Summer 6-27-2019

Fibrinogen, Factor XIII and Fibronectin: A Biophysical and Kinetic Characterization of Their Interactions

Frank Fabian
University of Nebraska - Lincoln, frankfabsan@gmail.com

Fibrinogen, Factor XIII and Fibronectin: A Biophysical and Kinetic Characterization of Their Interactions

by

Frank Marco Fabian Sanabria

A DISSERTATION

Presented to

The Graduate College at The University of Nebraska

In Partial Fulfillment of Requirements

For the Degree of Doctor of Philosophy

Major: Chemical and Biomolecular Engineering

Under the SUPERVISION of Professor William H. Velander

Lincoln, Nebraska

July, 2019

Fibrinogen, Factor XIII and Fibronectin: A Biophysical and Kinetic Characterization of Their Interactions

Frank M. Fabian Ph.D.

University of Nebraska,2019

Advisor: William H. Velander

The development of recombinant-based liquid fibrin tissue sealants having enhanced hemostatic and wound healing properties will involve understanding as yet not well characterized interactions between fibrinogen, fibrin (Fbn) factor XIII, thrombin and fibronectin. We study these phenomena in the context of comparing plasma derived fibrinogen to recombinant fibrinogen (rFI) produced in the milk of transgenic cows. An abundance of purified γγ and γγ' FI subspecies enables detailed study of γγ or γγ' biomonomer and their respective Fbn biopolymer formation as having different substrate behaviors of activated plasma derived factor XIII ($pFXIIIa_2b_2$). High pressure size exclusion (HPSEC) and anion chromatography technique were used along with dynamic light scattering (DLS) and an adapted solid phase peptide incorporation assay.

HPSEC analysis of the purified mixtures rFI with $pFXIIIa_2b_2$ showed greater $pFXIIIa_2b_2$ avidity for γγ'rFI than γγrFI. This mixture could also be isolated by weak anion exchange chromatography. The elution profile resolved both γγ and γγ'rFI and transglutaminase activity showed $pFXIIIa_2b_2$ activity specifically overlapping the γγ'rFI elution peak. DLS analysis of $pFXIIIa_2b_2$–γγ'rFI mixture showed a high level of polydispersity index suggesting the complexes of different sizes.

Kinetic studies on the effect of the γγ, γγ'rFI and rFbn in the rate of $pFXIIIa_2b_2$ activation were postulated to exist in three different stages. This mechanism resembles the proposed stages for in-vivo $pFXIIIa_2b_2$ activation. In stage I, it was showed that γγ' rFbn accelerates the rate of thrombin proteolytic removal of the $pFXIIIa_2b_2$ activation peptide. Stage II indicated that γγ' rFI and γγ'-rFbn induced the faster $pFXIIIa_2b_2$ B-subunit dissociation. In the final stage, neither rFI nor rFbn showed an effect on the $pFXIIIa_2b_2$. This was consistent with the previously reported role of B chains in fibrinogen binding.

The goal of this work focused on studying the existence and reversibility of a complex specifically formed between plasma derived γγ' fibrinogen (γγ'pFI) and plasma fibronectin (pFN) and postulated to exist in plasma circulation. HPSEC was used to identify and isolate the mixture while DLS was used to analyze the hydrodynamic size that ranged between γγ'pFI and pFN. Reconstitution studies using a degraded α-chain γγ' fibrinogen showed that the γ' chain of pFI is needed to initiate complex formation.

Dedication

I want to dedicate my work to my beloved wife Rosie for the daily support and to my daughter Brianna and my son Ian

Author's Acknowledgements

I want to express my sincere gratitude to Dr. William Velander for his guidance throughout my doctoral studies. In addition, I also want to thank to my lab group: Ayman Ismail, Weijie Xu, Nick Vanderslice and Jorge Ragusa. Finally, I want to thank all the staff of the Biological Process Development Facility (BPDF).

TABLE OF CONTENTS

List of Tables

List of Figures and Schemes

CHAPTER I

Hemostasis and Wound Healing Initiated by the Coagulation Cascade: the Physiology of Fibrin Formation by Fibrinogen, Factor XIII and Fibronectin.

1.1 Overview of fibrin function at the wound site

Injury and the physiologic response of wound stabilization and healing can be viewed as beginning simultaneously as the fibrin barrier acts to both seal the wound and as a foundation to begin healing. Fibrin is a wound adherent biopolymer of sufficient strength and density to stop bleeding by sealing the damaged blood vessels and surrounding wounded tissue. [1] It also presents structural features (such as by entrained platelets that are cross-linked into the polymer) that signal various cells to colonize it and to begin the healing process. [2, 3, 4, 5] The cessation of bleeding initiates a return to "steady-state" restoration of the coagulation system. The recovery from any systemic and local physiologic shock resulting from fluid loss (plasma and blood) is commensurate with "the re-establishment of hemostasis".

Almost instantly after injury and during the formation of the fibrin barrier to fluid loss, a pool of circulating inflammatory cells called neutrophils gather and occupy the fibrin barrier [6, 7, 8] . This is mediated by various neutrophil integrin receptors that bind to ligands displayed by both fibrin and by platelets. This is a needed initiation of an inflammatory process which proteolytically cleans up (a debridement) damaged tissue that results from injury. The neutrophils participate in a simultaneous cytokine and growth factor signaling that emanates from damaged vascular endothelium and platelets entrained within the fibrin barrier at the wound site. [9, 10, 11] A 24 hour

time lag accompanies signals arising from this process and its conveyance to the bone marrow. This results in activation, maturation and transport of macrophages from the bone marrow to the wound site. Macrophages are cells with exceptional plasticity and the ability to differentiate into fibroblasts and endothelial cells upon colonization of the fibrin matrix. [12, 13] In that context, fibrin acts as a 3-D provisional matrix for wound healing that is centered about staging macrophage colonization.

The next stage of healing then advances to the formation of a provisional tissue called granulation tissue. It is formed during the next 48 hours by a network of fibroblasts that support a 3-D network of vasculature formed within it by endothelial cells both arising from differentiated macrophages. Thus, granulation tissue is essentially derived from fibrin colonized macrophages. [14] This network provides the necessary 3-D scaffold that can deliver nutrients and oxygen and simultaneously remove metabolites and waste products to colonizing stem cells which must build and restore functional tissue to the wound site. [15] A total time of about 3 to 4 days is needed to install well-vascularized granulation tissue during which fibrin is proteolytically digested. [16] The susceptibility to proteolysis of fibrin is thus purposeful and at the core of the process for the rapid establishment of granulation tissue. Well-vascularized granulation tissue is necessary for the next stage of healing which seeks to restore functional tissue from stem cells which colonize granulation tissue.

1.2 **Fibrin generation and the coagulation cascade**

The biochemical pathway which polymerizes fibrinogen into the fibrin matrix that is both a barrier to fluid loss and a 3-D provisional matrix for healing is the initiated

by the blood coagulation enzymatic cascade (Figure 1.1.). The cascade is designed to amplify an enzymatic chain of reactions that are triggered by the exposure of blood components specifically to the subendothelial layers of the damaged vessel wall. [17, 18] The final amplified surge of enzyme activation is that of prothrombin to thrombin specifically at the wound site. Thrombin then polymerizes fibrinogen into fibrin polymer purposely confining the fibrin generation locally at and within the damaged vascular wound site. [19, 20] The specific confinement of a potent thrombin activity surge is essential to both generate sufficient wound adherent fibrin to stop bleeding while minimizing the risk of a blood borne, fibrin clot emboli that could become systemically lodged and would block blood flow. [21, 18]

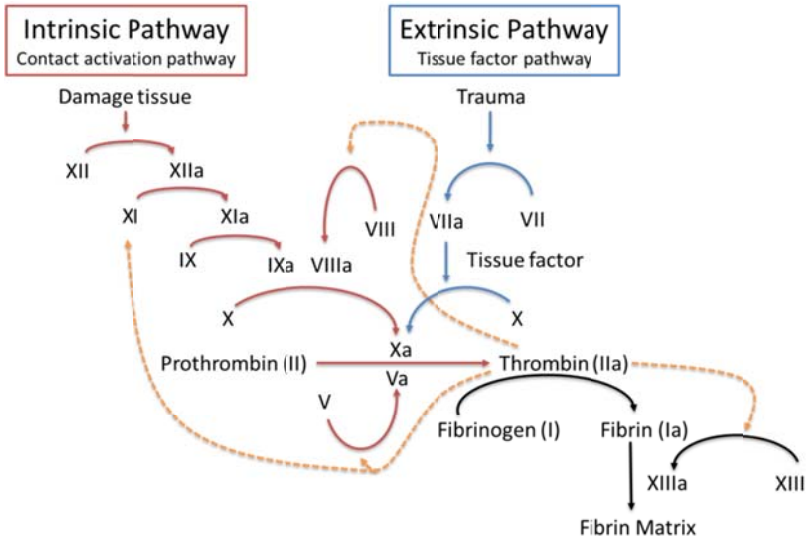

Figure 1.1: The Blood coagulation cascade. The extrinsic pathway and the intrinsic pathway have common steps once the activation of factor X takes place. Last steps on the process are directed to the formation of a stable, locally formed, wound adherent fibrin matrix.

The blood coagulation cascade can be divided in two distinct and essentially sequentially occurring amplification pathways: the extrinsic and the intrinsic coagulation pathways. [22, 23, 24, 25] In the extrinsic pathway, tissue factor (TF) is released after vascular injury leading to the first stabilizing pulse of fibrin called a hemostatic plug. It is sometimes referred to as the TF-FVIIa pathway. The hemostatic plug is characteristically a first responder effort to achieve hemostasis and includes entrained platelets which immediately catalyze both thrombin generation and cell signaling that gathers circulating neutrophils. After this initial fibrin generation, the same thrombin triggers the intrinsic pathway resulting in a >1500-fold kinetic surge of additional thrombin. It is this thrombin that generates the bulk of fibrin needed to ultimately finish the hemostatic and "provisional matrix for healing" roles of the fibrin barrier. [25] It is noted that thrombin acts penultimately in multiply nested enzyme reaction steps to assure insoluble fibrin formation including activation steps of fibrinogen to fibrin monomer and also of intrafibrin and wound ECM crosslinking.

The extrinsic pathway is centered about the initial exposure of TF caused by wounding. [23] It is a cell bound transmembrane glycoprotein and class II cytokine, operates as both a signal transduction and a factor VII cofactor. As a signal transduction, TF induces the genes involved in inflammation, embryonic development and cell migration and as cofactor TF binds and activates coagulation factor VII (FVII) in a process named blood coagulation initiation. The newly formed complex proteolytically activates the coagulation factor IX (FIX) and factor X (FX) into FIXa and FXa. The association of FXa with the cofactor Factor V activates small amounts of prothrombin to thrombin. [22]

Large amounts of FXa (>1500-fold kinetically higher amounts is generated than is by VIIa pathway) are generated by the formation of tenase complex involving FIXa and FVIIIa. [17, 22] The activation of FVIIIa and FIXa is catalyzed by small amounts of thrombin formed from the FVIIa activation pathway. This results in large amounts of prothrombinase complex to generate a very large surge of thrombin necessary to seal the wound in a lasting manner. It is noteworthy that the FIXa-FVIIIa-FXa tenase complex formation is precluded in individuals with hemophilia A and hemophilia B. [17] The formation of FXa forms a complex with FVa on the platelet surface receptors forming prothrombinase complex that converts prothrombin to thrombin. As final steps, thrombin activates fibrinogen and factor XIII to induce fibrin polymerization and the formation a stable fibrin matrix. [24, 25] Thus, thrombin activity is self amplifying. It is feedback controlled by inhibitors such as antithrombin III and the inactivation of Factor Va and Factor VIIIa caused by activated protein C. Protein C is activated by thrombin.

The polymerization of fibrinogen, figure 1.2, begins with the thrombin proteolytic cleavage of the fibrinopeptide A (fpA) contained on the fibrinogen (FI) Aα chain and the fibrinopeptide B (fpB) located in the Bβ chain. The release of the fpA and fpB generates the exposure of independent polymerization sites E_A and E_B which combines respectively with a constitutive complementary D_A and D_B pocket located in the D domain of adjacent FI molecules. [26, 27, 28, 29] The release of the fpA expose the Gly-Pro-Arg (GPR) motif which associates with D_A pocket resulting in the formation of a strong and stable double-stranded fibril which in turn undergo lateral association to form a complex fibrin network. In the other hand, the release of the fpB exposes the Gly-His-Arg-Pro (GHPR) motif allowing the interactions with the D_B pocket. This later interaction is not

completely required for lateral fibril association but it contributes to this process through cooperative interactions. The further assembly of fibrin begins with the formation of double stranded fibrils. Interactions of fibrin monomers occurs in a half staggered manner inducing the formation of large fibrin oligomers which lengthen further to make protofibrils. Protofibrils lateral aggregation leads to the formation thicker or thinners packed fibers which is catalyzed by the enzymatic activity of factor XIII. [30, 31] Further fiber branching occurs by bilateral and equilateral junction. The first occurs when a double –stranded fibril converges laterally with another fibril to form a four-stranded fibril. The equilateral junction occurs when three fibrin molecules converge they form a three double stranded fibril. Finally, these associations give rise to the formation of a 3-D network which in turn induce the formation of a fibrin clot and consequently the initial structure for the incorporation of different proteins including fibronectin, Von Willebrand factor (a circulating protein with platelet and ECM-collagen wound adherence, that is a large macromolecule with potential for polymeric structures >1M kDa) , vascular endothelial growth factor that contributes to tissue repair. [32, 33]

1.3 **The process for fibrin entrainment of Fibronectin needed for cell colonization signaling**

One form of Fibronectin (FN) is a large 440 kDa glycoprotein is produced and secreted by hepatocytes into blood plasma where circulates at 300–400 μg/mL. Other forms of FN are designated as “cellular fibronectin (cFN): and are produced by most cells for integration into their ECMs. For example, macrophages, fibroblasts and epithelial cells all produce cFN. pFN and cFN are can be distinguished by their differences in structure that impart solubility: plasma FN is soluble enabling it to circulate while cFN

has limited solubility leading to its immediate ECM incorporation upon its secretion. [34, 35, 36] However, pFN can be incorporated into the fibrin matrix evolving at the woundsite by the crosslinking provided transglutaminase factor XIII (FXIII).

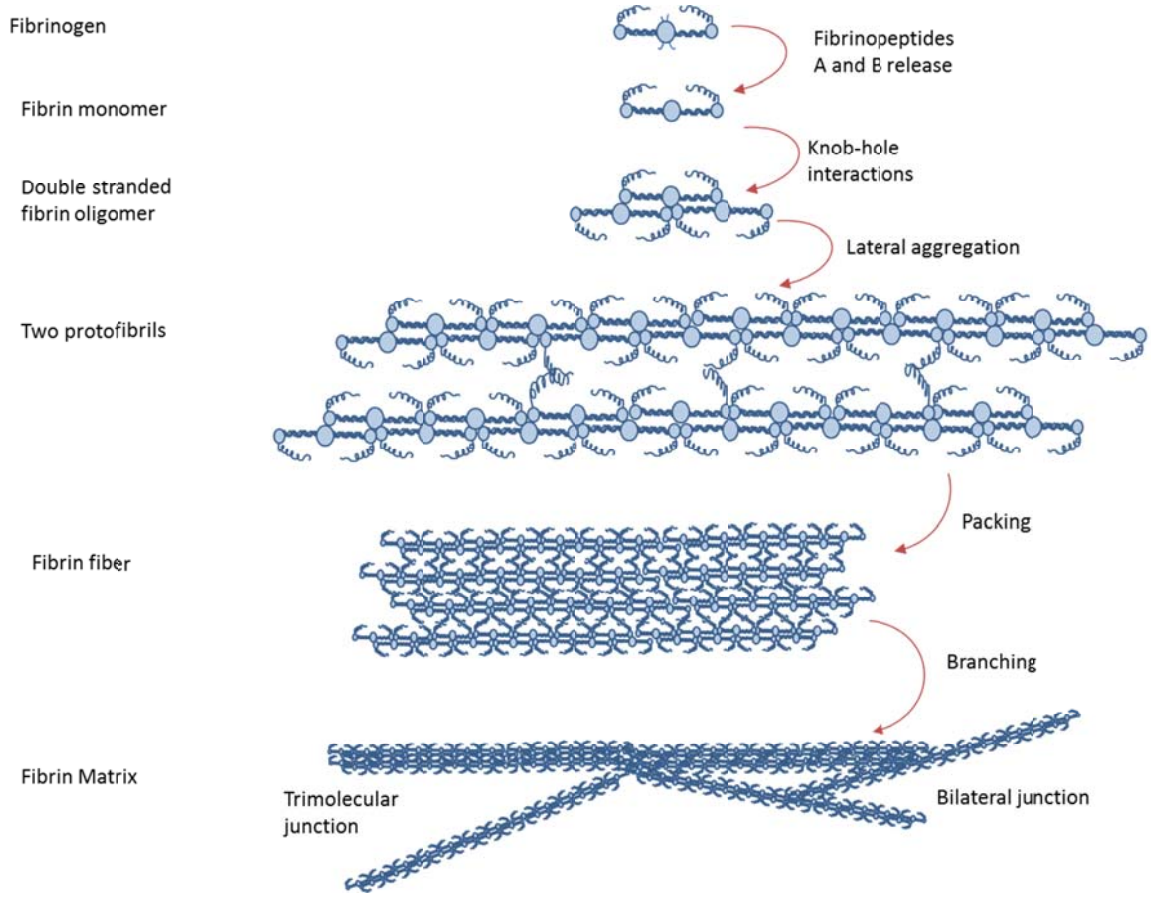

Figure 1.2.: Fibrin polymerization initiates by the proteolytic thrombin removal of fpA and fpB. Knob-hole interactions between D domains and E domains start lateral aggregation which induces further packing and branching. Bilateral junction occurs as the final step of the fibrin matrix formation.

Several important structural characteristics result from the installation of pFN into the fibrin matrix. pFN provides stability and viscoelastic strength to the nascent fibrin matrix. [32] In addition, the altered pFN conformation resulting from crosslinking into fibrin matrix exposes signaling residues for integrin receptors. These exposed ligands are key to triggering of angiogenesis. For example, cross-linked pFN induces the integrin expression of α4β1, α5β1 in quiescent endothelial cells and subsequently αvβ3, αvβ5 during angiogenesis. [37, 37]

The migration and proliferation of endothelial cells within the fibrin matrix during the early stages of wound healing and angiogenesis is dependent on the presence of cross-linked pFN. [37] pFN is also well known for its significance in physiological process such as cell adhesion, migration and wound healing. Once fibronectin is crosslinked into the fibrin matrix by the action of the transglutaminase factor XIII (FXIII), fibronectin RGD (Arg-Gly-Asp) peptide residues serves as a signal for the binding of transmembrane integrin proteins in endothelial cells. [26, 38, 39] Thus, the engineering of the incorporation of pFN into the fibrin matrix by FXIII can be used as method to regulate cellular association, migration and proliferation.

1.4 FXIII activity and the engineering of the incorporation of pFN into the fibrin matrix.

The *in vitro* and *in situ* engineering of strong fibrin matrices including those incorporating pFN such as occurs in fibrin based surgical sealants requires FXIII activity. In that context, the cross-linking by FXIII has a multi-faceted impact on fibrin stability. For example, the cross-linking of fibrin by FXIII renders resistance of the fibrin

to fibrinolysis. *In vivo*, a balance of resistance to fibrinolysis and fibrin stability is essential for the development of fibrin clot strength while mitigating the danger of emboli formation. The catalytic activity of FXIII on the fibrin cross-linking also regulates the plasminogen binding to the fibrin network. This fibrinolytic process is regulated by covalent binding presence of α2 antiplasmin to fibrin. FXIII also regulates the platelet attachment to fibrin matrix by crosslinking the γ-chains which in turn alters the platelet binding site inducing the down regulation of platelet adhesion to the fibrin matrix. [40] [41, 42] As mentioned above, the covalent attachment of FN to the fibrin matrix during this process influences the clot elastic properties and the fiber size and density. [43, 44] The physiologic impact of fibrin sealants used at wound sites will undoubtedly be complex and have wound healing properties impacted by FXIII activity and the fibrin:pFN polymer structure it catalyzes. Briefly, these can be anticipated by physiologic abnormalities associated with FXIII deficiencies. For example, FXIII has been demonstrated to be important to embryonic fibroblast growth. FXIII deficiencies affect the normal fibroblast growth producing cells of irregular shape which consequently affect the ECM associated collagen production associated with tissue development. [45]

1.5. References

[1] R. Litvinov and J. Weisel, "What is the biological and clinical relevance of fibrin," *Semin. Thromb Hemost ,* vol. 42, pp. 333-343, 2016.

[2] R. A. Clark, "Fibrin and Wound healing," *Annals New York Academy of Science,* vol. 936, pp. 355-367, 2001.

[3] M. Xue and C. J. Jackson, "Extracellular matrix reorganization during wound healing and its impact on abnormal scarring," *Advances in wound care,* vol. 4, pp. 119 - 136, 2015.

[4] P. Olczyk, L. MenCner and K. Komosinska-Vassev, "The role of the extracellular matrix components in cutaneous wound healing," *BioMed Research International,* pp. 1-8, 2014.

[5] R. Clark and P. Henson, "The Molecular and Cellular Biology of Wound Repair," pp. 51-93, 1988.

[6] J. D. Loike, B. Sodeik, L. Cao, S. Leucona, J. I. weitz, P. A. Detmers, S. D. Wright and S. C. Silverstein, "CD11c/CD18 on neutrophils recognizes a domain at the N terminus of the A alpha chain of fibrinogen," *Proc. Natl. Acad. Sci.,* vol. 88, pp. 1044-1048, 1991.

[7] D. Davalos and K. Akassoglou, "Fibrinogen as a key regulator of inflammation in disease," *Semin. Immunopathol,* vol. 34, pp. 43-62, 2012.

[8] H. Brem and M. Tomic-Canic, "Cellular and molecular basis of wound healing," *The journal of clinical investigation,* vol. 117, pp. 1219-1222, 2007.

[9] L. Koenderman, J. A. Van der Linden, H. Honing and L. H. Ulfman, "Integrins on neuthrophils are dispensable for migration into three dimensional fibrin gels," *Thrombosis and Haemostasis,* vol. 104, pp. 599-608, 2010.

[10] P. Kuijper, H. Gallardo Torres, J. Van der Linden, J. Lammers, J. Sixma, J. Swaginga and L. Koenderman, "neutrophil adehesion to fibrinogen and fibrin under flow conditions is diminished by activation and L-selectin shedding," *Blood,* vol. 89, pp. 2131-2138, 1997.

[11] F. Szaba and S. Smiley, "Roles for thrombin and fibrin(ogen) in cytokine/chemokine production and macrophage adhesion in vivo," *Blood,* vol. 99, pp. 1053-1059, 2002.

[12] J. Y. Hsieh, T. D. Smith, V. S. Meli, T. N. Tran, E. L. Botvinivk and W. F. Liu, "Differential regulation of macrophage inflammatory activation by fibrin and fibrinogen," *acta biomaterualia,* vol. 47, pp. 14-24, 2017.

[13] S. Smiley, J. King and W. Hancock, "Fibrinogen stimulates macrophage chemokine secretion through toll-like receptor 4," *J. Immunol,* vol. 167, pp. 2887-2894, 2001.

[14] K. K. Mathieu P. Rodero, "Skin wound healing modulation by macrophages," *Int J Clin Exp Pathol,* vol. 3, pp. 643-653, 2010.

[15] M. Lovett, K. Lee, A. Edwards and D. Kaplan, "Vascularization strategies for tissue engineering," *Tissue engineering part B,* vol. 15, pp. 353-370, 2009.

[16] J. Stroncek and m. Reichert, "Chapter 1: Overview of wound in different tissue types," in *Indwelling Neural Implants: Strategies for Contending with the In Vivo Environment.*, 2008.

[17] K. G. Mann and K. Brummel-Ziedins, "Blood Coagulation," in *Haematology of infancy and childhood*, Saunders Elsevier, 2009, pp. 964-983.

[18] H. H. Versteeg, J. W. Heemskerk, M. Levi and P. Reitsma, "New Fundamental in Hemostasis," *Physilogical Review,* vol. 93, pp. 327-358, 2013.

[19] N. Laurens, P. Koolwijk and P. De Maat, "Fibrin structure and wound healing," *Journal of Thrombosis and Haemostasis,* vol. 4, pp. 932-939, 2006.

[20] S. A. Smith, R. J. Travers and J. H. Morrissey, "How it all starts: initiation of the clotting cascade," *Crit. Rev. Biochem Mol Biol,* vol. 50, pp. 32-336, 2015.

[21] T. Velnar, T. Bailey and V. Smrholj, "The wound healing proces: and overview of the cellular and molecular mechanism," *The journal of international medical research,* vol. 37, pp. 1528 - 1542, 2009.

[22] M. P. McGee and C. L. Lynne, "Functional difference between intrinsic and extrinsic coagulation pathways," *The journal of biological chemistry,* vol. 266, pp. 8079-8085, 1991.

[23] N. Mackman, R. E. Tilley and N. S. Key, "Role of the extrinsic pathway of blood coagulation in hemostasis and thrombosis," *Arteriosclerosis, Thrombosis, and Vascular Biology,* vol. 27, pp. 1687-1693, 2007.

[24] D. Gailani and T. Renne, "The intrinsic pathway of coagulation: a target for treating thromboembolic disease?," *Journal of thrombosis and haemostasis,* vol. 5, pp. 1106-1112, 2007.

[25] D. Gailani and T. Renne, "Intrinsic pathway of coagulation and arterial thrombosis," *Arteriosclerosis, Thrombosis, and Vascular Biology,* vol. 27, pp. 2507-2513, 2007.

[26] M. W. Mosesson, K. R. Siebenlist and D. A. Meh, "The structure and biological features of fibrinogen and fibrin," *Annals new york academy of science,* vol. 936, pp. 11-30, 2001.

[27] J. W. Weisel and R. I. Litvinov, "Fibrin formation, structure and properties," *Subcell Biochem,* vol. 82, pp. 405-456, 2017.

[28] J. J. Sidelmann, J. Gram, J. Jespersen and C. Kluft, "Fibrin clot formation and lysis: basic mechasnism," *Seminar in thrombosis and hemostasis,* vol. 26, pp. 605-617, 2000.

[29] J. W. Weisel and R. I. Litvinov, "Mechanism of fibrin polymerization and clinical implications," *Blood,* vol. 121, pp. 1712-1719, 2013.

[30] E. Barry and D. Mosher, "Factor XIII cross linking of fibronectin at cellular matrix assembly sites," *Journal of Biological chemistry,* vol. 263, p. 25, 1988.

[31] R. A. Ariens, T.-S. Lai, J. W. Weisel, C. S. Greenberg and P. J. Grant, "Role of factor XIII in fibrin clot formation and effects of genetic polymorphisms," *Blood,* vol. 10, pp. 743-754, 2002.

[32] S. Corbett, L. Lee, C. Wilson and J. Schwarzbauer, "Covalent cross-linking of fibronectin to fibrin is required for maximal cell adhesion to a fibronectin-fibrin matrix," *Journal of biological chemistry,* vol. 272, pp. 24999-25005, 1997.

[33] S. Corbett, C. Wilson and C. Schwarzbauer, "Changes in cell spreading and cytoskeletal organization are induced by adhesion to a Fibronectin-Fibrin matrix," *Blood,* vol. 88, pp. 158-166, 1996.

[34] W. S. To and K. S. Midwood, "Plasma and cellular fibronectin: distinct and independent fucntions during tissue repair," *Fibrogenesis and tissue repair,* vol. 4, 2011.

[35] M. K. Magnusson and D. F. Mosher, "Fibronectin: Structure, Assembly and Cardiovascular implications," *Arteriosclerosis, thrombosis and vascular biology,* vol. 18, pp. 1363-1370, 1998.

[36] S. Johanson, G. Svineng, K. Wennerberg, A. Armulik and A. Lohikangas, "Fibronectin-Integrin interactions," *Frontiers in bioscience,* vol. 2, pp. 126-146, 1997.

[37] R. Clark, J. DellaPelle, P. Manseau, E. Dvorak and R. Colvin, "Fibronectin and fibrin provide a provisional matrix for epidermal cell migration during wound reepithelization," *Journal of investigative dermatology,* vol. 79, pp. 264-269, 1982.

[38] D. Donalson and J. Mahan, "Fibrinogen and fibronectin as substrates for epidermal cell migration during wound closure," *Journal of cell science,* vol. 62, pp. 117-127, 1983.

[39] N. Fournier and C. Doillon, "In-vitro angiogenesis in fibrin matrices containing fibronectin or hyaluronic acid," *Cell biology international reports,* vol. 16, pp. 1251-1263, 1992.

[40] C. Duval, P. Allan, S. Connell, V. Ridger, H. Philippou and R. Ariens, "Roles of fibrin alpha and gamma specific cross-linking by FXIIIa in fibrin structure adn function," *Blood coagulation fibrinolysis and cellular haemostasis,* vol. 111, pp. 842-850, 2014.

[41] L. Muszbek, Y. C. Vivien and Z. Hevessy, "Blood coagulation factor XIII: structure and function," *Thrombosis research,* vol. 94, pp. 271-305, 1999.

[42] K. Siebenlist , D. Meh and M. Mosesson, "Plasma factor XIII binds specifically to fibrinogen containing gamma prime chains," *Biochemistry,* vol. 35, pp. 10448-10453, 1996.

[43] A. Ismail, F. Fabian, O. Wang, L. Yugou, M. Carlson, W. Burgess and W. Velander, "The isolation of a plasma-derived γγ' fibrinogen: Fibronectin mixture that forms a novel polymeric matrix," *Process biochemistry,* vol. 75, pp. 257-265, 2018.

[44] E. Makogonenko, G. Tsurupa, K. Ingham and L. Medved, "Interaction of Fibrin(ogen) with fibronectin: further characterization and localization of the fibronectin binding site," *Biochemistry,* vol. 41, pp. 7907-7913, 2002.

[45] L. Lorand, "Factor XIII and the clotting of fibrinogen: from basic research to medicine," *Journal of thrombosis and haemostasis,* vol. 3, pp. 1337-1348, 2005.

CHAPTER II

Biophysical properties of Fibrinogen, Factor XIII and Fibronectin: molecular structure and interactions

2.1 Fibrinogen (FI) structure

Fibrinogen a 340 kDa human plasma glycoprotein that is comprised of two sets of disulfide-bridged Aα chain (66.5kDa), Bβ chain (52kDa), and γ chain (46.5). Each FI molecule symmetrically presents two D domains connected to a central E hub domain. [1, 2] FI is formed by 6 chains held together by disulfide bonds in the E region. These chains extend from the E region forming two symmetric half molecules. The D region is mainly conformed by the C-termini of the Bβ and γ which form a globular domain. At physiological conditions FI behaves as a straight rod shape molecule with a hydrodynamic radius (R_H) of 10 ± 0.1 nm as measured by dynamic light scattering (DLS) [3, 4]. FI presents two variants of γ chains arising from differential mRNA splicing leading to the substitution of 4 carboxy terminal amino acid residues of the γ chain by a more acidic 20 amino acid sequence. (Figure 2.1) [5, 6, 7] . The presence of this sequence leads to an approximate 90% occurrence of FI in normal human plasma containing a “homodimeric” γγ content with 10 % of FI containing “heterodimeric” γγ’. This variation introduces different biochemical characteristics that are mainly related to its interaction with plasma factor XIII, fibronectin and also fiber thickness, protofibril packing, intrafibrillar structure and clotting strength [8, 9, 10]

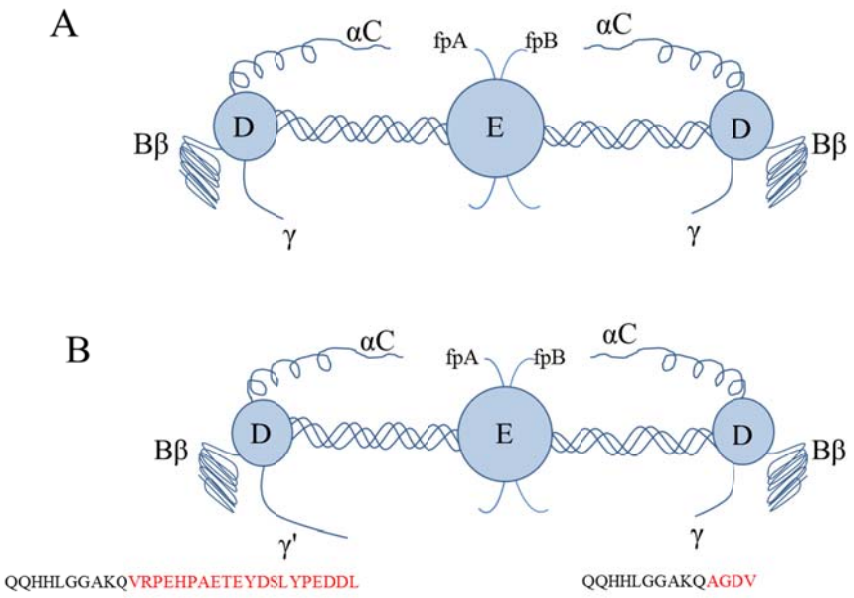

Figure 2.1: Schematic diagram of Fibrinogen (FI). Outer domains D are connected to the central E domain by coiled segments. Aα, Bβ, and γ chains are located within the D domains. **(A)** The homodimer γγ **(B)** The heterodimer γγ' with additional 20 amino acids.

2.1.1. Fibrin polymer structural properties when made from FI alone.

Fibrin formation begins with FI activation to form soluble fibrin monomers that are catalyzed by the thrombin proteolytic removal of fibrinopeptides A and B (fpA and fpBP). Each of these peptides is located at the N-terminal of the Aα and Bβ chains, respectively. Assembly of fibrin monomers into fibrin begins with the formation of a double-stranded fibrils which are also induced by conformational changes from the removal of fpA and fpB. Interactions between fibrin monomers induces the formation of large aggregations of fibrin oligomers. These oligomeric structures further lengthen into protofibrils where several pathways for fibril growth have been proposed. [11, 12, 13] For example, a lateral aggregation of these "protofibrils" can leads to the formation of

thicker fibers. These structures are rendered insoluble by the enzymatic cross-linking activity of factor XIII. Fiber branching occurs when a double-stranded fibril converges laterally aligns with another fibril to form a four-stranded fibril. A "three double stranded fibril" occurs when three fibrin molecules converge they form a fibril. Finally, these associations and cross-linking give rise to the formation of an insoluble 3 dimensional network that is a core part of the fibrin barrier and provisional matrix. [11, 12, 14, 15, 16]. However, the specific pathways for pFN integration have not been detailed and are a function of FXIII activity. Structural differences in fibrin polymer occur when polymerized from γγ versus γγ' F1. For example, fibrin polymer made *in vitro* with γγ' exhibits smaller pores when visualized by Transmission Electron Microscopy (TEM). [17, 8, 18, 10]

2.2 Factor XIII (FXIII) structure

Plasma factor XIII ($pFXIIIA_2B_2$) is composed of two A catalytic sub-unit and two B carrier subunits (Figure 2.2). [19] Factor XIII also occurs on the surface of platelets as a dimer of two A catalytic sub-units. This dimeric form is also named cellular factor XIII ($cFXIIIA_2$). Both $pFXIIIA_2B_2$ and $cFXIIIA_2$ of platelets are transformed to the same activated dimers by thrombin proteolysis in the presence of physiological levels of calcium which induces to structural modifications. About 50% of the resulting factor XIII crosslinking activity is supplied to the polymerization reaction of fibrin by $pFXIIIA_2B_2$. This cross-linking is catalyzed by transglutaminase activity which forms covalent bonds between γ-γ, γ-α and α-α of adjacent fibrin molecules stabilizing the protofibrils. [20, 21, 22]

The pFXIII is transformed to its enzymatically form (pFXIIIA$_2$*) by the successive action of thrombin and Ca^{2+} in the presence of fibrinogen (figure 2.3). This enzymatic conversion occurs in two steps. In the first step, thrombin cleaves the 4kDa activation peptide at the N-terminus from each of the two A chains and gives the formation of an inactive intermediate. In the second step, calcium, in the presence of fibrin, causes the dissociation of the B subunits forming the active functional dimeric pFXIIIA$_2$* [23, 24, 25] The structural re-arrangement exposes the catalytic core domain composed of three amino acids residues: Cys314, His373, and Asp396 that are responsible for the interchain peptide bond formation between glutamine and lysine residues in the fibrin clot. [26] The catalytic activity of pFXIIIA$_2$a accelerates the intramolecular formation of γ-glutamyl-ε-lysil isopeptide bond also known as cross-linking. The covalent links resulting in dimerization of the γ-chains can be observed by SDS-PAGE as can be cross-linking products of the α-chains. [27, 28]

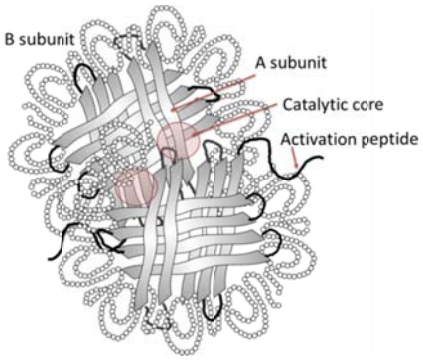

Figure 2.2. : Schematic representation of plasma factor XIII. Two A subunits represented by Beta strands and two B subunits represented by sushi domains are depicted in the figure above. The catalytic triad (red circle) is conformed of Cys314, His373, and Asp396.

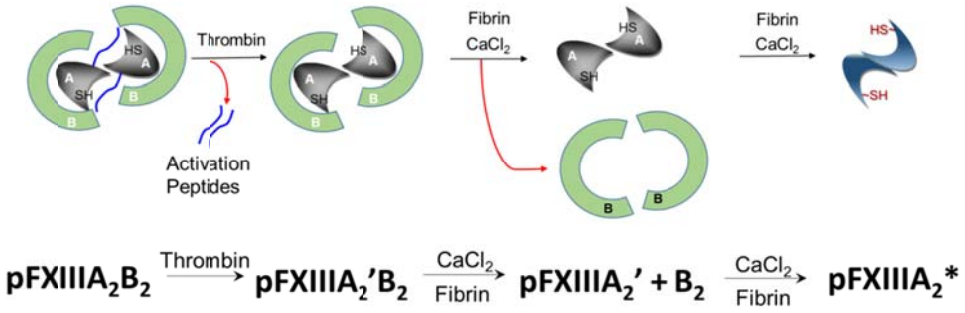

Figure 2.3. : Schematic representation of plasma factor XIII activation mechanism. Thrombin removes the activation peptide from the A subunit. B-subunit dissociation is induced by the presence of Ca^{2+} in the presence of fibrin. Conformational changes induced by fibrin expose the Cysteine catalytic core of the factor XIII.

2.3 Fibronectin (FN) Structure

FN exists as plasma and cellular FN. plasma FN is synthesized in the liver by hepatocytes and secreted into blood plasma where circulates at 300–400 µg/mL [29] meanwhile cellular FN is produced by fibroblasts, endothelial cells, chondrocytes, synovial cells and myocytes contributing to the formation of a large numbers of FN isoforms. [30, 31] These two forms of FN are mainly distinguished by its structure and functionality during wound healing. [29, 32] Structurally, FN exists as a dimer consisting of similar but no identical chains of approximately 220kDa in size joined by a pair of disulfide bonds (figure 2.4) [33]. Each chain consists of a linear arrangement of repeating units known as: type I, type II and type III. FN contains 12 type I repeats (about 40 amino acid and 2 disulfide bonds), 2 type II repeats (60 amino acids and 2 intrachain disulfide) and 15-17 type III repeats (90 amino acid). [33, 31] Each repeating unit operates as distinct domain which possesses specific arrangement that allows flexibility within the

molecule to adopt different shapes and facilitates its interaction with other proteins like collagen and FI. Structurally, FN is defined as a semi-globular protein with a R_H of 11.5 ± 0.1 nm with significant degree of chain flexibility [30, 34, 35] Additional studies showed that FN contains two major fibrin binding sites located at the amino terminal (Fib-1) and carboxyl terminal (Fib-2). [36, 37]

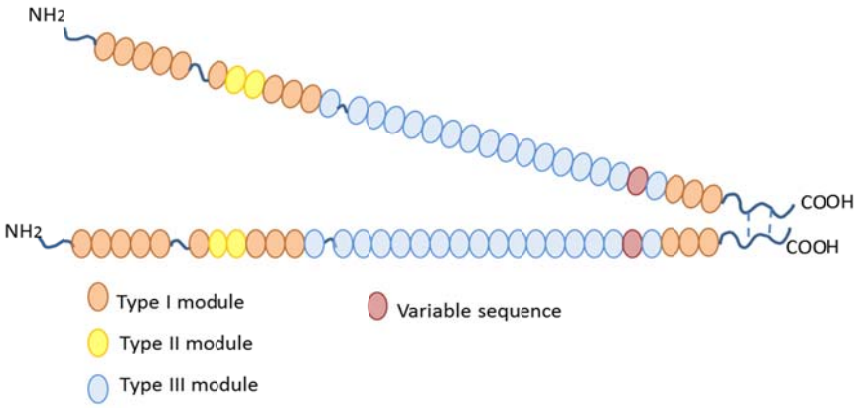

Figure 2.4.: Schematic diagram of Fibronectin (FN), two identical amino acids sequence are connected by disulfide bonds on the Carboxyl terminus. Three different modules are depicted in orange, yellow and blue circles.

2.4 **Interaction between fibrinogen-factor XIII and Fibrin-factor XIII**

The interaction between fibrinogen-FXIIIA_2B_2 and fibrin-FXIIIA_2B_2 has been a theme of interest due to its importance in the blood clot formation in hemostasis and their role in the initial step in wound healing. In plasma, fibrinogen solubility plays and important role as its free motion exposes binding sites for many proteins as: factor XIII, thrombin, plasminogen, fibronectin and α2-antiplasmin. However, during the activation of the blood coagulation cascade, fibrinogen solubility is precluded by the thrombin

proteolytic removal of the fibrinopeptides A and B respectively converting fibrinogen into fibrin. Fibrin monomers, a less soluble molecule, is rapidly induced to lateral aggregation to form long double stranded oligomers which are lengthen to form protofibrils and aggregate to make fibers. Further crosslinking of fibrin fibers is achieved by the transglutaminase activity of the active factor XIII ($pFXIIIA_2$*, figure 2.3) forming an insoluble fibrin clot. As detailed above, three important stages of fibrinogen conversion into fibrin can be identified based in its solubility and the capability of interaction with plasma factor XIII ($pFXIIIA_2B_2$). It is important to highlight that fibrin ability to interact with factor XIII, thrombin and fibronectin are quite different from fibrinogen.

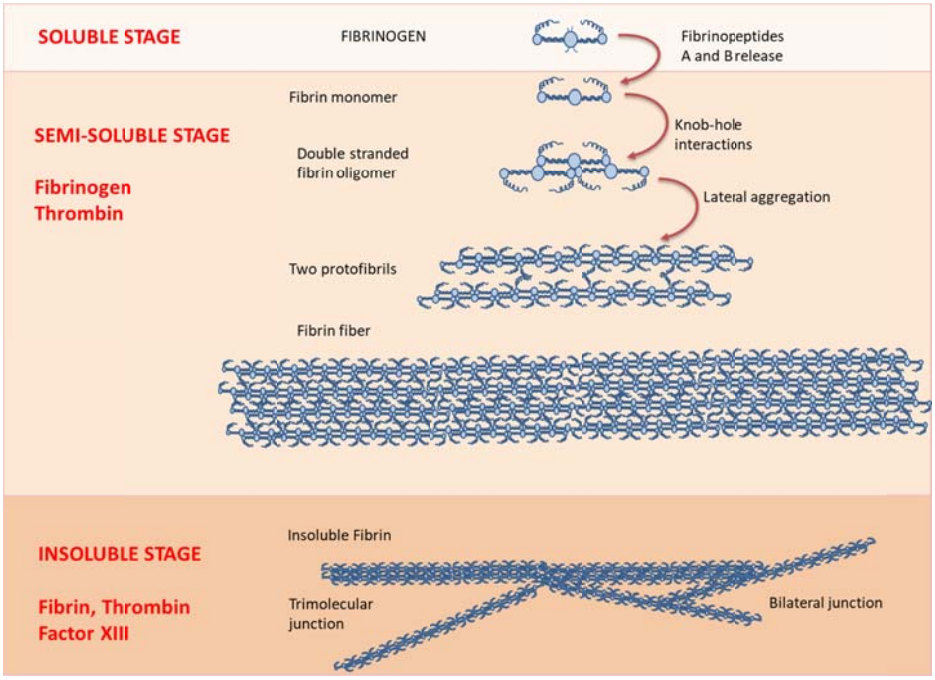

Figure 2.5: Schematic representation of the fibrinogen conversion into fibrin by the action of thrombin and factor XIII. Stages were subdivided based on molecule solubility.

2.4.1 Fibrinogen and factor XIII ($pFXIIIA_2B_2$)

It was initially stated that plasma factor XIII binds fibrinogen trough the factor XIII-A subunit suggesting that $pFXIIIA_2B_2$ circulates in plasma bound to fibrinogen. [38] Later studies focused on the identification of the fibrinogen binding site for $pFXIIIA_2B_2$, indicated that the fibrinogen γ' peptide chain is responsible for the interaction with $pFXIIIA_2B_2$ via the B subunit. [39] However, studies using surface plasmon resonance (SPR) identified a $pFXIIIA_2B_2$ binding region located in the αC region of fibrinogen. [40] Further investigation in the plasma Fibrinogen–Factor XIII interactions, showed that the fibrinogen γ chain residues 390-396 provides binding sites for $pFXIIIA_2B_2$ via the B subunit [41]. Based on these findings, it was suggested that the stoichiometric ratio of $pFXIIIA_2B_2$-fibrinogen interaction is 1:1 [41] However, due to the tetrameric nature of the factor XIII (2 subunit-B and 2 sub-unit A) it was also suggested that the interaction $pFXIIIA_2B_2$-fibrinogen occurs in a 2:1 ratio via the factor XIII subunit-B [42]. All these results presented above showed convincing evidence of the intrinsic nature of the interaction between the soluble FI with $pFXIIIA_2B_2$. However, some characteristics of these interactions are not quite completely explained. First, it is not quite clear what biophysical changes emerge from the interaction between the two main variants of fibrinogen: the homodimer γγ and the heterodimer γγ'. Second, it was stated that preparations of factor XIII free fibrinogen are quite complicated to obtain and it is only achievable by thermal denaturing of FI. Thus, all the previous experiments conducted using plasma fibrinogen may have misleading results as pFXIIIA2B2 may be present as an impurity. The previous statement is important during the activation assays as some

$pFXIIIA_2B_2$ content may affect the real contribution of the fibrinogen variants on the $pFXIIIA_2B_2$ activation mechanism.

2.4.2 Fibrin and factor XIII

While the interaction between fibrinogen and $pFXIIIA_2B_2$ has been extensively studied, the specific binding phenomenon is complicated by the heterologous nature of the cross-linking of fibrin by activated $FXIIIA_2$*. This is related to the fibrin matrix changes as it becomes insoluble due to the cross-linking process (figure 2.5 Insoluble phase). Specifically, $pFXIIIA_2B_2$-fibrin interactions were studied on the basis of the $pFXIIIA_2B_2$ activation mechanism. As presented in figure 2.3, the complete exposure of the $pFXIIIA_2$* catalytic triad occurs only in the presence of fibrin which reduces the concentration of calcium required for both the B-subunit dissociation and the structural modification to expose the catalytic core in the enzymatic pFXIII A subunit. [43, 44]. The nature of this interaction was also investigated by the formation of a termolecular complex between Fibrin–Thrombin–$pFXIIIA_2B_2$ which enhances the rate of proteolitic removal of the activation peptide within the $pFXIIIA_2B_2$. [45] However the major interaction between Fibrin–$pFXIIIA_2$* occurs during the fibrin crosslinking as fibrin acts as both cofactor and substrate during the crosslinking process. As a substrate, fibrin provides amino acid residues glutamine and lysine which are involved on the crosslinking phenomena. In short, the cysteine residue in the active pFXIIIA2* acts as nucleophile attacking the side chain of the glutamine (Q) residues on fibrin. Then, after the release of the ammonia from glutamine the acyl glutamil residue bond to the factor XIII catalytic triad, binds the primary amine from a lysine (K) residue forming the isopeptide bond. Crosslinking occurs more rapidly on the γ-chains between the γQ398 and or γQ399 and

γK406 [46]. Then, crosslinking of the α-chains occurs between αQ221, αQ237, αQ328, αQ366, and various Lysine residues. In the other hand, fibrin acts as cofactor by (a) reducing the amount of calcium required to separate A and B factor XIII subunits, (b) inducing the factor XIII B subunit dissociation from the previously thrombin $pFXIIIA_2B_2$, (c) triggering conformational changes on the $pFXIIIA_2$' to form the fully active $pFXIIIA_2$* (Figure 2.3). Thus, the predominant effect of fibrinogen on the activation of the $pFXIIIA_2B_2$ is as a cofactor. However, due to the fact the plasma fibrinogen preparations contain traces of $pFXIIIA_2B_2$ the actual evaluation of the FI effect on the rate of $pFXIIIA_2B_2$ activation may incur in unexpected deviations.

2.5 Interactions between Fibrinogen and fibronectin

As in the $pFXIIIA_2B_2$–FI interactions, the analysis of the plasma fibronectin–fibrinogen (pFN-FI) interactions were studied based in the pFN ability to bind fibrinogen and/or fibrin. Previous work suggested that the cold insoluble globulin (CIg), later renamed as fibronectin, induce the cryoprecipitation of fractions containing fibrin-fibrinogen complexes but not fibrinogen alone suggesting the pFN greater avidity toward fibrin molecules.[52] Further studies showed that the fibrinogen conversion to fibrin was necessary for the interaction of the fibrin αC chain and fibronectin [53]. However, the identification of a soluble 1:1 ratio FI–FN complexed molecule was detected by hydrodynamic light scattering studies of plasma collected from patients with rheumatoid arthritis suggesting that the intrinsic interaction of fibrinogen and fibronectin was facilitated by the FN structural flexibility in free motion. [48] In our recent work, we observed the formation of a γγ'FI-FN complex molecule in human plasma cryoprecipated

and isolated by DEAE at room temperature. Moreover, the thromboelastographic analysis showed that the γγ'FI-FN complex increases the clotting strength when compare with γγ'FI and γγ'FI at the same concentration. Our findings were also extended to the crosslinking characterization of the γγ'FI-FN mixture which present a periodical pFN crosslink into fibrin fibers a phenomenon that was not observed with the γγFI-FN mixture. [9] These finding lead us to perform a deep biophysical evaluation of interactions between pFN and the two major variants of FI: (a) the homodimer γγ and (b) the heterodimer γγ' and have a complete understanding on the nature of the FN and γγFI-FN, γγ'FI interactions.

2.6 Dissertation Objectives

In an effort to reconcile previous studies and present new evidence of interaction between fibrinogen and $pFXIIIa_2b_2$ and the effect of fibrinogen on the activation mechanism of $pFXIIIa_2b_2$ the present work have the following specific objectives.

1. Provide evidence of the role of the fibrinogen γ' chain on the interaction with the plasma derived factor XIII by analytical methods including high pressure size exclusion and dynamic light scattering.
2. Identify the stage at which the γγ and γγ' variants of fibrinogen exert the co-factor effect in the $pFXIIIa_2b_2$ activation mechanism.

This work is also extended to the characterization of the non-covalent binding between fibrinogen and fibronectin. Thus, the additional objectives are included in this dissertation.

3. Characterize the interaction of plasma fibrinogen and plasma fibronectin by analytical methods including dynamic light scattering.
4. Evaluate the effect of fibrin on the formation of a stable fibrinogen-fibronectin mixture.
5. Assess the influence of the fibrinogen γ' and α chain and their interactions with fibronectin.

2.7. References

[1] M. Mosesson, "Fibrinogen and fibrin structure and functions," *Journal of thrombosis and haemostasis,* vol. 3, pp. 1894-1904, 2005.

[2] J. W. Wiesel and R. I. Litvinov, "Fibrin formation, structure and properties," *Subcell Biochemistry,* vol. 82, pp. 405-456, 2017.

[3] M. Wasilewska, Z. Adamczyk and B. Jachimska, "Structure of fibrinogen in electrolyte solutions derived from dynamic light scattering (DLS) and viscosity measurements," *Langmuir,* vol. 25, pp. 3698-3704, 2009.

[4] Z. Adamczyk, B. Cichocki, M. Ekiel-Jezewska, A. Slowicka, E. Wajnryb and M. Wasilewska, "Fibrinogen conformations and charge in electrolyte solutions derived from DLS and dynamic viscosity measurements," *Journal of Colloid and Interface Science,* vol. 385, pp. 244-257, 2012.

[5] M. W. Mosesson, J. S. Finlayson and R. A. Umfleet, "Human Fibrinogen Heterogeneities: Identification of gamma chain variants," *Journal of Biological Chemistry,* vol. 247, pp. 5223-5227, 1972.

[6] D. W. Chung and E. W. Davie, "gamma and gamma-prime chains of human fibrinogen are produced by alternative mRNA processing," *Biochemistry,* vol. 23, pp. 4232-4236, 1984.

[7] S. Kattula, J. Byrnes and A. Wolberg, "Fibrinogen and fibrin in hemostasis and thrombosis," *Arterioscler Thromb Vasc Biol,* vol. 37, pp. 13-21, 2017.

[8] J. Calcaterra, K. E. Van Cott, S. P. Butler, G. C. Gil, M. Germano, H. A. Van Veen, K. Nelson, E. J. Forsberg, M. A. Carlson and W. H. Velander, "Recombinant Human Fibrinogen that produces thick fibrin fibers with increased wound adhesion and clot density," *Biomacromolecules,* vol. 14, pp. 169-178, 2013.

[9] E. A. Ismail, F. M. Fabian, O. Wang, Y. Lei, M. A. Carlson, W. H. Burgess and W. H. Velander, "The isolation of a plasma derived gamma/gamma-prime fibrinogen:fibronectin mixture that forms a novel polymeric matrix," *Process Biochemistry,* 2019.

[10] M. Dominguez, F. L. Macrae, C. Duval, H. R. McPherson, K. I. Bridge, R. A. Ajjan, V. C. Ridger, S. D. Connell, H. Phillippou and R. A. Ariens, "Thrombin and fibrinogen γ′ impact clot structure by marked effects on intrafibrillar structure and protofibril packing," *Blood,* vol. 127, pp. 487-495, 2016.

[11] M. W. Mosesson, "Fibrin polymerization and its regulatory role in hemostasis," *Journal of Laboratory and Clinical Medicine,* vol. 116, pp. 8-17, 1990.

[12] J. W. Weisel and R. I. Litvinov, "Mechanism of fibrin polymerization and clinical implications," *Blood,* vol. 121, pp. 1712-1719, 2013.

[13] R. F. Doolittle, "Fibrinogen adn Fibrin," *Annual Review Biochemistry,* vol. 53, pp. 195-229, 1984.

[14] P. A. McKee, P. Mattock and R. L. Hill, "Subunit structure of human fibrinogen, soluble fibrin and cross-linked insoluble fibrin," *PNAS,* vol. 66, pp. 738-744, 1970.

[15] L. Huang and S. T. Lord, "The isolation of fibrinogen monomer dramatically influences fibrin polymerization," *Thrombosis research,* vol. 131, pp. 258-263, 2013.

[16] U. Larson, B. Blomback and R. Rigler, "Fibrinogen and the early stages of polymerization to fibrin as studied by dynamic laser light scattering," *Biochimica et*

Biophysica acta, vol. 915, pp. 172-179, 1987.

[17] J. Collet, C. Nagawasmi, D. Farrell, G. Montalescot and J. Weisel, "Influence of gamma-prime fibrinogen splice variant of fibrin physical properties and fibrinolysis rate," *Arthroscleorosis thrombosis Vascular Biology,* vol. 24, pp. 382-386, 2004.

[18] M. W. Mosesson, J. S. Finlayson, R. A. Umfleet and D. Galanakis, "Human Fibrinogen Heterogeneities: Structural and related studies of plasma fibrinogens which are high solubility catabolic intermediates," *Journal of Biological Chemistry,* vol. 247, pp. 5210-5219, 1972.

[19] E. Katona, K. Penzes, A. Csapo, F. Fazakas, M. Udvardy, Z. Bagoly, Z. Z. Orosz and L. Muszbek, "Interactions of factor XIII subunits," *Thrombosis and Haemostasis,* vol. 123, pp. 1757 - 1763, 2014.

[20] I. Komaromi, Z. Bagoly and L. Muszbek, "Factor XIII: Novel Structural and Functional Aspects," *Journal of Thrombosis and Heamostasis,* no. 9, pp. 9-20, 2010.

[21] R. Ariens, T.-S. Lai, J. Weisel, C. S. Greenberg and P. Grant, "Role of factor XIII in fibrin clot formation and effects of genetic polymorphisms," *Blood,* vol. 100, pp. 743-754, 2002.

[22] E. L. Hethershaw, A. L. Cilia la Corte, A. M. Duval, P. J. Grant, R. A. Ariens and H. Philippou, "The effect of blood coagulation factor XIII on fibrin clor structure and fibrinolysis," *Journal of thrombosis and haemostasis,* vol. 12, pp. 197-205, 2013.

[23] L. Lorand and K. Konishi, "Activation of the fibrin stabilizing factor of plasma by thrombin," *Archives of Biochemistry and Biophysics,* vol. 105, pp. 58-67, 1964.

[24] L. Lorand, R. B. Credo and T. J. Janus, "Factor XIII (Fibrin-Stabilizing Factor)," *Methods in Enzymology,* vol. 80, pp. 333-341, 1981.

[25] L. Muszbek, V. C. Yee and Z. Hevessy, "Blood Coagulation Factor XIII: Structure and Function," *Thrombosis Research,* no. 94, pp. 271-305, 1999.

[26] K. A. Smith, R. J. Pease, C. Avery, J. Brown, P. Adamson, E. J. Cooke, S. Neergaard-Petersen, P. Cordell, R. A. Ariens, C. W. Fishwick, H. Philippou and P. J. Grant, "The activation peptide cleft exposed by thrombin cleavage of FXIII-A2 contains a recognition site for the fibrinogen alpha chain," *Thrombosis and Hemostasis,* vol. 121, pp. 2117-2126, 2013.

[27] T. Hornayk and J. Shafer, "Interactions of factor XIII with fibrin as substrate and cofactor," *Biochemistry,* vol. 31, pp. 423-429, 1992.

[28] L. Muszbek, Z. Bereczky, Z. Bagoly, I. Komaromi and E. Katona, "Factor XIII: A coagulation factor with multiple plasmatic and cellular functions," *Physiological Reviews,* vol. 91, pp. 931-972, 2011.

[29] Y. Wang, A. Reheman, C. M. Spring, J. Kalantari, A. H. Marshall, A. Wolberg, P. L. Gross, J. I. Weitz, M. L. Rand, D. F. Mosher, J. Freedman and H. Ni, "Plasma fibronectin supports hemostasis and regulates thrombosis," *The journal of clinical investigation,* vol. 124, pp. 4281-4293, 2014.

[30] M. W. Mosesson and D. L. Amrani, "The structural and biologic activities of plasma fibronectin," *Blood,* vol. 56, pp. 145-158, 1980.

[31] D. Romberger, "Molecules in focus: Fibronectin," *Journal of biochemistry Cell Biology,* vol. 29, pp. 939-943, 1997.

[32] W. S. To and K. S. Midwood, "Plasma and cellular fibronectin: distinct and independent funtions during tissue repair," *fibrinogenesis & tissue repair,* vol. 4, 2011.

[33] M. K. Magnusson and F. D. Mosher, "Fibronectin: Structure, assembly and cardiovascular implications," *Arteriosclerosis Thrombosis and Vascular Biology,* vol. 18, pp. 1363-1370, 1998.

[34] E. C. Williams, P. A. Janmey, J. D. Ferry and D. F. Mosher, "Conformational states of fibronectin: Effects of pH, Ionic strength, and collagen binding," *The journal of biological chemistry,* vol. 257, pp. 14973-14978, 1982.

[35] J. Pelta, H. Berry, G. C. Fadda, E. Pauthe and D. Lairez, "Statistical conformation of human plasma fibronectin," *Biochemistry,* vol. 39, pp. 5146-5154, 2000.

[36] Y. V. Matzuka, L. V. Medved, S. A. Brew and K. C. Ingham, "the NH2-terminal Fibrin-binding site of fibronectin is formed by interacting fourth and fifth finger domains," *Journal of Biological Chemistry,* vol. 269, pp. 9539-9546, 1994.

[37] A. Rostagno, M. J. Williams, M. Baron, I. D. Campbell and L. I. Gold, "Further characterization of the NH-2 terminal fibrin binsding site on fibronectin," *Journal of Biological Chemistry,* vol. 269, pp. 31938-31945, 1994.

[38] K. R. Siebenlist, D. A. Meh and M. W. Mosesson, "Plasma Factor XIII Binds Specifically to Fibrinogen Molecules Containing gamma prime chain," *Biochemistry,* no. 35, pp. 10448-10453, 1996.

[39] M. Moaddel, D. H. Farrell, M. A. Daugherty and M. G. Fried, "Interactions of human fibrinogens with factor XIII: roles of calcium and the g' peptide," *Biochemistry,* vol. 39, pp. 6698-6705, 2000.

[40] S. I. Chung and J. E. Folk, "Kinetic studies with transglutaminases," *The Journal of Biological Chemistry,* vol. 247, pp. 2798-2807, 1972.

[41] T. J. Hornyak and J. A. Shafer, "Interaction of factor XIII with Fibrin as Substrate and Cofactor," *Biochemistry,* vol. 31, pp. 423-429, 1992.

[42] J. R. Byrnes, C. Wilson, A. M. Boutelle, C. B. Brandner, M. J. Flick, H. Philippou and A. S. Wolberg, "The interaction between fibrinogen and zymogen FXIIIA2B2 is mediated by fibrinogen residues gamma390-396 and FXIII-B subunits," *Thrombosis and hemostasis,* vol. 128, pp. 1969-1978, 2016.

[43] K. A. Smith, P. J. Adamson, R. J. Pease, J. M. Brown, A. J. Balmforth, P. A. Cordell, R. A. Ariens, H. Philippou and P. J. Grant, "Interactions between factor XIII and the Alpha-C region of fibrinogen," *Thrombosis and Hemostasis,* vol. 117, pp. 3460-3468, 2011.

[44] C. S. Greenberg and M. A. Shuman, "The zymogen forms of blood coagulation factor XIII bind specifically to fibrinogen," *The Journal of Biological Chemistry,* vol. 257, pp. 6096-6101, 1982.

[45] S. D. Lewis, T. J. Janus, L. Lorand and J. A. Shafer, "Regulation of formation of Factor XIIIa by its Fibrin Substrates," *Biochemistry,* vol. 24, pp. 6772-6777, 1985.

[46] J. T. Janus, D. S. Lewis, L. Lorand and A. J. Shafer, "Promotion of thrombin-catalyzed activation of factor XIII by fibrinogen," *Biochemistry,* vol. 22, pp. 6269-6272, 1983.

[47] C. G. Curtis, J. T. Janus, B. R. Credo and L. Lorand, "Regulation of factor XIIIa generation by fibrinogen," *Annals New York Academy of Science,* vol. 83, pp. 567-576, 1983.

[48] C. S. Greenberg, K. E. Achyuthan and J. W. Fenton II, "Factor XIIIa formation promoted by complexing of alpha-thrombin, Fibrin, and plasma factor XIII," *Blood,*

vol. 69, pp. 867-871, 1987.

[49] C. S. Greenberg, K. E. Achyuthan, S. Rajagopalan and S. V. Pizzo, "Characterization of the fibrin polymer structure that accelerates thrombin cleavage of plasma factor XIII," *Archives of Biochemistry and Biophysics,* vol. 262, pp. 142-148, 1988.

[50] B. R. Credo, G. C. Curtis and L. Lorand, "Alpha-chain domain of fibrinogen controls gneration of fibrinoligase (coagulation factor XIIIa) Calcium Ion regulatory aspects," *Biochemistry,* vol. 20, pp. 3770-3778, 1981.

[51] M. Moaddel, L. A. Falls and D. H. Farrell, "The role of gammaA/gamma' firbrinogen in plasma factor XIII activation," *The Journal of Biological Chemistry,* vol. 275, pp. 32135-32140, 2000.

[52] N. E. Stathakis, M. W. Mosesson, A. B. Chen and D. k. Galanakis, "Cryoprecipitation of fibrin-fibrinogen complexes induced by the cols-insoluble globulin of plasma," *Blood,* vol. 51, pp. 1211-1222, 1978.

[53] E. Makogonenko, G. Tsuruoa, K. Ingham and L. Medved, "Interaction of fibrin(ogen) with fibronectin: further characterization and localization of the fibronectin-binding site," *Biochemistry,* vol. 41, pp. 7907-7913, 2002.

[54] K. A. Smith, P. J. Adamson, R. J. Pease, J. M. Brown, A. J. Balmforth, P. A. Cordell, R. A. S. Ariens, H. Philippou and P. J. Grant, "Interactions between factor XIII and the alpha C region of fibrinogen," *Thrombosis and Hemostasis,* vol. 10, pp. 3460-3468, 2010.

[55] J. R. Byrnes, C. Wilson, A. M. Boutelle, C. B. Brandner, M. J. Flick, H. Philippou and A. S. Wolberg, "The interaction between fibrinogen and zymogen FXIII-A2B2 is mediated by fibrinogen residues g390-396 and the FXIII-B subunits," *Blood,* vol. 128, pp. 1969-1978, 2016.

CHAPTER III

Interactions with γγ and γγ' Recombinant Fibrinogen: Tetrameric Plasma factor XIII and Recombinant Monomeric Factor XIII Binding

3.1.Summary and Background.

Past reports describing the binding of tetrameric plasma derived plasma factor XIII ($pFXIIIA_2B_2$) to γγ'pF1 used the coincidentally eluting anion chromatographic fractions of these two proteins as evidence of the complexation. [1] $pFXIIIA_2B_2$ normally occurs in plasma at about only 3-4 ug/ml (about 0.07 um) while γγ'pF1 occurs in plasma circulation at only 300 ug/ml (at about 9 uM). These studies estimated that $pFXIIIA_2B_2$ binds about 1 out every 100 γγ'rF1 and thus the ratio of cross-linking enzyme to fibrin substrate is typical of enzyme catalyzed reaction masses. [2, 3] The complexation with γγ'pF1 serves to target the delivery of FXIII zymogen to the wound where fibrin polymer must be cross-linked by activated FXIII that decomplexes from the γγ'pF1 after thrombin activation. [4, 5, 6]

The future medical uses of this unique and abundant source of recombinant human fibrinogen and the recombinant FXIII made by Pichia Pastoris would logically benefit from a full characterization of their behavior together relative to that of pF1 and $pFXIIIA_2B_2$. The post-translational character of the γγ'rF1 contains less sulfation of the tyrosines contained in the carboxy terminal end of the γ' chain. [7] The monomeric recombinant A subunit factor XIII ($rFXIIIA_1$) studied here has a contrasting absence of the B domain subunits to that occurring in pFXIII. In this chapter we characterize the

binding of $pFXIIIA_2B_2$ and also monomeric recombinant Factor XIII (γγ'rF1) to γγpF1 and γγ'pF1 and also γγrF1 and γγ'rF. We use a combination of anion exchange and HPSEC chromatographic fractionation techniques along with dynamic light scattering (DLS) of the fractionated samples. In contrast to the 10:1 presence of γγpF1 and γγ'pF1 in plasma, we also evaluated γγrF1 and γγ'rF1 which are both expressed at about 2 g/l in the milk of transgenic cows. We have also made $rFXIIIA_1$ in Pichia and find it a useful component in the recombinant fibrin surgical sealant formulations we have studied.

HPSEC was shown to resolve $pXIIIA_2B_2$ from γγ'pF1 and also from γγ'rF1 as well as $pXIIIA_2B_2$ from γγpF1 and also from γγrF1. The binding of $pXIIIA_2B_2$ to γγ'pF1 was indicated by a single peak eluted from a mixture made of $pFXIIIA_2B_2$ and γγ'pF1. This contrasted separate peaks eluting from a mixture made of $pXIIIA_2B_2$ and γγpF1 that showed no significant binding behavior. The presence of functional $pFXIIIA_2B_2$ zymogen was tracked by transglutaminase activity assay that we have adapted from past reported studies. Transglutaminase activity assessment of the above chromatography product eluates showed that the majority of $pFXIIIA_2B_2$ activity did not form an association with the γγpF1. However, the mixture made of $pFXIIIA_2B_2$ and γγ'pF1 showed transglutaminase activity superimposed with the single peak containing γγ'pF1 that was eluted by HPSEC processing of that mixture.

A similar behavior was observed when mixing $pFXIIIA_2B_2$ with γγ'rF1. Of particular significance was that γγ'rF1 and γγrF1 which are both recombinantly produced and therefore contain no $pFXIIIA_2B_2$. Thus, a mixture of $pFXIIIA_2B_2$ together with γγ'rF1 and γγrF1 enabled the study of $pFXIIIA_2B_2$ avidity for γγ'rF1 that was without

background $pFXIIIA_2B_2$ activity. For example, the study of an association of transglutaminase activity specifically with γγ'rF1 was done when a mixture of $pFXIIIA_2B_2$ together with γγ'rF1 and γγrF1 was followed by the resolution of the γγ'rF1 by processing the mixture by DEAE chromatography. The DEAE chromatography resolved γγ'rF1 from γγ'rF1 where the activity assay indicated that the majority of the $pFXIIIA_2B_2$ that was added to the mixture co-eluted as a coincidental peak along with the γγ'rF1. The role of B domain in γ' chain binding of the heterodimeric γγ'pF1 as reported in previous studies was also investigated using $rFXIIIA_1$. In contrast to γγ'pF1 studies using $pFXIIIA_2B_2$, neither γγrF1 or γγ'rF1 were observed to associate with $rFXIIIA_1$ when evaluated by HPSEC. Thus, the absence of the B domain in $rFXIIIA_1$ is consistent with the lack of binding with γγ'rF1 by $rFXIIIA_1$ as observed in our HPSEC studies.

3.2.Introduction

Plasma factor XIII ($pFXIIIA_2B_2$) is a member of the transglutaminase enzyme family that circulates in plasma as a hetero-tetrameric protein conformed of 2A and 2B sub-units which act as the enzymatic and carrier peptide respectively. [8, 9, 4, 10] The A subunit is a single polypeptide chain consisting of 731 amino acids with a molecular mass of 83kDa and it is composed of two β barrels, a β sandwich, the catalytic core peptide and the activation peptide residue at the N-terminal that is removed upon thrombin activation. [11, 2, 6, 12] The B subunit consists of 641 amino acids organized in 10 tandem repeats termed sushi domains which prolong the lifespan of the catalytic subunit. [13, 14, 10] The activation of $pFXIIIA_2B_2$ occurs in two sequential steps. First, thrombin cleaves an activation peptide from the N-terminal in the A subunit. Then, the dimeric dissociation

from the B subunit takes place on the presence of calcium giving rise to the dimeric structure of activated factor XIII ($pFXIIIA_2$*) which stabilize the nascent fibrin matrix in the early stages of blood clot formation. [15, 16, 17, 18]

The interaction between fibrinogen and $pFXIIIA_2B_2$ has been largely studied. [3, 19, 1, 20, 21, 22, 4] Greenberg and Shuman showed specific $pFXIIIA_2B_2$ binding to fibrinogen by the A_2 subunit suggesting that $pFXIIIA_2B_2$ circulates in plasma bound to fibrinogen. Hornyak and Shafer studied the non-active $pFXIIIA_2B_2$ and platelet $FXIIIA_2$ binding to fibrin. [19] They indicated that the binding of platelet $FXIIIA_2$ was weaker than the zymogen $pFXIIIA_2B_2$. Additional studies focused on the identification of the fibrinogen binding site for $pFXIIIA_2B_2$, indicated that the fibrinogen γ' peptide chain is responsible for the interaction with $pFXIIIA_2B_2$ via the B subunit. [1]Smith et al. used surface plasmon resonance to show that the $pFXIIIA_2B_2$ binds to the αC region of fibrinogen [20]. In a recent study, Byrnes et al. identified the fibrinogen γ chain residues 390-396 as the primary binding residues for $pFXIIIA_2B_2$ via the B subunit. Based on these findings, Byrnes suggested that the interaction of $pFXIIIA_2B_2$-fibrinogen occurs in a 1:1 stoichiometric which differs from the 1:2 $pFXIIIA_2B_2$:fibrinogen proposed by Moadel. [21] In either case, binding of $pFXIIIA_2B_2$ to the α, γ or γ' chains generates physical and conformational changes on the fibrinogen structure.

Physical studies characterized fibrinogen as a straight rod shaped molecule with an over-all length of 47.5±2.5 nmand a hydrodynamic radius (R_H) ranging from 10nm to 18nm determined by dynamic light scattering (DLS) under physiological conditions. [23, 24, 25] Huang and Lord identified fibrinogen species of high molecular weight with a R_H

from 11nm to 200nm. [26] However the isolation of fibrinogen monomers via size exclusion chromatography showed a R_H of 10±0.1nm which is consistent with previous findings. Further studies on the fibrinogen polymerization showed large fluctuations on the fibrinogen diffusion constant due to conformational changes after enzymatic activation [27, 28, 6] which can be interpreted as the increase of the R_H. Same results were observed by Ping et al. during the polymerization of fibrinogen monomers. A rapid increase on the R_H was detected after the enzymatic thrombin activation. [29] Here, we assess the conformational changes arising from the interaction between the non-activated zymogen $pFXIIIA_2B_2$ and the two major variants of a recombinant fibrinogen (rF1), γγ and γγ', produced in milk of transgenic cows. [30] Furthermore, we used high performance size exclusion chromatography (HPSEC) to isolate complexed molecules formed by either $pFXIIIA_2B_2$:γγrF1 or $pFXIIIA_2B_2$:γγ'rF1. A second pass of the concentrated fractions was performed in order to confirm the existence of a single complexed molecule. Our HPSEC results confirmed the high affinity of the $pFXIIIA_2B_2$ towards γγ'rF1. Meanwhile, An increased on the R_H and the polydispersity percentage suggests the formation of complexed molecules when $pFXIIIA_2B_2$:γγ'rF1 is evaluated by DLS. These findings contribute to resolve the apparent contradictions in the role of the γ' chain in the interaction with the $pFXIIIA_2B_2$ and provide new insights into the complex $pFXIIIA_2B_2$:γγ'rF1 conformational rearrangements.

3.3. Materials and Methods

3.3.1. **Materials.** All reagents were purchased form Fisher-Scientific unless otherwise stated. Recombinant activated thrombin (20000 units) was purchased from

Zymogenetics (WA). 1000U/mL aliquots were prepared in 0.9% NaCl and stored at -80 ^{0}C until use. Human plasma factor XIII, (pFXIIIA_2B_2) containing a specific crosslink activity of 2650 Loewy units/mg was purchased from Enzyme Research Laboratories (IN). FPR-chloromethylketone (PPACK) was purchased form Haematologic Technologies Inc. VT.

3.3.2. **Recombinant factor XIII.** Monomeric recombinant factor XIII (rFXIIIA) was intracellular expressed in the yeast Pichia pastoris X-33 as previously described [31]. rFXIIIA was purified in a His-Bind® nickel charged resin column. rFXIII specific activity was estimated to be 153 PEU/mg using a peptide incorporation assay.

3.3.3. Recombinant fibrinogen.(rF1). The human recombinant fibrinogen was expressed in the milk of transgenic dairy cows and purified by a two-column purification procedure using cation exchange (CIEX) and hydrophobic interaction chromatography (HIC). [7, 1]

3.3.4. Anion Exchange Chromatography. Purified rF1 was loaded to the weak anion exchange DEAE Sepharose™ Fast Flow column to isolate γγ and γγ' species by pH gradient as previously described. [1] After γγ and γγ' were isolated, 1:9 molar ratio γγ': γγ rF1 were mixed with pFXIII to a final molar ratio 1:10 pFXIII: total rF1. The mixture was loaded onto a DEAE sepharose equilibrated with 50nm Sodium Citrate, 150mM NaCl, pH7.4. Gradient elution was performed increasing salt concentration. Collected fractions were pooled and concentrated down to determine the pFXIII activity using peptide incorporation assay.

3.3.5. High Pressure Size Exclusion Chromatography (HPSEC). Mixtures of factor XIII and fibrinogen (γγ or γγ') were prepared in 50mM Tris buffer, 115 mM NaCl, pH 7.5 maintaining ionic strength of 0.15. The mixtures were incubated for 1 hour at 37°C and 200µg of the mixture were loaded into two superose 6 10/300 (GE lifescience) columns connected in series to a Knauer (Berlin, Germany) Smartline chromatography station. The columns were isocratically eluted using Tris Buffer at a flow rate of 0.35 mL/min and the length of the run was 90 minutes for all the samples. Effluent's absorbance was read at 280nm and collected fractions were assayed for Factor XIII activity, SDS-Page, and particle size distribution using a Dynamic Light Scattering instrument.

3.3.6. SDS PAGE gel electrophoresis. Non-reduced and reduced samples of pFXIII, γγ and γγ'rF and their mixtures were evaluated by sodium dodecylsulfate polyacrylamide gel electrophoresis (SDS-PAGE) on 4-12% NuPage Bis-Tris pre-cast gels (Thermofisher, CA). All the gels ran for 1 hour at 200 volts and then stained with colloidal Blue gel stain (Invitrogen, CA, USA).

3.3.7. Factor XIII Biotinamino-pentylamine incorporation activity assay. The factor XIII mediated incorporation of Biotinamino-pentylamine to γγ or γγ' rF1 was determined using the 5 Biotionamido-pentylamine assay. [20] In brief, 100 µL of 40µg/mL of γγ or γγ'rF1 were poured into each well of a 96 high binding microtiter plate. Then plates were incubated for 1 hour at 37°C. Blocking buffer (1%BSA in TBS) was added to the wells and incubated overnight at room temperature. The adsorbed fibrinogen was converted to fibrin monomers by adding 100µL of 1.11 NIH U/mL rFIIa. Then, 50µL of crosslink substrate mix

(0.25mM 5bapa, 0.1mM DTT and 1.1 mM $CaCl_2$) was added to each well and incubated for 10 minutes at room temperature. Thereafter, 50µL of activated $pFXIIIA_2$* or rFXIIIA* was added to each well and the plate was incubated for 30 minutes at room temperature. 200µL of 200mM EDTA were added to each well to quench transglutaminase reaction. 100µL of 2.0 µg/mL Streptavidin alkaline phosphatase solution was added to each well and incubated at 37^0C for 1 hour. After incubation, plates were washed and 100µL of para-nitrophenyl phosphate (p-NPP) dissolved in 1M Diethanoalamine was added to the wells. The color developing (clear to yellow) indicated the phosphatase activity on the p-NPP substrate. Finally, the reaction was stopped by adding 200µL of 4N NaOH after 2 minutes reaction. The plates were read at 405nm using Beckman Coulter AD340 plate reader. The results were expressed in units of optical density.

3.3.8. Dynamic Light Scattering. The hydrodynamic radius (R_h) and particle size distribution were estimated by dynamic light scattering using the DynaPro99 Titan Instrument (Wyatt Technology, CA). In Brief, 20µL of samples containing either rγγF1 or rγγ'F1 or in mixture with pFXIII were illuminated by a 830nm laser and the intensity of light scattered was measured by an avalanche photodiode. The fluctuations in the measured intensity specify the diffusion coefficient which is estimated by autocorrelation analysis. Finally, the particle hydrodynamic radius is determined by using the Stroke-Einsten relationship which assumes the uniform sphere shape of the analyzed particle. Isolated samples of rγγF1, rγγ'F1, pFXIII and their combinations were prepared and

analyzed at different concentrations ranging from 0.5 to 2.5 mg/mL. The buffer ionic strength was controlled by adding NaCl from 0.15.

3.4. Results

3.4.1. **γγ/γγ'rF1 isolation**. Purified rF1 was loaded into DEAE fast flow sepharose column and eluted by linear salt gradient. [1] Two peaks were observed in the chromatogram and further SDS-PAGE peak analysis indicates that the first and the second peak correspond to the γγrF1 and γγ'rF1species respectively. Figure 2.1 shows the chromatogram profile for the γγ and γγ' rF1 isolation.

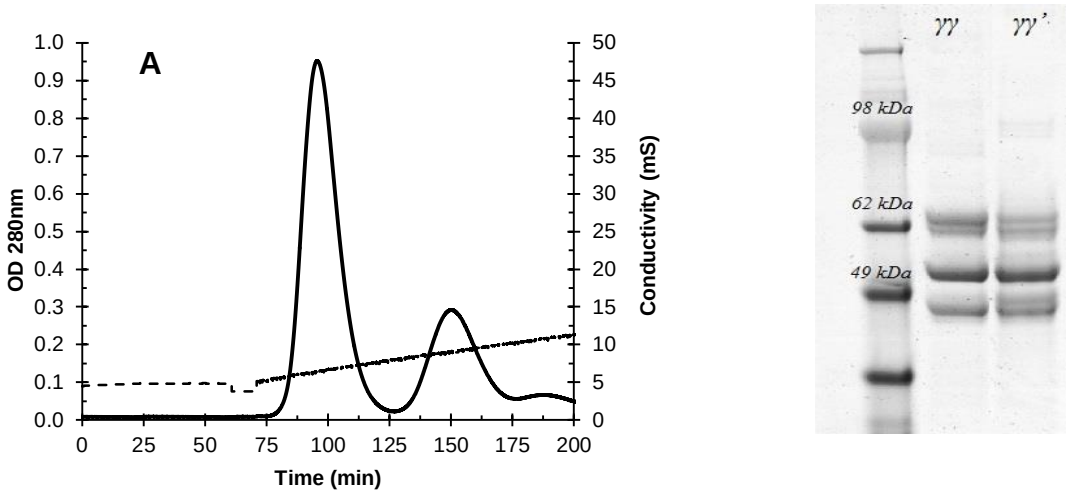

Figure 3.1: DEAE-Sepharose chromatography of γγ and γγ' rF1 isolation.

3.4.2. **HPSEC pFXIII- γγ/γγ'rF1 interaction.** In order to understand the interactions of pFXIII and fibrinogen species γγ and γγ', free factor XIII recombinant γγ and γγ' fibrinogen were mixed with pFXIII and evaluated by high pressure size exclusion chromatography. Figure 2.1 shows the HPSEC γγ rF1 and pFXIII chromatograms profile. In these experiments, γγ rF1 and pFXIII eluted as a

single peak at minute 61.2 and 68.9 respectively (figure 2.1 panel A). When pFXIII and γγ rF1 were mixed in a 1:10 molar ratio, two peaks were eluted as presented in panel B. The eluate was collected in 3 fractions (1,2,3) and analyzed by non-reduced SDS-PAGE (panel C). It is observed that fraction 1 which corresponds to the first peak is mainly composed of γγ rF1 without any observable pFXIII. However, some pFXIII can be observed in Fraction 2 which corresponds to the intersection of peak 1 and peak 2. Fraction 3 is composed mostly of pFXIII and corresponds to the second peak in the chromatogram (panel B). To evaluate if the collected fractions correspond to a single complexed molecule, fractions 1, 2 and 3 were reloaded to the HPSEC and evaluated it as indicated in the methods section. The chromatogram profiles along with their corresponding SDS-PAGE gels are presented in panels D to I. In panel D, fraction 1 eluted as a sharped peak followed by a long tail which may indicate the presence of some of small quantity of complexed γγrF1:pFXII molecules. However, No visible pdFXIII is observed in the SDS-PAGE gel (panel E). Panel F represents the chromatogram profile for fraction 2. Two consecutive peaks centered at minute 61 and minute 68 were observed in the chromatogram. The SDS-PAGE demonstrates that the main peak is mainly composed of γγ rF1 meanwhile pFXIII is the main component of the small peak centered at minute 68. This result proves that fraction 2 in panel C is not composed of a single complexed molecule but represents the intersection of γγ rF1 tail and the front head of pFXIII. Finally, fraction 3 which corresponds to the second peak in panel B was reloaded into the HPSEC system. Panel H represents the elution profile of

fraction 3 and panel I its corresponding SDS PAGE. The chromatogram shows the formation of a single peak which is mainly composed of pFXIII with no observable γγ rF1 as indicated by the SDS-PAGE.

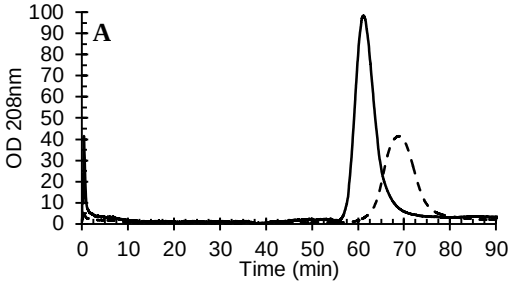

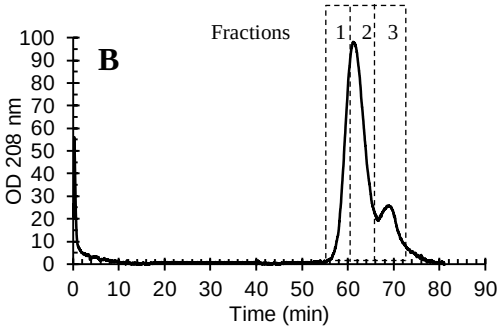

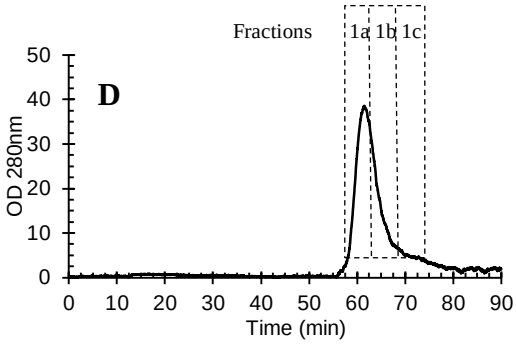

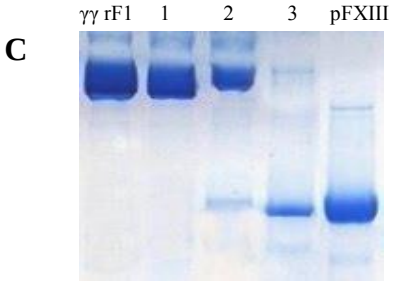

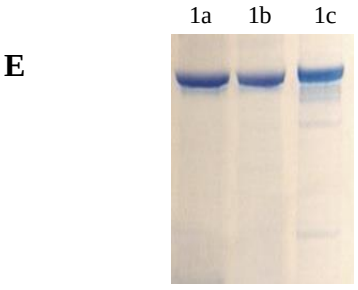

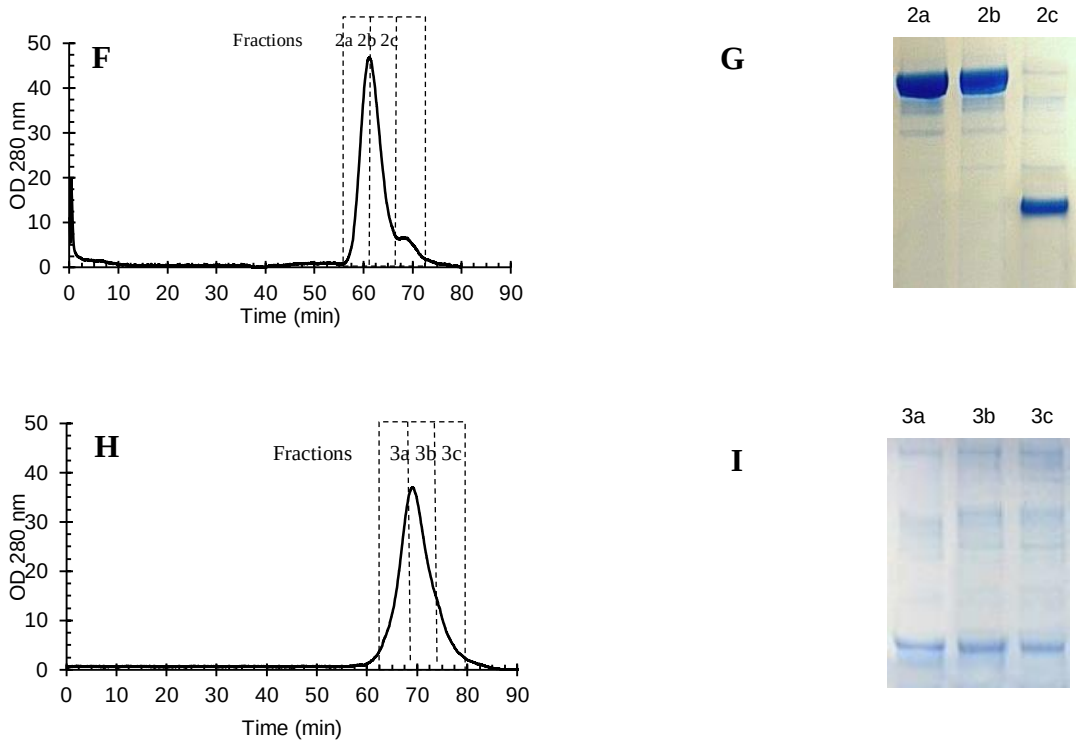

Figure 3.2: High Pressure Size Exclusion, **Panel A**: γγ rF1 (solid line), pFXIII (dashed line), **Panel B**: γγ rF1 with pFXIII (10:1 mass ratio). **Panel C:** Non-reduced SDS-PAGE γγ rF1-pFXIII mixture. Lane 1: γγ rF1, Lane 2: Fraction 1, Lane 3: Fraction 2, Lane 4: Fraction 3, Lane 5: pFXIII. **Panel D**: HPSEC fraction 1 **Panel E:** Non-reduced SDS-PAGE fraction 1 γγ rF1-pFXIII mixture. Lane 1: fraction 1a, Lane 2: fraction 1b, Lane 3: fraction 1c, **Panel F**: HPSEC fraction 2 **Panel G:** Non-reduced SDS-PAGE fraction 2 γγ rF1-pFXIII mixture. Lane 1: fraction 2a, Lane 2: fraction 2b, Lane 3: fraction 2c, **Panel H**: HPSEC fraction 3 **Panel I:** Non-reduced SDS-PAGE fraction 3 γγ rF1-pFXIII mixture. Lane 1: fraction 3a, Lane 2: fraction 3b, Lane 3: fraction 3c.

When γγ'rF1 and pFXIII were mixed and loaded into a HPSEC system, a peak centered at minute 60.74 and shoulder protruding at minute 65 can be observed in the

chromatogram profile presented in figure 2.2 panel B. The displacement in the normal elution of pFXIII showed in panel A may indicate an intrinsic interaction between γγ'rF1 and pFXIII. To prove this reasoning, the eluted fractions 1,2 and 3 were collected and analyzed in a non-denatured SDS-PAGE. From the gel presented in panel C, It can be observed that all the fractions contained pFXIII. To identified if those fraction form a single complexed molecule, all the fractions were reloaded to the HPSEC system. Fraction 1 elutes as a single peak centered at minute 60.7 which prove the existence of a single complexed molecule. The analyzed fractions, 1a, 1b and 1c, indicates the interaction of γγ'rF1 and pFXIII. When fraction 2 was reloaded to the HPSEC system, a main peak centered at minute 60.8 and a shoulder protruding around minute 65 was observed in the chromatogram profile (panel F). The collected fractions were analyzed by SDS-PAGE and presented in panel G. It is observed that pFXIII is presented in all fractions (b1,b2 and b3). We can state that the observed shoulder in the chromatogram profile may indicated the saturation of γγ'rF1 and a residual pFXIII separates from the main peak. When fraction 3 was reloaded to the HPSEC a main peak centered at minute 69 with a shoulder protruding at the leading edge (panel H). The SDS-PAGE shows the conformation of a complexed molecule in the leading edges fractions meanwhile the trailing edge.

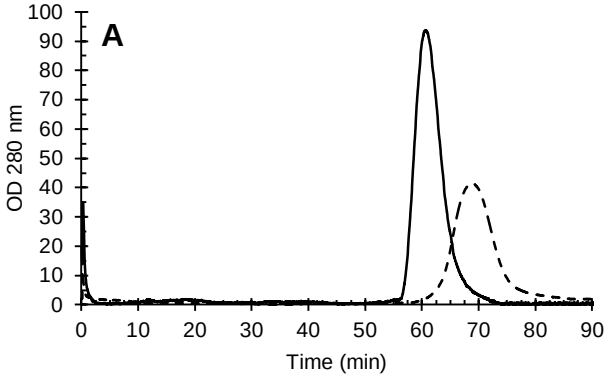
A
OD 280 nm
Time (min)

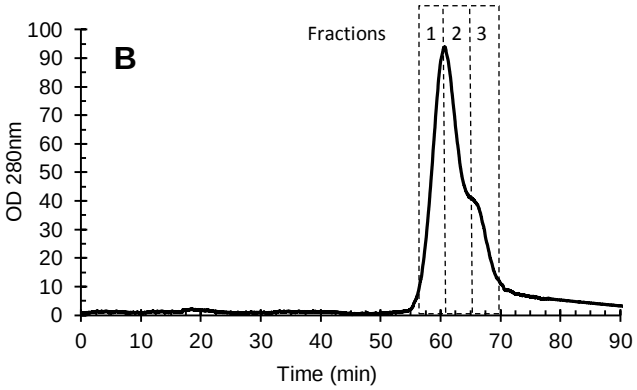
B
Fractions
1 2 3
OD 280nm
Time (min)

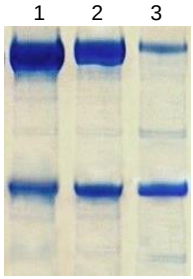
1
2
3

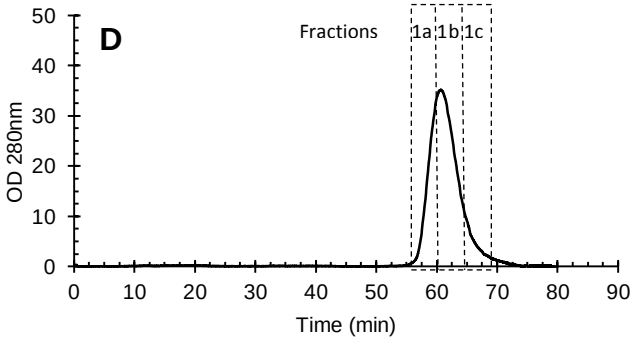
D
Fractions
1a 1b 1c
OD 280nm
Time (min)

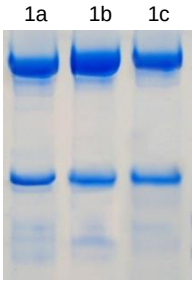
1a
1b
1c

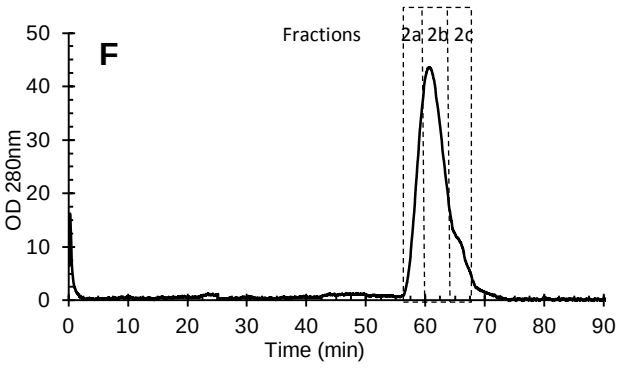
F
Fractions
2a 2b 2c
OD 280nm
Time (min)

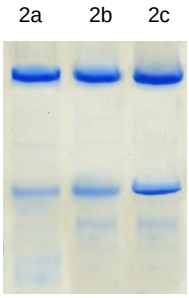
2a
2b
2c

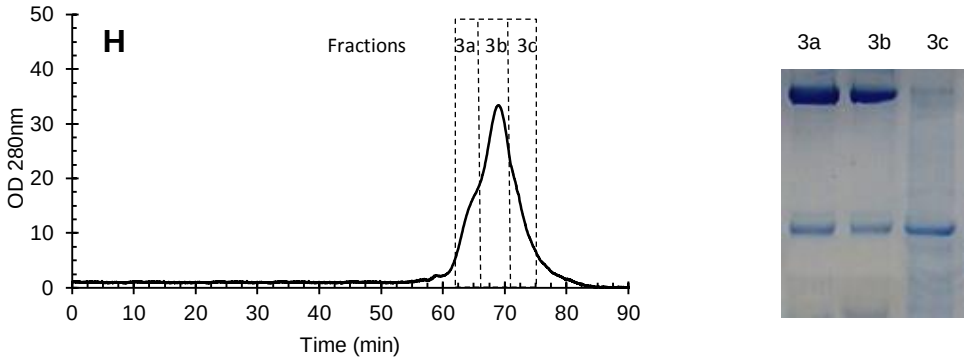

Figure 3.3: High Pressure Size Exclusion, **Panel A**: γγ' rF1 (solid line), pFXIII (dashed line), **Panel B**: γγ' rF1 with pFXIII (10:1 mass ratio). **Panel C:** Non-reduced SDS-PAGE γγ' rF1-pFXIII mixture. Lane 1: Fraction 1, Lane 2: Fraction 2, Lane 3: Fraction 3, **Panel D**: HPSEC fraction 1 **Panel E:** Non-reduced SDS-PAGE fraction 1 γγ'rF1-pFXIII mixture. Lane 1: fraction 1a, Lane 2: fraction 1b, Lane 3: fraction 1c, **Panel F**: HPSEC fraction 2 **Panel G:** Non-reduced SDS-PAGE fraction 2 γγ'rF1-pFXIII mixture. Lane 1: fraction 2a, Lane 2: fraction 2b, Lane 3: fraction 2c, **Panel H**: HPSEC fraction 3 **Panel I:** Non-reduced SDS-PAGE fraction 3 γγ'rF1-pFXIII mixture. Lane 1: fraction 3a, Lane 2: fraction 3b, Lane 3: fraction 3c.

3.4.3. **Peptide incorporation assay.** The interactions between pFXIII and γγrF1 and γγ'rF1 were also investigated by the peptide incorporation assay. Figure 2.3 shows the pFXIII activity in the collected fractions for the mixture γγrF1-pFXIII. Panel A shows that pFXIII activity is mostly localized in the HPSEC second peak that match the elution time for the pFXIII. The collected fractions 1, 2 and 3 were reloaded to the HPSEC system and the results presented in panel B, C and D. In panel B which corresponds to fraction 1, low levels of pFXIII activity is detected.

This low level of pFXIII activity indicates that pFXIII has a limited affinity for γγrF1. The Fraction 2 elution chromatogram presented in panel C shows maximum level of pFXIII activity in the second peak. This result confirmed that the γγrF1:pFXIII doesn't form a complexed molecule instead most of the remaining pFXIII eluted along with γγrF1 during the first pass (fraction 2) is removed from the main peak and forms a protuberance that displays the no interaction. Panel D, mostly formed of the second peak in panel A, contains high level of pFXIII activity in all the collected fractions. The high level of pFXIII activity in this fraction indicates that most of the pFXIII is contained in this region. Even though some traces of pFXIII activity can be detected in previous HPSEC fractions this is not an indication of the formation of single complexed molecule but because of the closeness in the elution of γγrF1 and pFXIII some pFXIII are captured in the same collected fraction and apparently forming a single complexed molecule.

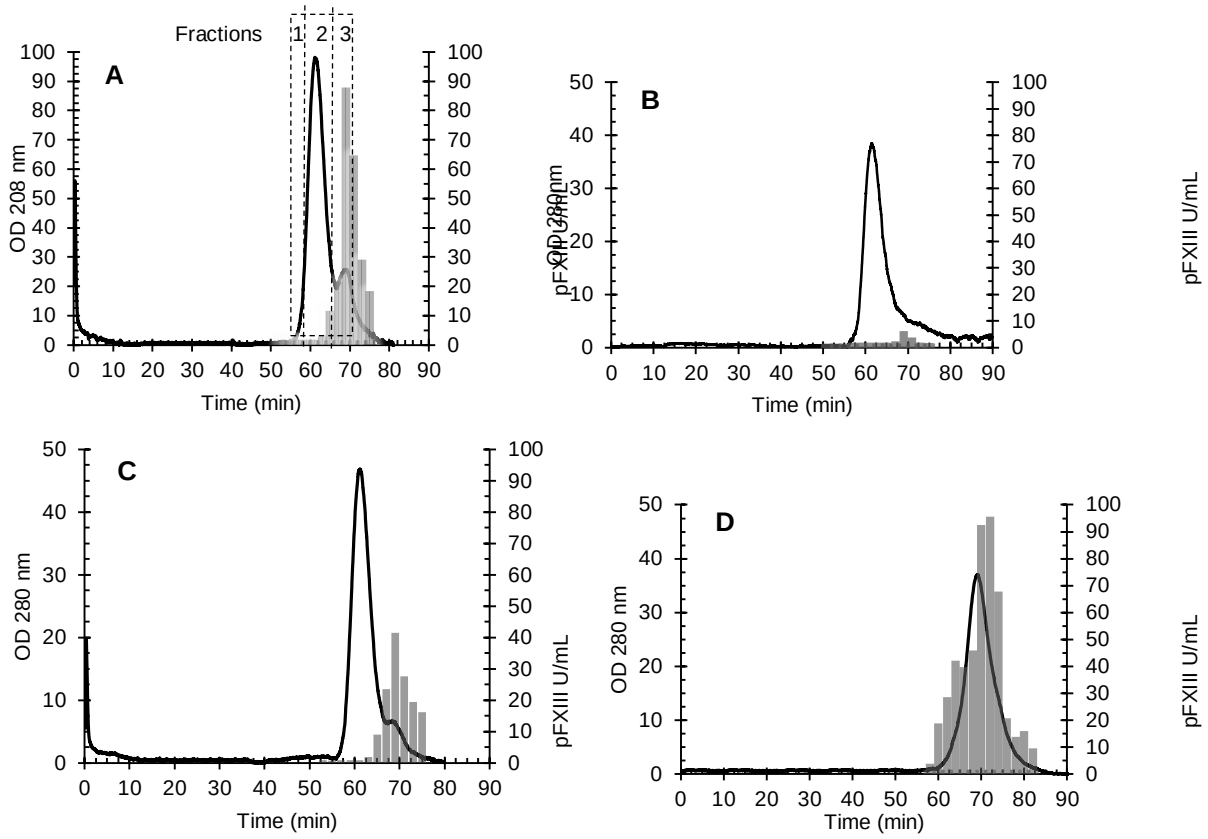

Figure 3.4: HPSEC and pFXIII activity (solid bars). Panel A: γγrF1 with pdFXIII (10:1 molar ratio), Panel B: Fraction 1 HPSEC (second pass). Panel C: Fraction 2 HPSEC (second pass). Panel D: Fraction 3 (second pass). pFXIII activity estimated by peptide incorporation assay.

In other hand, when γγ'rF1 is mixed with pFXIII, measureable levels of pFXIII are localized in throughout the chromatogram peak presented in panel A figure 2.4. Highest activity can be observed towards the center of the peak (875 U/mL). The collected factions were reloaded to the HPSEC system and the individual chromatograms presented in panel B, C, and D. Panel B is conformed of a single peak with pFXIII activity present in all the collected fractions. Same results are observed for fractions 2 and 3 which are presented in panel C and D. As expected, these results presented in panel

A, B and C confirm the formation of a single complexed molecule which is mainly biased by the presence of the γ' chain in the rF1.

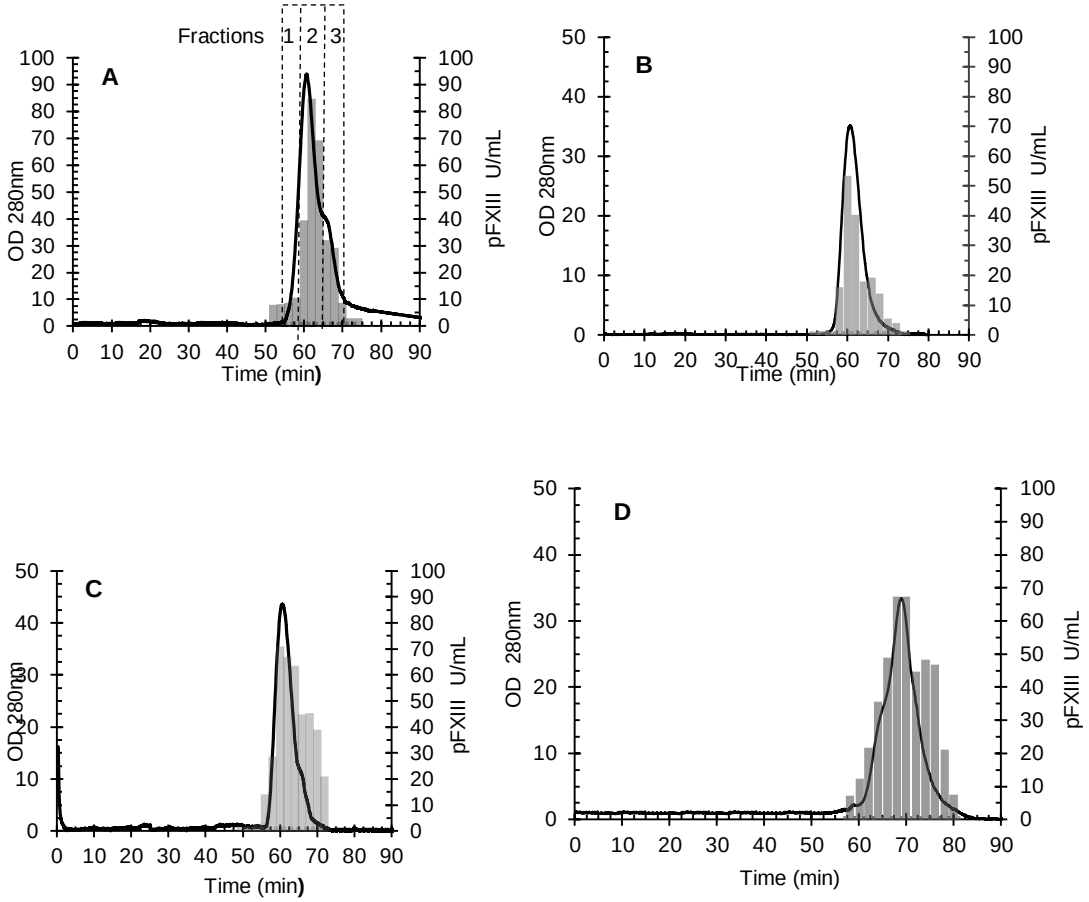

Figure 3.5: HPSEC and pFXIII activity (solid bars). Panel A: γγrF1 with pdFXIII (10:1 molar ratio), Panel B: Fraction 1 HPSEC (second pass). Panel C: Fraction 2 HPSEC (second pass). Panel D: Fraction 3 (second pass). pFXIII activity estimated by peptide incorporation assay.

3.4.4. **HPSEC rFXIIIA: γγ and γγ' rF1 interactions.** In order to further explore the nature of the interactions between the γγ'rF1 and pFXIII, we mixed rFXIIIA with either γγ rF1 or γγ'rF1. The mixture was incubated for 1 hour at 37°C and the

elution chromatograms profile presented in figure 2.5. The standard elution profile for γγ rF1 and rFXIIIA are presented in panel A. Panel B represents the chromatogram profile for the γγ rF1 and pFXIII mixture. Two peaks were observed in the eluate which indicates the existence of two distinct and immiscible molecules that match exactly the elution time for the individual γγ rF1 and rFXIIIA. Same result was observed when γγ'rF1 and rFXIIIA were mixed and incubated for 1 hour at 37°C (panel D).

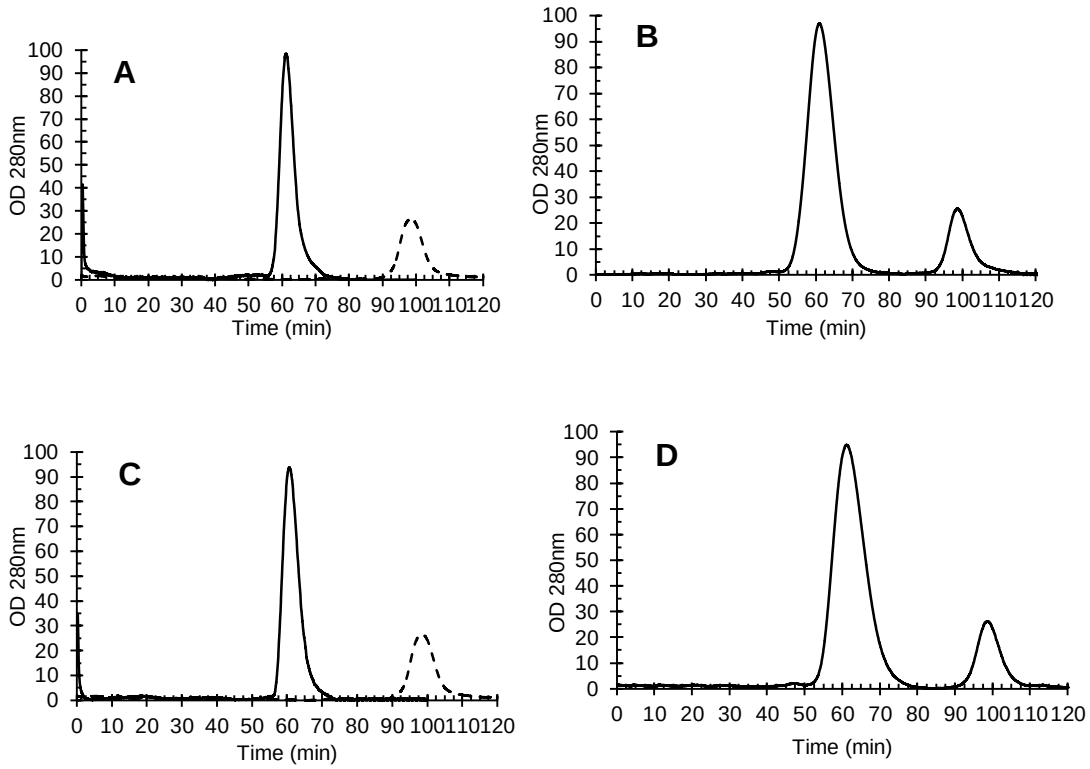

Figure 3.6: HPSEC, Panel A: γγrF1 (solid line), rFXIIIA (dashed line), Panel B: γγrF1 with rFXIIIA (10:1 molar ratio), panel C: γγ'rF1 (solid line), rFXIIIA (dashed line). Panel D: γγ'rF1 with rFXIIIA (10:1 molar ratio).

3.4.5. **DEAE γγrF1/γγ'rF1 pFXIII reconstitution.** A mixture of rF1 (γγ/γγ' 10:1) and pFXIII was loaded onto a DEAE sepharose and eluted as described in the methodology section. The elution chromatogram is presented in figure 2.7. Panel A shows the elution profile of the mixture pFXIII:rF1 (1:10). As expected, during the salt gradient profile elution two peaks were eluted resembling the γγ/γγ' isolation of rF1. The pdFXIII added was contained on the second peak showing the grater affinity of pFXIII towards the acidic γ' residue.

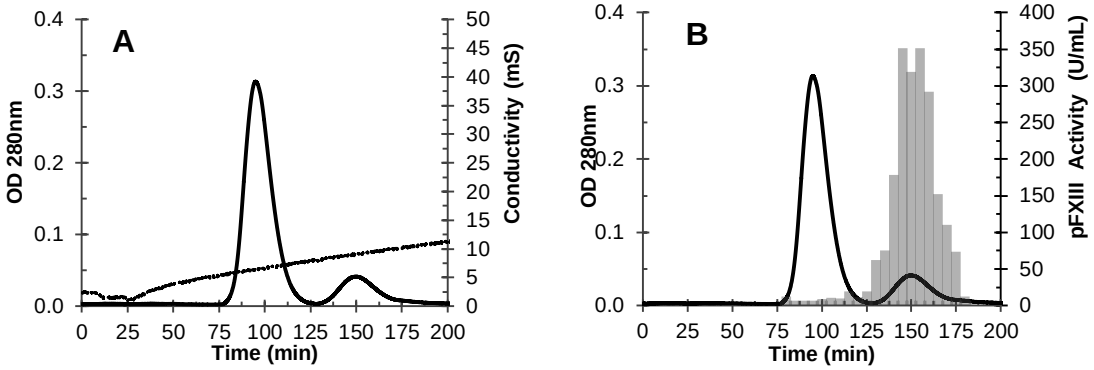

Figure 3.7: DEAE-Sepharose chromatography of γγ/γγ'rF1 with the addition of pFXIIIA_2B_2. Samples were loaded onto a DEAE-Sepharose fast flow column (0.9 x 5 cm) and eluted by gradient salt. Panel A: Elution profile of γγ/γγ'rF110:1 molar ratio. Panel B: pFXIII activity assayed by Biotin peptide incorporation.

3.4.6. **Dynamic Ligth Scattering.** We used DLS to estimate the molecular size of the individual pFXIIIA_2B_2, γγrF1 and γγ'rF1and their mixtures γγrF1: pFXIIIA_2B_2 and γγ'rF1:pFXIII. The hydrodynamic radius (R_H) along with the percentage of polydispercity and the intensity percentage are presented in table 1. When pFXIIIA_2B_2 are mixed with either γγrF1 or γγ'rF1 the R_H increases which may

indicate the natural interaction of pFXIII to γγrF1 and γγ'rF1. However the percentage of polydispercity which directly measures the heterogeneity of each species showed the heterogeneous composition of the γγ'rF1: pFXIIIA_2B_2 mixture that indicates the existence of molecules of different sizes. The particle size distribution histogram presented in figure 2.8 confirmed that the addtion of pFXIIIA_2B_2 to γγ'rF1 contributes to the formation of high size molecules.

Table 3.1: γγ/γγ'rF1, pFXIII and mixture γγrF1:pFXIIIA_2B_2 and γγ'rF1: pFXIIIA_2B_2 Hydrodynamic radius (R_H). All samples were diluted into 50mM TRIS, 115mM NaCl pH 7.5 (μ=0.15M)

Species	R_H (nm)	Polydispercity %	% Intensity
γγ rF1	11.9 ± 0.3	20.6 ± 2.7	93.7
γγ' rF1	11.8 ± 0.4	19.8 ± 2.1	97.9
pFXIII	10.7 ± 0.4	24.7 ± 0.7	86.2
γγrF1: pFXIIIA_2B_2	13.6 ± 0.3	26.7 ± 8.8	96.5
γγ'rF1: pFXIIIA_2B_2	16.4 ± 1.5	48.1 ± 14.1	96.9

When γγrF1 is mixed with pFXIIIA_2B_2 the hydrodynamic radius increases up to 13.6 ± 0.3 nm. The particle size distribution histogram showed a prominent peak with an intensity distribution of 96.5%. The polydispersity of 26.7 indicates that the molecule is slightly polydisperse. In other hand, when γγ'rF1 is mixed with pFXIII the hydrodynamic radius increases up to 16.4 nm with an intensity percentage of 96.9. the

polydispercity indicates the high heterogeneity of the sample. The particle size distribution presented in panel D indicates the formation of high molecular size particles which can be due to some fibrinogen aggregation. In the same histogram, a prominent peak with a radius of 40.1nm indicates the existence of particles of high molecular size.

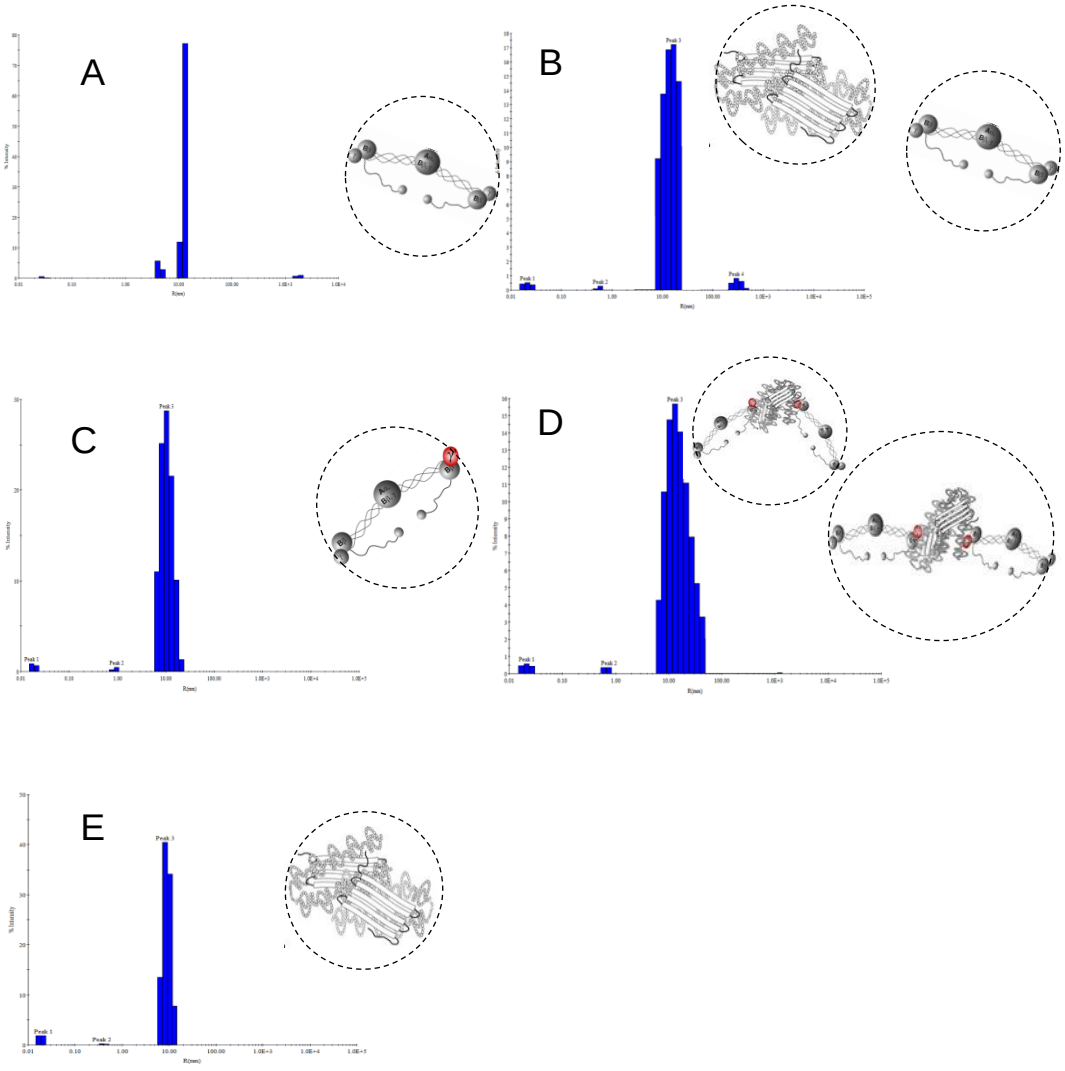

Figure 3.8: particle distibution histogram. Panel A: γγrF1, panel B: γγrF1: pFXIIIA_2B_2, panel C: γγ'rF1 panel D: γγ'rF1: pFXIIIA_2B_2, panel E: pFXIIIA_2B_2.

3.5. Discussion

Previous studies focused on the interaction between $pFXIIIA_2B_2$ and the two major species of pdF1, γγ and γγ', suggested that the γ' chain was responsible for the interaction with $pFXIIIA_2B_2$ via B subunit. However inconsistent results led to discrepancies about the role of γ' as the primary binding site for the zymogen $pFXIIIA_2B_2$. We suspect that many of those inconsistencies arose from the fact that fibrinogen preparations from normal human plasma content traces of $pFXIIIA_2B_2$ as we assessed our pF1 preparations by western blot 9 (data not shown). In fact, Farrell pointed out that the discrepancies between his results and Siebenlist's group were due to the uncounted pFXIII bound onto the γγ'pF1 preparations which induced the high rate of crosslink when compared with that of γγpF1 [32]. In order to avoid misleading results, we used rF1 expressed in milk of transgenic cows which is free factor XIII and possess same activation kinetics and rate of polymerization as the of pF1. [7] In our studies, we employed size exclusion chromatographic techniques and dynamic light scattering to assess the binding of the zymogen $pFXIIIA_2B_2$ to the major fibrinogen variants γγ and γγ' isolated from recombinant fibrinogen.

In our experiments, we observed that the γ' chain is the main peptide responsible for the interactions with the zymogen $pFXIIIA_2B_2$. The tendency of $pFXIIIA_2B_2$ to migrate towards the γγ'rF1 position when analyzed by HPSEC showed the intrinsic affinity between these molecules. This results were in clear concordance with Siebenlist's work as they reported the formation of a single peak when a mixture of 25mg γγ'pF1 and 5mg $pFXIIIA_2B_2$ were loaded onto a pair of Superose 6 size exclusion columns. [1] However

in order to confirm the $pFXIIIA_2B_2$:γγ'rF1 complex formation, the collected the fractions from the $pFXIIIA_2B_2$:γγ'rF1 eluate were reloaded onto the Superose 6 HPSEC system to confirm the existence of a single species. In fact, we observed that each fraction eludes as a single peak. The non-reduced SDS-PAGE analysis of each peak conforms the coexistence of $pFXIIIA_2B_2$ and γγ'rF1 as a single complex molecule. In addition, the factor XIII activity determined by the peptide incorporation assay showed that each collected $pFXIIIA_2B_2$:γγ'rF1 fraction contain high levels of FXIII activity which reaffirm the $pFXIIIA_2B_2$ incorporation into the γ' chain.

Based on results reported by Moaddel [22] and Siebenlist [20], it is expected to observe no interaction between $pFXIIIA_2B_2$ and γγrF1, however our HPSEC experiments determined that there's not complete dissociation of the mixture $pFXIIIA_2B_2$ and γγrF1 what can be assumed that exits some level of interaction that creates an incomplete integration of both $pFXIIIA_2B_2$ and γγrF1. In order to elucidate a possible interaction between $pFXIIIA_2B_2$ and γγrF1, we reloaded the collected eluate fractions to the HPSEC system. Our results indicated the formation of a single peak which confirms the existence of the complex $pFXIIIA_2B_2$:γγrF1. In addition, the FXIII activity assay showed low level of activity compared with the of $pFXIIIA_2B_2$:γγ'rF1. We assume that this level of activity is related to a low binding affinity of $pFXIIIA_2B_2$ to γγrF1. In fact, Byrnes determined that the γ chain amino acids 390-396 are key residues that act as binding site for the zymogen $pFXIIIA_2B_2$. [21] In addition, Smith constructed recombinant truncations of the fibrinogen αC region and identified a high affinity interaction between $pFXIIIA_2B_2$ and amino acid residues localized in the αC region 371-425. [20] Even though those findings

suggest the high affinity between the zymogen $pFXIIIA_2B_2$ and the γ and αC chains, our results demonstrated that $pFXIIIA_2B_2$ may have a low binding affinity to both α the γ chain as the majority of the $pFXIIIA_2B_2$ is displaced forming a second peak as observed in figure 2.2 panel B. This suggestion is supported by our analysis of the pFXIII incorporation peptide assay in which high level of pFXIII activity is located in the second peak.

We also investigated the binding of the factor XIII A-subunit to γγ and γγ' rF1. As showed in the HPSEC profile for the mixtures $rFXIIIA_1$-γγ'rF1 and $rFXIIIA_1$:γγrF1, no binding was observed what suggest that this interaction depends exclusively on the FXIII B subunit. Our results are in total agreement with the reports presented by Siebenlist, [1] Moaddel [22] and Byrnes [21] who performed an extensive evaluation of this interaction.

Although all previous experiments presented here showed an intrinsic interaction between pFXIII and either γγrF1 or γγ'rF1, chromatographic technique do not provide information about the structural rearrangements during the formation of the complexes. Our DLS experiments showed that HPSEC isolated γγrF1, γγ'rF1 and $pFXIIIA_2B_2$ samples exhibited monodisperse behavior which agrees with previous results presented by Huang & Lord. [33] However when mixed the percentage of polydispersity increases which indicated the existence of particles of different sizes. In previous studies, Wasilewska who assessed the fibrinogen R_H under different pH values observed the rapid increase of the R_H induced by the formation of aggregates as the value approaches to the fibrinogen isoelectric point (i.p 5.8). [23] In our studies we maintained a constant pH of 7.5 which leaves $pFXIIIA_2B_2$ as the only protein with the ability to form complexes with

γγrF1 and γγ'rF1. As presented in our results, we might suggest that the pFXIIIA_2B_2:γγ'rF1 mixture has a higher tendency to form complexes as the percentage of polydispercity increases which indicates the presence of larger complexed particles with flexible arrangements.

3.6 References

[1] K. R. Siebenlist, D. A. Meh and M. W. Mosesson, "Plasma Factor XIII Binds Specifically to Fibrinogen Molecules Containing gamma prime chain," *Biochemistry,* no. 35, pp. 10448-10453, 1996.

[2] R. Ariens, T.-S. Lai, J. Weisel, C. S. Greenberg and P. Grant, "Role of factor XIII in fibrin clot formation and effects of genetic polymorphisms," *Blood,* vol. 100, pp. 743-754, 2002.

[3] C. S. Greenberg and M. A. Shuman, "The zymogen forms of blood coagulation factor XIII bind specifically to fibrinogen," *The Journal of Biological Chemistry,* vol. 257, pp. 6096-6101, 1982.

[4] L. Lorand, R. B. Credo and T. J. Janus, "Factor XIII (Fibrin-Stabilizing Factor)," *Methods in Enzymology,* vol. 80, pp. 333-341, 1981.

[5] R. F. Doolittle, S. Hong and D. Wilcox, "Evolution of the fibrinogen g' chain: implications for the binding of factor XIII, thrombin and platelets," *Journal of Thrombosis and Heamostasis,* vol. 7, pp. 1431-1433, 2009.

[6] K. R. Siebenlist, D. A. Meh and M. W. Mosesson, "Protransglutaminase (Factor XIII) Mediated Crosslinking of Fibrinogen and Fibrin," *Thrombosis and Hemostasis,* vol. 5, no. 86, pp. 1221-1228, 2001.

[7] J. Calcaterra, K. E. Van Cott, S. P. Butler, G. C. Gil, M. Germano, H. A. Van Veen, K. Nelson, E. J. Forsberg, M. A. Carlson and W. H. Velander, "Recombinant Human Fibrinogen that produces thick fibrin fibers with increased wound adhesion and clot density," *Biomacromolecules,* vol. 14, pp. 169-178, 2013.

[8] M. L. Schwartz, S. V. Pizzo, R. L. Hill and P. A. McKee, "Human Factor XIII from Plasma and Platelets. Molecular weight, subunit structures, proteolytic activation, and cross-linking of fibrinogen and fibrin," *The Journal of Biological Chemistry,* vol. 248, pp. 1395-1407, 1973.

[9] I. Komaromi, Z. Bagoly and L. Muszbek, "Factor XIII: Novel Structural and Functional Aspects," *Journal of Thrombosis and Heamostasis,* no. 9, pp. 9-20, 2010.

[10] E. Katona, K. Penzes, A. Csapo, F. Fazakas, M. Udvardy, Z. Bagoly, Z. Orosz and L. Muszbek, "Interactions of factor XIII subunits," *Blood,* vol. 123, pp. 1757-1763, 2014.

[11] A. Ichinose, L. E. Hendrickson, K. Fujikawa and E. W. Davie, "Amino Acid Sequence of the A Subunit of Human Factor XIII," *Biochemistry,* vol. 25, pp. 6900-6906, 1986.

[12] V. Yee, L. C. Pedersen, I. Le Trong, P. Bishop, R. E. Stenkamp and D. C. Teller, "Three-dimensional structure of a transglutaminase: human blood coagulation factor XIII.," *PNAS,* vol. 91, pp. 7296-7300, 1997.

[13] A. Ichinose, B. A. Mcmullen, K. Fujikawa and E. W. Davie, "Amino Acid Sequence of the B Subunit of Human Factor XIII, a Protein Composed of Ten Repetitive Segments," *Biochemistry,* vol. 25, pp. 4633-4638, 1986.

[14] M. Souri, T. Osaki and A. Ichinose, "The Non-catalytic B Subunit of Coagulation factor XIII Accelerates Fibrin Cross-linking," *Journal of Biological Chemistry,* vol. 290, no. 19, pp. 12027-12039, 2015.

[15] L. Lorand and K. Konishi, "Activation of the fibrin stabilizing factor of plasma by thrombin," *Archives of Biochemistry and Biophysics,* vol. 105, pp. 58-67, 1964.

[16] T. Takagi and R. Doolittle, "Amino acid sequence studies on factor XIII and the peptide released during its activation by thrombin," *Biochemistry,* vol. 12, pp. 750-756, 1974.

[17] L. Lorand, A. J. Gray, K. Brown, R. B. Credo, C. G. Curtis, R. A. Domanik and P. Stenberg, "Dissociation of the Subunit structure of fibrin stabilizing factor during activation of the zymogen," *Biochemical and Biophysical Research Communications,* vol. 56, pp. 914-922, 1974.

[18] L. Muszbek, V. C. Yee and Z. Hevessy, "Blood Coagulation Factor XIII: Structure and Function," *Thrombosis Research,* no. 94, pp. 271-305, 1999.

[19] T. J. Hornyak and J. A. Shafer, "Interactions of Factor XIII with Fibrin as substrate and cofactor," *Biochemistry,* vol. 31, pp. 423-429, 1992.

[20] K. A. Smith, P. J. Adamson, R. J. Pease, J. M. Brown, A. J. Balmforth, P. A. Cordell, R. A. S. Ariens, H. Philippou and P. J. Grant, "Interactions between factor XIII and the alpha C region of fibrinogen," *Thrombosis and Hemostasis,* vol. 10, pp. 3460-3468, 2010.

[21] J. R. Byrnes, C. Wilson, A. M. Boutelle, C. B. Brandner, M. J. Flick, H. Philippou and A. S. Wolberg, "The interaction between fibrinogen and zymogen FXIII-A2B2 is mediated by fibrinogen residues g390-396 and the FXIII-B subunits," *Blood,* vol. 128, pp. 1969-1978, 2016.

[22] M. Moaddel, D. H. Farrell, M. A. Daugherty and M. G. Fried, "Interactions of human fibrinogens with factor XIII: roles of calcium and the g' peptide," *Biochemistry,* vol. 39, pp. 6698-6705, 2000.

[23] M. Wasilewska, Z. Adamczyk and B. Jachimska, "Structure of fibrinogen in electrolyte solutions derived from dynamic light scattering (DLS) and viscosity measurements," *Langmuir,* vol. 25, pp. 3698-3704, 2009.

[24] C. E. Hall and H. S. Slayter, "The fibrinogen molecule: Its size, shape and mode of polymerization," *Journal of Biophysical Biochemical Cytology,* vol. 5, pp. 11-27, 1959.

[25] Z. Adamczyk, B. Cichocki, M. Ekiel-Jezewska, A. Slowicka, E. Wajnryb and M. Wasilewska, "Fibrinogen conformations and charge in electrolyte solutions derived from DLS and dynamic viscosity measurements," *Journal of Colloid and Interface Science,* vol. 385, pp. 244-257, 2012.

[26] L. Huang and S. T. Lord, "The isolation of fibrinogen monomer dreamatically influences fibrin polymerization," *Thrombosis Research,* vol. 131, pp. 258-263, 2013.

[27] U. Larson, B. Blomback and R. Rigler, "Fibrinogen and the early stages of polymerization to fibrin as studied by dynamic laser light scattering," *Biochimica et Biophysica acta,* vol. 915, pp. 172-179, 1987.

[28] J. W. Wiesel and R. I. Litvinov, "Fibrin formation, structure and properties," *Subcell Biochemistry,* vol. 82, pp. 405-456, 2017.

[29] L. Ping, L. Huang, B. Cardinali, A. Profumo, O. V. Gorkun and S. T. Lord, "Substitution of the human αC region with the analogous chicken domain generates a fibrinogen with severely impaired lateral aggregation: fibrin monomers assemble into protofibrils but protofibrils do not assemble into fibers.," *Biochemistry,* vol. 50, pp. 9066-9075, 2011.

[30] J. Calcaterra, K. E. Van Cott, S. P. Butler, G. C. Gil, M. Germano, H. A. Van Veen, K. Nelson, E. J. Forsberg, M. A. Carlson and W. H. Velander, "Recombinant human fibrinogen that produces thick fibrin fibers with incrased wound adhesion and clot density," *Biomacromolecules,* vol. 14, pp. 169-178, 2012.

[31] D.-S. Park, J.-H. Kim, S. W. Lee and J.-M. Jeong, "Secretory expression of the alpha-subunit of human coagulation factor XIII in the yeast Pichia pastoris," *Biotechnology Letters,* vol. 24, pp. 97-101, 2002.

[32] Farrell, "Letter to the Editor: Fibrinogen containing g' chains," *Blood,* vol. 107, pp. 3011-3012, 2006.

[33] L. Huang and S. T. Lord, "The isolation of fibrinogen monomer dramatically influences fibrin polymerization," *Thrombosis Research,* vol. 131, pp. e258-e263, 2013.

CHAPTER IV

The plasma factor XIII activation is regulated by the γγ' fibrinogen chain

4.1. Summary

In the presence of Factor XIII cross-linking activity, the process of fibrinogen polymerization rapidly proceeds from a short-lived soluble phase initiated at low viscosity, to within a semi-soluble and partially cross-linked fibrin hydrogel environment, to a highly cross-linked totally insoluble viscoelastic solid. Thus, the reactions occur mostly in a heterologous manner with restricted mass transfer from the liquid phase and where most enzymatic reactions are occurring entirely within the evolving aqueous hydrogel polymer phase. The high level reaction efficiency that can occur within the fibrin hydrogel are seen by thromboelastography in the presence of higher levels of thrombin and Factor XIII enzyme activity that almost instantly catalyze the formation of a thoroughly dense, cross-linked viscoelastic fibrin polymer. This efficiency is essential to rapidly re-establishing hemostasis under threatening conditions of hemorrhage.

In this chapter, we assessed the effect of the two major variants of a recombinant fibrinogen (rFI) and fibrin (rFbn) γγ and γγ' on the rate of $pFXIIIa_2b_2$ activation. This provides information about how a rF1 fundamentally interacts with FXIII and an advantage of evaluating FXIII interactions in the absence of a fibrinogen having no endogenous Factor XIII activity. It is noted that plasma-derived fibrinogen contains complexed Factor XIII which complicates evaluation of subtle kinetic interactions with fibrinogen and exogenously added Factor XIII activity. Two advantages Three main stages that resembled the activation mechanism of $pFXIIIa_2b_2$ were studied using a 5-

(biotinamino pentylamine) peptide incorporation assay which permits the analysis of heterologous reactions occurring within a solid phase containing an immobilized fibrinogen species. Thus, the liquid phase solutions containing (A) the non-active tetramer ($pFXIIIa_2b_2$), (B) the thrombin cleaved ($pFXIIIa_2'b_2$) and (C) the thrombin cleaved non-active dimeric plasma factor XIII a-subunit ($pFXIIIa_2'$) were individually place in contact with a previously immobilized γγ, γγ' rFI or γγ, γγ' rFbn (immobilized solid phase). This heterologous setting allows the evaluation of the effect of fibrinogen and fibrin (solid phase) on the rate of $pFXIIIa_2b_2$ activation (delivered from the liquid phase). In general, the results indicated that the presence of γγ or γγ' rFbn increased the rate of $pFXIIIa_2$* generation when compared with that of γγ or γγ' rFI. A detailed analysis for each stage suggested that in "stage I" γγ'rFbn enhances the rate of proteolytic activation of $pFXIIIa_2b_2$ yielding $pFXIIIa_2'b_2$. It is consistent with past reports of the γγ'rFbn induction of the formation of a ternary molecular complex between Fbn, thrombin and $pFXIIIa_2b_2$ that results in the enzymatic removal of the $pFXIIIa_2b_2$ activation peptide. In "stage II", the $pFXIIIa_2'b_2$ dimeric dissociation into pFXIII-A_2 and pFXIII-B_2 subunits was expedited by the presence of the γγ'rFbn which interacts with pFXIII-B_2 subunit. However when $pFXIIIa_2'$ was incubated with either γγ or γγ' rFI and rFbn, no significance difference on the rate of $pFXIIIa_2$* generated was observed suggesting that the γγ'rFbn enhances the rate of $pFXIIIa_2b_2$ activation. From this we conclude that the enzymatic activation of the tetramer plasma factor XIII ($pFXIIIa_2b_2$) is regulated by the γγ' fibrin variant which operates as both substrate and cofactor. The γγ' fibrin modulates the thrombin enzymatic cleavage of the factor XIII activation peptide and accelerates the rate of the factor XIII B-subunit dissociation.

4.2. Introduction

Whether in solution in the short-lived absence of fibrin polymer hydrogel or within the evolving fibrin polymer hydrogel, the active transglutaminase plasma factor XIII ($pFXIIIa_2$*) is generated from the zymogen plasma factor XIII ($pFXIIIa_2b_2$) which undergoes proteolytic and conformational modifications to expose its catalytic core. [1, 2] The $pFXIIIa_2b_2$ activation mechanism, as presented in Scheme A, consists of a series of sequential step that can be divided in 3 main stages [3, 4]. In the first stage, thrombin removes a 4kDa factor XIII activation peptide (AP_{FXIII}) from the N-terminal of the A subunit (83kDa) yielding the non-active thrombin cleaved factor XIII ($pFXIIIa_2'b_2$) [5, 6]. Subsequently, $pFXIIIa_2'b_2$ dissociates into two A and two B subunits in the presence of fibrin/fibrinogen and Ca^{2+} at physiological levels [7, 8]. In the final stage, $pFXIIIa_2$' undergoes conformational changes to form the fully active factor XIII ($pFXIIIa_2$*) which catalyzes formation of the γ-glutamyl–ε-lysyl peptide cross link between adjacent glutamine–lysine residues in the γ and α chains of fibrin units. [9, 10, 11, 12].

$$FXIII\ a_2b_2 \xleftrightarrow{rFIIa} FXIII\ a_2'b_2 + AP_{FXIII} \quad \text{[Stage I]}$$

$$FXIII\ a_2'b_2 \xleftrightarrow{Ca^{2+},\ Fibrinogen/Fibrin} FXIII\ a_2' + FXIIIb_2 \quad \text{[Stage II]}$$

$$FXIII\ a_2' \xleftrightarrow{Ca^{2+},\ Fibrinogen/Fibrin} FXIII\ a_2^* \quad \text{[Stage III]}$$

Scheme A: The overall $pFXIIIa_2b_2$ activation mechanism in the presence of thrombin, FI/Fbn and Ca^{2+} at physiological levels.

The factor XIII catalytic core domain is conformed of both β-cheets and α helices. This domain contains the catalytic triad comprising Cys 314, His 373 and Asp 396 that interact with each other through a hydrogen bonding network. [13, 14] The factor XIII

transamidation reaction mechanism (Scheme B) begins by the recognition of the glutamine residues followed by a nucleophilic attack of the thiolate sulfur Cys 314 to the side chain of the glutamine residue. Then, the formation of a thioester bond is achieved by the release of ammonia from glutamine forming an acyl glutamil residue. The following step consists of the binding of the enzyme-substrate complex to a primary amine from a lysine residue. Because of the high reactivity of the thioester group the formation of the isopeptide bond occurs rapidly. [15, 16]

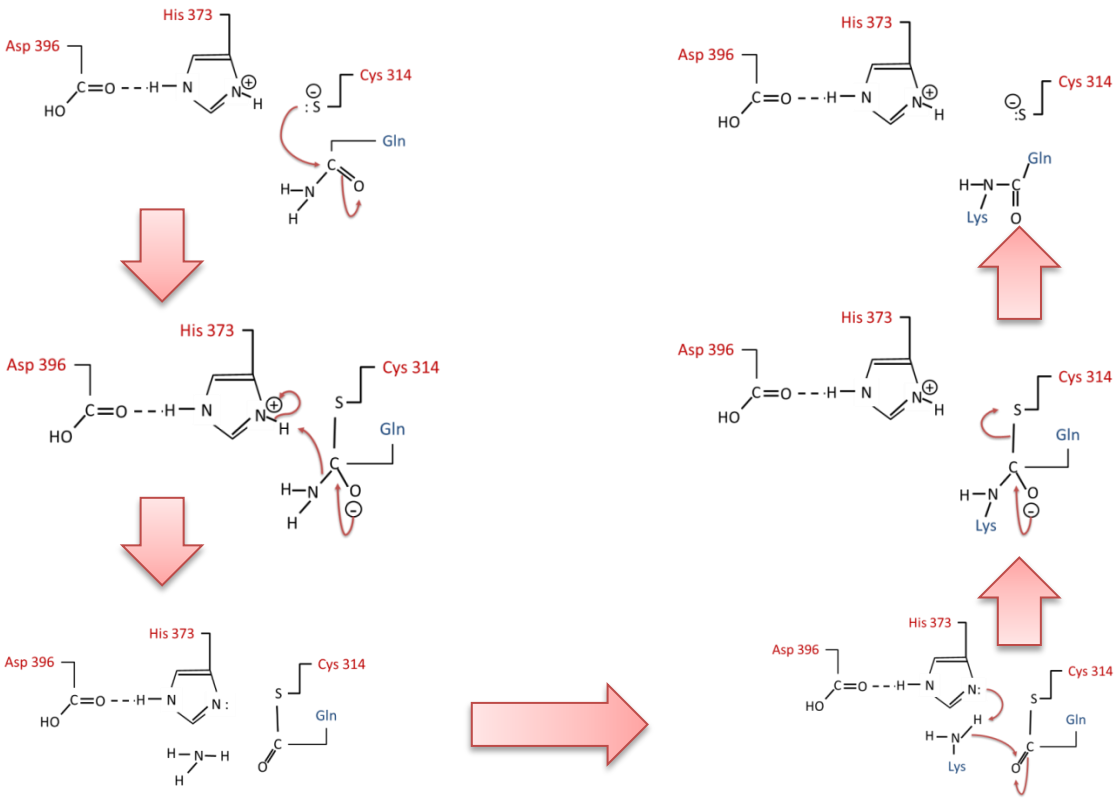

Scheme B: transglutaminase reaction mechanism of the enzyme factor XIII. Gln and Lys are the residues in fibrin monomers.

Studies on the $pFXIIIa_2b_2$ activation mechanism suggested that generation of $pFXIIIa_2$* is regulated by the presence of fibrin. In particular, the γγ' fibrinogen variant which represent about 10% of the total normal fibrinogen was reported to interact with the pFXIII-B subunit and thrombin forming a termolecular complex that expedite the cleavage of the AP_{FXIII}. [3, 2, 13, 14, 15]In addition, the γ'-pFXIII-B subunit interaction facilitates the $pFXIIIa_2b_2$ subunit dissociation increasing the rate of $pFXIIIa_2$* formation. [16, 17] Further investigations suggested that $pFXIIIa_2$* formation is regulated by fragments derived from the fibrin plasmin degradation emerging from the midsection of the α chain. It was also suggested that fibrinogen residues in the γ chain regulate the $pFXIIIa_2b_2$ activation in a $pFXIIIb_2$ dependent mechanism. These observations proposed that fibrinogen and/or fibrin acts a cofactor during the $pFXIIIa_2b_2$ activation and provide regulation for the $pFXIIIa_2$* catalysis. [5]

The transglutaminase kinetic behavior of $pFXIIIa_2$* was found to be in accord with a ping-pong mechanism as suggested by Chung and Folk. (Scheme B) [18]In their study, the isotope exchange method was used to define the $pFXIIIa_2b_2$ reaction pathway in the absence of one or more reactants. However in order to estimate kinetic constant (K_d. K_{cat}, K_m), a simplified sequential activation pathway scheme was proposed by Shafer's group. They reported that fibrinogen and fibrin are required to promote the release of AP_{FXIII} and lower the K_m value. [4]

In an effort to reconcile previous studies and present new evidence on the effect of fibrinogen in the $pFXIIIa_2b_2$ activation mechanism, we recreated the 3 main stages of the

$pFXIIIa_2b_2$ activation process to identify the stage at which the γγ and γγ' variants of fibrinogen and fibrin exert the co-factor effect in the $pFXIIIa_2b_2$ activation mechanism.

4.3. Materials and Methods

All reagents were purchased from Fisher Scientific unless otherwise stated. 5-Biotinamide pentylamine (5bapa) was obtained from Thermo Scientific. D-Phe-Pro-Arg-CMK-HCl (PPACK) was acquired from HaemTech Inc. (VT), p-Nitrophenyl phosphate (pNPP) tablets and Streptavidin-Alkaline phosphatase was purchased from Sigma Life Science. DL-Dithiothreitol (DTT), Diethanolamine and Albumin from Bovine Serum (BSA) were acquired from Sigma-Aldrich. High Binding microtiter plates were purchased from FisherScientific. Rabbit monoclonal Anti-Factor XIIIA subunit antibody and murine monoclonal Anti-Factor XIIIB subunit was purchased from abcam (ab79759) and green mountains antibodies (GMA-033) respectively.

4.3.1. **Plasma factor XIII**, ($pFXIIIa_2b_2$) was purchased from Enzyme Research Laboratories (IN). The $pFXIIIa_2b_2$ was diluted to concentrations ranging from 5nM to 21nM for microtiter plate assay. Thrombin cleaved $pFXIIIa_2'b_2$ was prepared by incubating $pFXIIIa_2b_2$ with 1.1 NIH U/mL rFIIa for 15 minutes and isolated by size exclusion chromatography (SEC) using TRIS buffer with 115mM NaCl pH7.5. In the same manner, the thrombin cleaved dimeric A subunit $pFXIIIa_2'$ was prepared by incubating $pFXIIIa_2b_2$ with 1.5 NIH U/mL and 30mM of $CaCl_2$ for 15 minutes. Then $pFXIIIa_2'$ was isolated by size exclusion chromatography (SEC) Finally, the fully active $pFXIIIa_2$* was prepared by incubating $pFXIIIa_2b_2$ with both 1.1 NIH U/mL and 30mM CaCl2. The solution

was added to immobilize fibrin or fibrinogen in microtiter plate to a final concentration of 1.1mM CaCl2.

4.3.2. **Monomeric recombinant factor XIII** (rFXIIIA) was intracellular expressed in the yeast Pichia pastoris X-33 as previously described [19]. rFXIIIA was purified in a His-Bind® nickel charged resin column.

4.3.3. γγ and γγ recombinant fibrinogen (rFI). rFI was expressed in the milk of transgenic dairy cows and purified by a two-column purification procedure using cation exchange (CIEX) and hydrophobic interaction chromatography (HIC) [20]. The γγ and γγ rF1 isolation was carried out in a weak anion exchange DEAE Sepharose™ Fast Flow column by pH gradient as previously described [14].

4.3.4. **Recombinant activated thrombin (rFIIa)** was purchased from Zymogenetics (WA). 1000U/mL aliquots were prepared in 0.9% NaCl and stored at -80 ^{0}C.

4.3.5. **Factor XIII 5-Biotinamino-pentylamine (5-bapa) incorporation activity assay.** The factor XIII mediated incorporation of biotinamino-pentylamine to γγ or γγ' rF1 was determined using an assay adapted from a previously developed 5 biotionamido-pentylamine (5-bapa) assay. [21, 22, 23] In general, 100 μL of 40μg/mL of γγ or γγ'rF1 were poured into each well of a 96 high binding microtiter plate. Then plates were incubated for 1 hour at 37°C. Blocking buffer (1%BSA in TBS) was added to the wells and incubated overnight at room temperature. To evaluate the effect of fibrinogen (FI) and fibrin (Fbn) in the assay, the adsorbed FI was converted to fbn by adding 100μL of 1.11 NIH U/mL rFIIa. Then, 50μL of crosslink substrate mix (0.25mM 5bapa, 0.1mM DTT and 1.1 mM $CaCl_2$) was added to each well and incubated for 10 minutes at room

temperature. To evaluate the effect of γγ and γγ' FI and Fbn, 4 different settings that resemble the $pFXIIIa_2b_2$ activation stages were prepared as indicated in the $pFXIIIa_2b_2$ section. Then 50µL of either $pFXIIIa_2b_2$, $pFXIIIa_2'b_2$, $pFXIIIa_2$ or $pFXIIIa_2$* was added to each well and the plate was incubated for 30 minutes at room temperature. 200µL of 200mM EDTA were added to each well to quench transglutaminase reaction. The same procedure without previous conversion to fibrin was followed when fibrinogen was immobilized in wells. Then, 100µL of 2.0 µg/mL Streptavidin alkaline phosphatase solution was added to each well and incubated at 37^0C for 1 hour. After incubation, plates were washed and 100µL of para-nitrophenyl phosphate (p-NPP) dissolved in 1M Diethanoalamine was added to the wells. The color developing (clear to yellow) indicated the phosphatase activity on the p-NPP substrate. Finally, the reaction was stopped by adding 200µL of 4N NaOH after 2 minutes reaction. The plates were read at 405nm using Beckman Coulter AD340 plate reader. The results were expressed in units of optical density.

4.3.6. **Estimation of kinetic constants: Michaelis-Menten (K_M) and Maximal Velocity (Vmax).** The 5-BAPA incorporation activity assay was used to estimate the kinetic constants Michaelis-Menten (K_M) and maximal velocity (Vmax). A proposed reaction mechanism is presented in Scheme B1 as suggested by et.al. Chung. In order to estimate the kinetic constants, the reaction mechanism presented in Scheme B1 was linearized (Scheme B2). Further reduction of the reaction mechanism in scheme B2 is obtained by assuming high concentration of factor XIII (E) and fibrin (F) and the pre activation of both fibrinogen to fibrin

and factor XIII ($pFXIIIa_2b_2$) to active factor XIII ($pFXIIIa_2$'). Scheme B3 shows the reaction mechanism proposed for the estimation of the kinetic constants K_M and Vmax. Algebraic deduction of the main equations for K_M and Vmax estimation is presented in scheme C.

C1

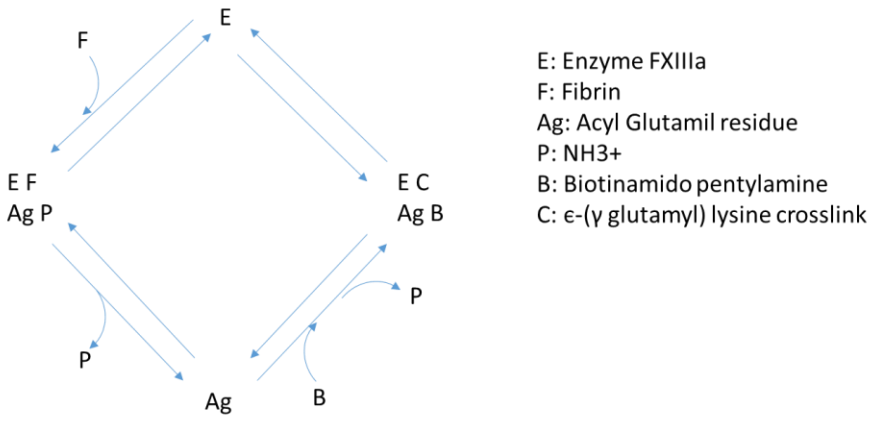

C2

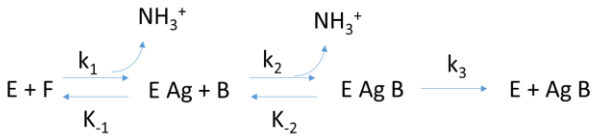

C3

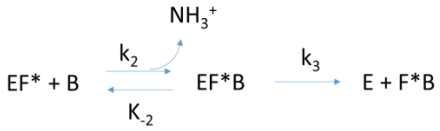

Scheme C: Transglutaminase reaction mechanism suggesting the incorporation of the Biotin peptide. In short, the active transglutaminase FXIII ($pFXIIIa_2$') acts on the fibrin glutamine residues inducing deamination and formation of glutamyl acyl residue. Thus, Gln residue behaves as acyl donor. Then, the 5BAPA, that simulates a Lysine residue, is integrated to the glutamyl acyl residue previous deamination. The Lys like chain

incorporated to the Biotin resemble the acyl group receptor. Finally, s ternary complex is formed by ϵ (γ-glutamyl) Lysine crosslink. (C2) Linearized reaction mechanism of C1. (C3) Simplified reaction mechanism considering high concentration of Fibrin (F) and factor XIII (E).

Estimation of K_M and Vmax were possible by changing the concentration of the Biotin peptide on the microtiter plate. Concentrations of 5BAPA were in the range of 0.25 to 2.5 mM and incubated for 0.5 to 15 minutes. In order to obtain quantifiable data, each reaction was performed in triplicate. The averaged values were used to construct a Reaction Time vs Absorbance plot. Fitted linear regression equations were obtained for each of the plotted lines and used to estimate the initial velocity (Vo). Inverse values of both Vo and substrate concentration (S) were used to prepare the Lineweaver Burk plot. Experimental values obtained from the proposed reaction mechanism were used to estimate Vmax and Km.

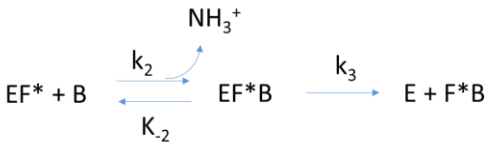

$$[EF^*B] = K_2 [EF^*] + [B]$$

Total enzyme coupled with fibrin monomer E_TF^*

$$[E_TF^*] = [EF^*] + [EF^*B]$$

$$[EF^*] = [E_TF^*] - [EF^*B]$$

$$[EF^*B] = K_2 [B] ([E_TF^*] - [EF^*B])$$

$$[EF^*B] = K_{-2} [EF^*B] - K_3 [EF^*B]$$

Then: K_{-2} [EF*B] – K_3 [EF*B] = K_2 [B] [E_TF*] – K_2 [EF*B] [B]

$$[EF^*B] = \frac{k_2\,[B]\,[E_T F^*]}{k_{-2} + k_3 + k_2[B]}$$

Then:

$$Vmax = k_3\,[E_T F^*]$$

$$[EF^*B] = Vo/k_3$$

$$Km = \frac{k_{-2} + k_3}{k_2}$$

$$Vo = \frac{Vmax\,[B]}{Km + [B]}$$

Scheme D: Algebraic representation of the equation used to estimate Km and Vmax.

4.3.7. **High Pressure Size Exclusion Chromatography. (HPSEC)** Mixtures of pFXIIIa_2b_2 and fibrinogen (γγ or γγ') were prepared in 50mM Tris buffer, 115 mM NaCl, pH 7.5 maintaining ionic strength of 0.15. The mixtures were loaded into two superose 6 10/300 (GE lifescience) columns connected in series to a Knauer (Berlin, Germany) Smartline chromatography station. The columns were isocratically eluted using Tris Buffer at a flow rate of 0.50 mL/min and the length of the run was 90 minutes. Effluent's absorbance was read at 280nm and collected fractions were assayed for Factor XIII activity and SDS-Page.

4.3.8. **SDS PAGE gel electrophoresis.** Non-reduced and reduced samples of pFXIII, γγ and γγ'rF and their mixtures were evaluated by sodium dodecylsulfate polyacrylamide gel electrophoresis (SDS-PAGE) on 4-12% NuPage Bis-Tris pre-cast gels (Thermofisher, CA). All the gels ran for 1 hour at 200 volts and then stained with colloidal Blue gel stain (Invitrogen, CA, USA).

4.4. Results

We evaluated the effect of the two major variants, γγ and γγ', of a recombinant fibrinogen and recombinant fibrin on the three stages of the $pFXIIIa_2b_2$ activation using the peptide incorporation microtiter plate assay. Previous Studies determined that fibrin acts as both substrate and cofactor during the $pFXIIIa_2b_2$ activation suggesting the formation of a termolecular complex fibrin-thrombin- $FXIIIa_2b_2$ which enhances the cleavage of the factor XIII activation peptide (AP_{FXIII}) and promotes the generation of $pFXIIIa_2'b_2$. [2, 28] Further investigations indicates that the non-covalent binding of $pFXIIIa_2b_2$ to the fibrinogen γ' variant increases the rate of $pFXIIIa_2b_2$ activation by accelerating the rate of B subunit dissociation. [5] Although these past investigations provides convincing information about the $pFXIIIa_2b_2$ activation mechanism, it is unknown the stage at which the γγ or γγ' variants have higher influence over the $pFXIIIa_2b_2$ activation. In our study, we recreated the main 3 stages of the $pFXIIIa_2b_2$ activation in the presence or absence of γγ and γγ' FI and Fbn. Schemes E to F represent the different stages of $pFXIIIa_2b_2$ activation.

a) pFXIIIa$_2$b$_2$ – γγ Fibrinogen

$$[\alpha\beta]_2\gamma\gamma + FXIII\ a_2b_2 + rFIIa \longleftrightarrow \boldsymbol{FXIII\ a_2b_2 \bullet [\alpha^*\beta]_2\gamma\gamma \bullet rFIIa} + fpA + fpB$$

$$\boldsymbol{FXIII\ a_2b_2 \bullet [\alpha^*\beta]_2\gamma\gamma \bullet rFIIa} \longleftrightarrow \boldsymbol{FXIII\ a_2'b_2 \bullet [\alpha^*\beta]_2\gamma\gamma} + rFIIa + AP_{FXIII}$$

$$\boldsymbol{FXIII\ a_2'b_2 \bullet [\alpha^*\beta]_2\gamma\gamma + rFIIa} \xleftrightarrow{1.1mM\ CaCl_2} \boldsymbol{FXIII\ a_2^* \bullet [\alpha^*\beta]_2\gamma\gamma - Ag + rFIIa + b_2}$$

b) pFXIIIa$_2$b$_2$ – γγ' Fibrinogen

$$[\alpha\beta]_2\gamma\gamma' + FXIII\ a_2b_2 + rFIIa \longleftrightarrow \boldsymbol{FXIII\ a_2b_2 \bullet [\alpha^*\beta]_2\gamma\gamma' \bullet rFIIa} + fpA + fpB$$

$$\boldsymbol{FXIII\ a_2b_2 \bullet [\alpha^*\beta]_2\gamma\gamma' \bullet rFIIa} \longleftrightarrow \boldsymbol{FXIII\ a_2'b_2 \bullet [\alpha^*\beta]_2\gamma\gamma'} + rFIIa + AP_{FXIII}$$

$$\boldsymbol{FXIII\ a_2'b_2 \bullet [\alpha^*\beta]_2\gamma\gamma' + rFIIa} \xleftrightarrow{1.1mM\ CaCl_2} \boldsymbol{FXIII\ a_2^* \bullet [\alpha^*\beta]_2\gamma\gamma' - Ag + rFIIa + b_2}$$

c) pFXIIIa$_2$b$_2$ – γγ Fibrin

$$[\alpha\beta]_2\gamma\gamma \xleftrightarrow{rFIIa} \boldsymbol{[\alpha^*\beta]_2\gamma\gamma} + fpA + fpB$$

$$\boldsymbol{[\alpha^*\beta]_2\gamma\gamma} + FXIII\ a_2b_2 + rFIIa \longleftrightarrow \boldsymbol{FXIII\ a_2b_2 \bullet [\alpha^*\beta]_2\gamma\gamma \bullet rFIIa}$$

$$\boldsymbol{FXIII\ a_2b_2 \bullet [\alpha^*\beta]_2\gamma\gamma \bullet rFIIa} \longleftrightarrow \boldsymbol{FXIII\ a_2'b_2 \bullet [\alpha^*\beta]_2\gamma\gamma} + rFIIa + AP_{FXIII}$$

$$\boldsymbol{FXIII\ a_2'b_2 \bullet [\alpha^*\beta]_2\gamma\gamma} + rFIIa \xleftrightarrow{1.1mM\ CaCl_2} \boldsymbol{FXIII\ a_2^* \bullet [\alpha^*\beta]_2\gamma\gamma - Ag} + rFIIa + b_2$$

d) pFXIIIa$_2$b$_2$ – γγ' Fibrin

$$[\alpha\beta]_2\gamma\gamma' \xleftrightarrow{rFIIa} \boldsymbol{[\alpha^*\beta]_2\gamma\gamma} + fpA + fpB$$

$$\boldsymbol{[\alpha^*\beta]_2\gamma\gamma'} + FXIII\ a_2b_2 + rFIIa \longleftrightarrow \boldsymbol{FXIII\ a_2b_2 \bullet [\alpha^*\beta]_2\gamma\gamma' \bullet rFIIa}$$

$$\boldsymbol{FXIII\ a_2b_2 \bullet [\alpha^*\beta]_2\gamma\gamma' \bullet rFIIa} \longleftrightarrow \boldsymbol{FXIII\ a_2'b_2 \bullet [\alpha^*\beta]_2\gamma\gamma'} + rFIIa + AP_{FXIII}$$

$$\boldsymbol{FXIII\ a_2'b_2 \bullet [\alpha^*\beta]_2\gamma\gamma'} + rFIIa \xleftrightarrow{1.1mM\ CaCl_2} \boldsymbol{FXIII\ a_2^* \bullet [\alpha^*\beta]_2\gamma\gamma - Ag} + rFIIa + b_2$$

Scheme E: pFXIIIa$_2$b$_2$ activation pathway in the presence of : a) γγ Fibrinogen b) γγ' Fibrinogen c) γγ Fibrin d) γγ' Fibrin.

$$pFXIII\ a_2b_2 \xleftrightarrow{rFIIa} pFXIII\ a_2'b_2 + AP_{FXIII}$$

a) pFXIIIa$_2$'b$_2$ – γγ Fibrinogen

$$[\alpha\beta]_2\gamma\gamma + FXIII\ a_2'b_2 + rFIIa \longleftrightarrow FXIII\ a_2'b_2 \bullet [\alpha^*\beta]_2\gamma\gamma + rFIIa + fpA + fpB$$

$$FXIII\ a_2'b_2 \bullet [\alpha^*\beta]_2\gamma\gamma + rFIIa \xleftrightarrow{1.5mM\ CaCl_2} FXIII\ a_2^* \bullet [\alpha^*\beta]_2\gamma\gamma - Ag + rFIIa + b_2$$

b) pFXIIIa$_2$'b$_2$ – γγ' Fibrinogen

$$[\alpha\beta]_2\gamma\gamma' + FXIIIa_2'b_2 + rFIIa \longleftrightarrow FXIIIa_2'b_2 \bullet [\alpha^*\beta]_2\gamma\gamma' + rFIIa + fpA + fpB$$

$$FXIII\ a_2'b_2 \bullet [\alpha^*\beta]_2\gamma\gamma' + rFIIa \xleftrightarrow{1.5mM\ CaCl_2} FXIII\ a_2^* \bullet [\alpha^*\beta]_2\gamma\gamma' - Ag + rFIIa + b_2$$

c) pFXIIIa$_2$'b$_2$ – γγ' Fibrin

$$[\alpha\beta]_2\gamma\gamma \xleftrightarrow{rFIIa} [\alpha^*\beta]_2\gamma\gamma + fpA + fpB$$

$$[\alpha^*\beta]_2\gamma\gamma + \underset{-Ag}{FXIII\ a_2'b_2} \underset{+\ b_2}{\longleftrightarrow} FXIII\ a_2'b_2 \bullet [\alpha^*\beta]_2\gamma\gamma \xleftrightarrow{1.5mM\ CaCl_2} FXIII\ a_2^* \bullet [\alpha^*\beta]_2\gamma\gamma$$

d) pFXIIIa$_2$'b$_2$ – γγ' Fibrin

$$[\alpha\beta]_2\gamma\gamma' \xleftrightarrow{rFIIa} [\alpha^*\beta]_2\gamma\gamma' + fpA + fpB$$

$$[\alpha^*\beta]_2\gamma\gamma' + \underset{+\ b_2}{FXIII\ a_2'b_2} \longleftrightarrow FXIII\ a_2'b_2 \bullet [\alpha^*\beta]_2\gamma\gamma' \xleftrightarrow{1.5mM\ CaCl_2} FXIII\ a_2^* \bullet [\alpha^*\beta]_2\gamma\gamma' - Ag$$

Scheme F: pFXIIIa$_2$'b$_2$ activation pathway in the presence of : a) γγ Fibrinogen b) γγ' Fibrinogen c) γγ Fibrin d) γγ' Fibrin.

$$pFXIII\ a_2b_2 \xleftrightarrow{rFIIa} pFXIII\ a_2'b_2 + AP_{FXIII}$$

$$pFXIII\ a_2'b_2 \xleftrightarrow{rFIIa} pFXIII\ a_2' + b_2$$

a) pFXIIIa$_2$'b$_2$ – γγ Fibrinogen

$$FXIII\ a_2' + \left[\alpha\ \ \beta\right]_2\gamma\gamma + rFIIa \xleftrightarrow{1.5mM\ CaCl_2} FXIII\ a_2^* \bullet [\alpha^*\beta]_2\gamma\gamma - Ag + rFIIa$$

b) pFXIIIa$_2$'b$_2$ – γγ' Fibrinogen

$$FXIII\ a_2' + [\alpha^*\beta]_2\gamma\gamma' + rFIIa \xleftrightarrow{1.5mM\ CaCl_2} FXIII\ a_2^* \bullet [\alpha^*\beta]_2\gamma\gamma' - Ag + rFIIa$$

c) pFXIIIa$_2$'b$_2$ – γγ' Fibrin

$$[\alpha\beta]_2\gamma\gamma \xleftrightarrow{rFIIa} [\alpha^*\beta]_2\gamma\gamma + fpA + fpB$$

$$[\alpha^*\beta]_2\gamma\gamma + FXIII\ a_2' \longleftrightarrow FXIII\ a_2' \bullet [\alpha^*\beta]_2\gamma\gamma \xleftrightarrow{1.5mM\ CaCl_2} FXIII\ a_2^* \bullet [\alpha^*\beta]_2\gamma\gamma - Ag$$

d) pFXIIIa$_2$'b$_2$ – γγ' Fibrin

$$[\alpha\beta]_2\gamma\gamma' \xleftrightarrow{rFIIa} [\alpha^*\beta]_2\gamma\gamma' + fpA + fpB$$

$$[\alpha^*\beta]_2\gamma\gamma' + FXIII\ a_2' \longleftrightarrow FXIII\ a_2' \bullet [\alpha^*\beta]_2\gamma\gamma' \xleftrightarrow{1.5mM\ CaCl_2} FXIII\ a_2^* \bullet [\alpha^*\beta]_2\gamma\gamma' - Ag$$

Scheme G: pFXIIIa$_2$' activation pathway in the presence of : a) γγ Fibrinogen b) γγ' Fibrinogen c) γγ Fibrin d) γγ' Fibrin.

4.4.1. **γγ'rFbn promotes the Activation peptide FXIII (AP_{FXIII}) cleavage** . We tested the hypothesis that the AP_{FXIII} cleavage is accelerated by the formation of a termolecular complex between pFXIIIa$_2$b$_2$, rFIIa and either γγ or γγ' rFbn. Scheme E summaries the reactions steps that includes the formation of a

termolecular complex previous to the generation of $pFXIIIa_2$*. Figure 1, panel A and B, presents the results of the 5-bapa peptide incorporation assay after incubating γγ, γγ'rFI or γγ, γγ'rFbn with 1.5 U/mL active recombinant thrombin (rFIIa) from 0.5 to 15 minutes. The X axis showed the thrombin incubation time quenched by the addition of 1.0mM PPACK. We observed that both γγ and γγ' rFbn increased the generation of $pFXIIIa_2$* when compared with that of γγ and γγ' rFI. However, the rate of $pFXIIIa_2$* formation was particularly enhanced by the presence of γγ'rFbn in the mixture. As presented in figure 1B, after 5 minutes of rFIIa incubation the absorbance signal at 405nm exhibited an increase of approximate 23% when γγ'rFbn is compared to γγ rFbn. Furthermore, a 37% increase on the absorbance signal was observed when γγ'rFbn is compared to the γγ'rFI. In other hand, our experiments using either γγ or γγ' rFI, figure 1 panel A, indicated that γγ'rFI enhanced the generation of $pFXIIIa_2$* by only approximately 8.0% when compared with that of γγrFI.

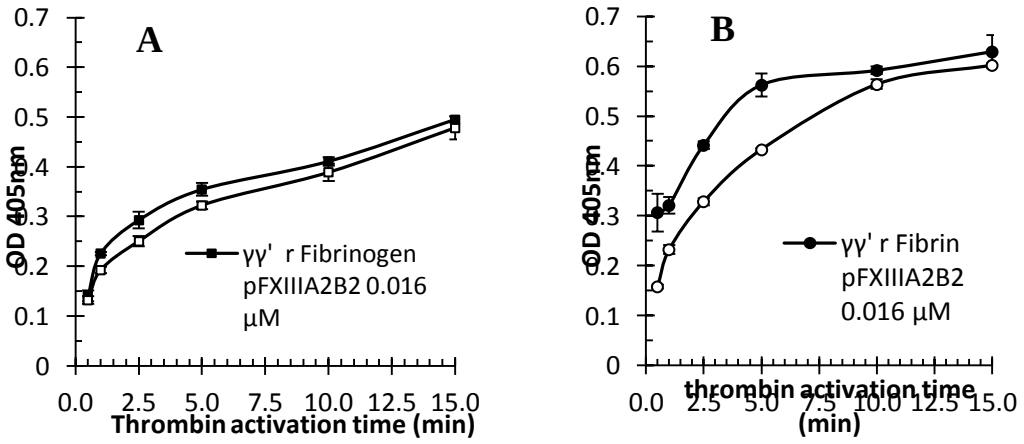

Figure 4.1: $pFXIIIa_2b_2$ activation kinetics by r-α Thrombin in the presence of: (■) γγ'rFI, (□) γγrFI, (●) γγ'rFbn, (○) γγ rFbn.

4.4.2. **The γγ' increases the rate of pFXIIIa$_2$* generation by enhancing the B subunit dissociation.** In addition to our results presented in Figure 1, we assessed the effect of the pFXIIIb$_2$ – γ' chain non-covalent interaction in the rate of pFXIIIa$_2$* generation. To evaluated this effect, we tested the pFXIIIa$_2$'b$_2$ and pFXIIIa$_2$' along with γγ, γγ' rFI and rFbn using the peptide incorporation microtiter plate assay.

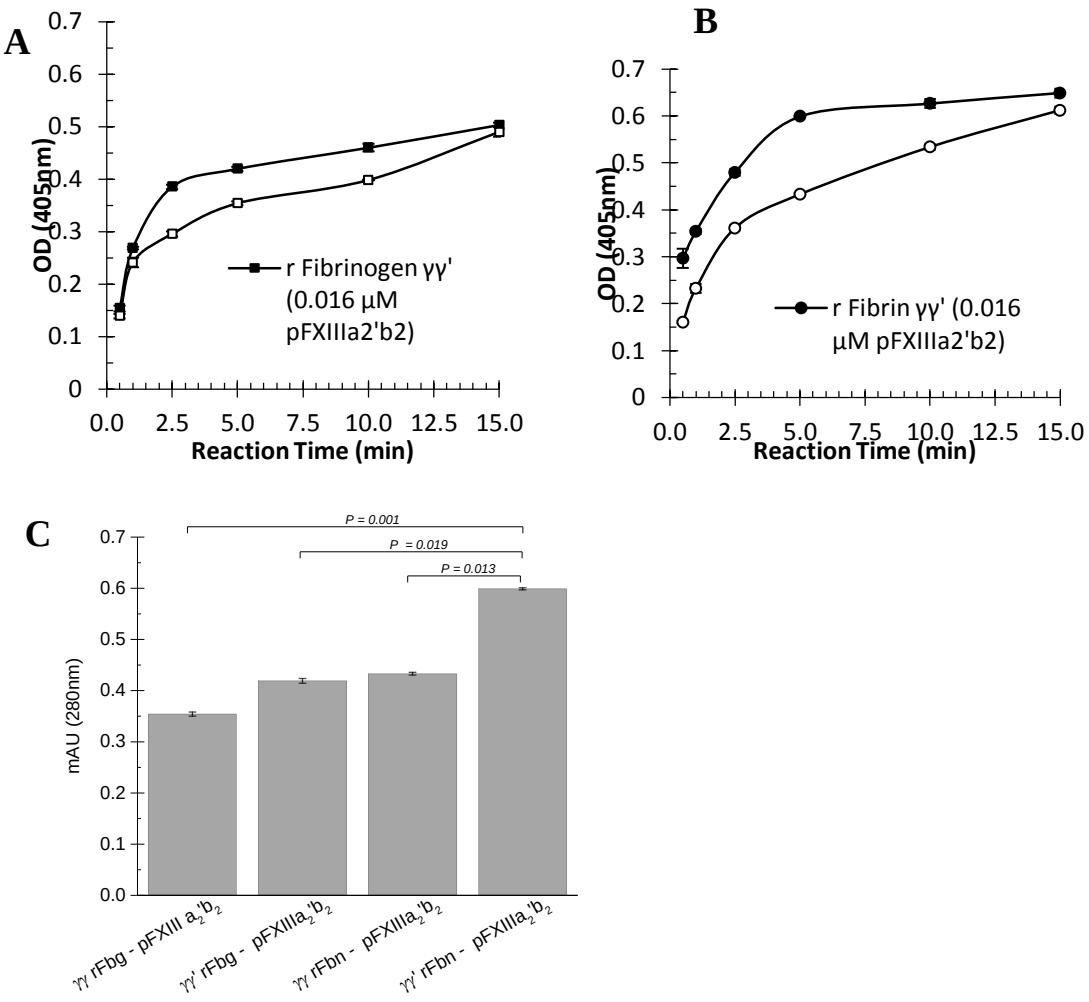

Figure 4.2: pFXIIIa$_2$'b$_2$ activation kinetics in the presence of: **A)** (■) γγ'rFI, (□) γγrFI, **B)** (●) γγ'rFbn, (○) γγrFbn. **C)** Bar diagram representing signal absorbance at 405nm. Bars are means ± SD, N=6.

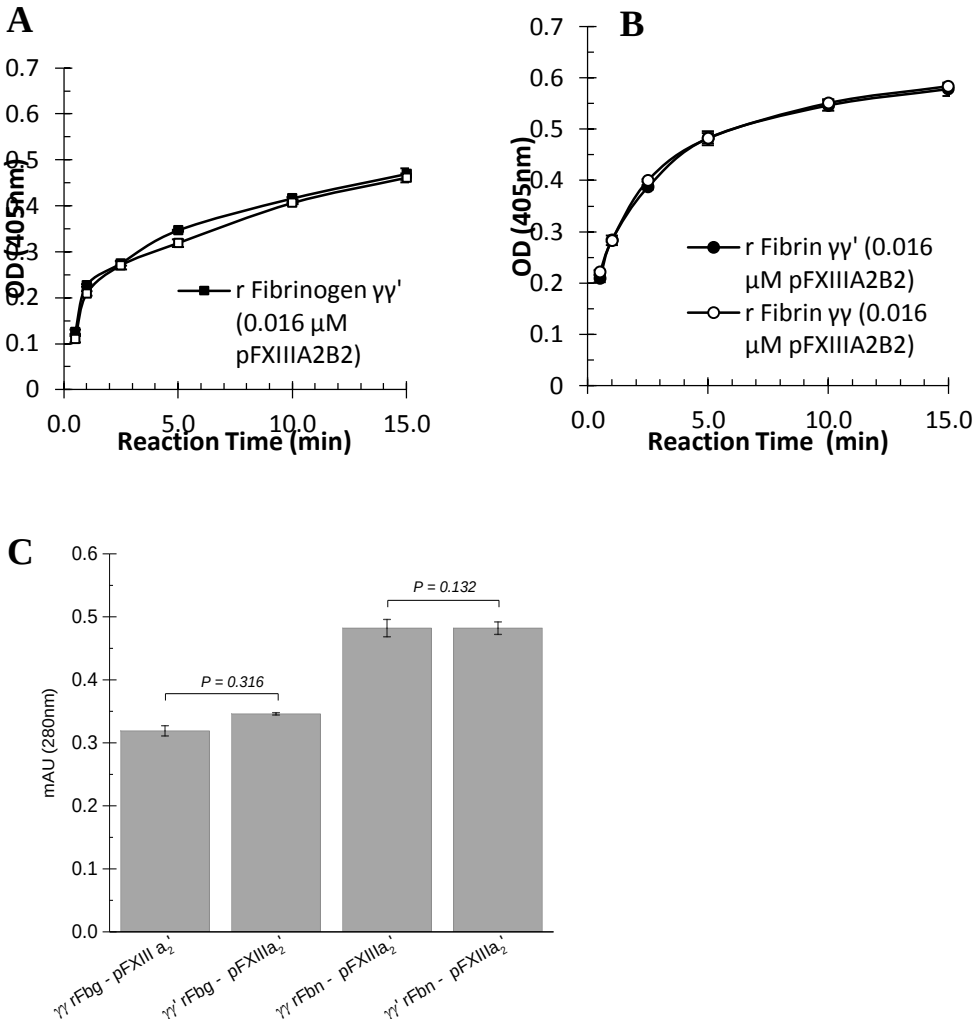

Figure 4.3: pFXIIIa_2' activation kinetics in the presence of: **A)** (■) γγ'rFI, (□) γγrFI, **B)** (●) γγ'rFbn, (○) γγrFbn. **C)** Bar diagram representing signal absorbance at 405nm. Bars are means ± SD, N=6.

Scheme E and F summarize the suggested steps for pFXIIIa_2* generation and the results are presented in figure 4.2 and 4.3 respectively. In figure 2 (panel A and B) the presence of rFbn accelerated the rate of pFXIIIa_2* formation when compared with that of FI. We also observed that γγ'rFbn increased the rate of pFXIIIa_2* generation by approximately 28% when compared with that of γγ rFbn. (figure

2B). Statistical analysis (P value <0.05) indicated the statistical significance of γγ'rFbn over the γγrFbn and both γγ and γγ' rFI (Figure 4.2C) .Surprisingly, the effect of γγ'rFbn over the rate of $pFXIIIa_2$* formation was minimized when the thrombin cleaved dimeric subunit factor XIII A subunit ($pFXIIIa_2$') was incubated with FI or Fbn (figure 4.3B). The results presented no statistical significance between γγ'rFbn and γγrFbn. Similar results were observed when γγ or γγ' rFI were incubated with $pFXIIIa_2$' (figure 4.3C). The decrease in the OD signal is related to the fibrinogen fibrinopeptide release by thrombin. These results indicated that the pFXIII-B sub-unit enhance the rate of $pFXIIIa_2$* formation which can be attributed to the interactions with the γ' chain.

4.4.3. **The combine effect of the pFXIII-B subunit and the γγ'rFI accelerates $pFXIIIa_2b_2$ activation.** To expand our assessment of the combine effect of the γ' chain on the rate of $pFXIIIa_2$* generation, we perform HPSEC to investigate the $pFXIIIa_2b_2$ dissociation. Figure 4.4 panel A shows the HPSEC chromatography profile of the calcium induced $pFXIIIa_2b_2$ dissociation, the γγrFI $pFXIIIa_2'b_2$ and the γγ'rFI $pFXIIIa_2'b_2$ in the presence of physiological calcium concentration (1.5mM). The $pFXIIIa_2b_2$ dissociation was promoted by the removal of AP_{FXIII} in 30mM $CaCl_2$. The dimeric $pFXIIIa_2$ and $pFXIIIb_2$ elutes as a single peak centered at minute 51.3 and 59.6 respectively.

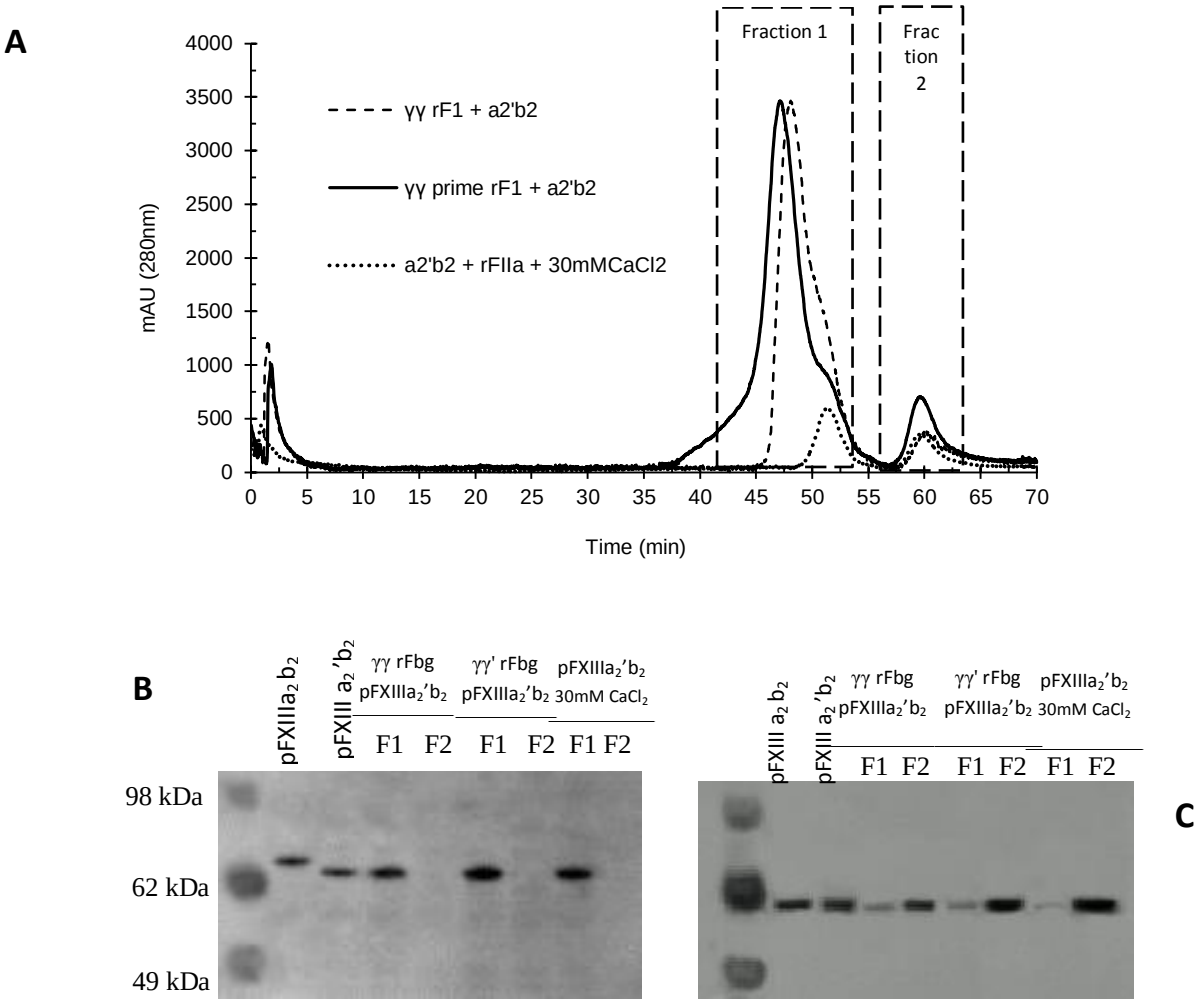

Figure 4.4: A) HPSEC profile of: (••) pFXIIIa$_2$'b$_2$+rFIIa+30mMCaCl$_2$, (--) pFXIIIa$_2$'b$_2$+γγrFI, (–-) pFXIIIa$_2$'b$_2$+γγ'rFI. Pooled fractions F1 and F2 were individually collected for each mixture. **B)** Anti factor XIII-A subunit western blot. **C)** Anti factor XIII-B subunit western blot.

When γγrFI was mixed and incubate for 5 minutes with pFXIIIa$_2$'b$_2$ two peaks centered at minute 48.1 and 60.2 with absorbance of 3465.06 and 388.31 mAU respectively were observed. In similar conditions and concentrations, γγ'rFI and pFXIIIa$_2$'b$_2$ were incubated for 5 minutes and loaded on the HPSEC. The

chromatogram profile showed the elution of two main peaks centered at minute 47.12 and 59.63 with absorbance of 3462.50 and 706.40 mAU respectively. The collected fractions were analyzed by western blotting using an anti-human FXIII-A and FXIII-B antibody. In figure 4.4 panel B, no presence of FXIII-A subunit was detected in all fractions 2 (F2). In the same figure, we noticed that all fractions 1 (F1) are mainly composed of the thrombin cleaved FXIIIA'. However when F1 and F2 were analyzed with FXIII-B antibody (figure 4.4 panel C), the presence of FXIII-B subunit was detected in both fractions. The densitometric analysis of the western blots indicates that the presence of γγ' increased the FXIII-B subunit dissociation by about 40 % when compared to the γγ.

To further assess the effect of γγ'rFbn and the pFXIII-B, we performed non-denatured SDS-Page on the mixtures of γγrFbn/pFXIIIa_2b_2/rFIIa and γγ'rFbn/pFXIIIa_2b_2/rFIIa. As presented in figure 4.5, densitometry analysis indicated that the mixture γγ'rFI-pFXIIIa_2'b_2 increased the rate of pFXIIIa_2'b_2 dissociation by about 10% when compared with that of γγrFI-pFXIIIa_2'b_2. We also observed the formation of high molecular weight fibrin species suggesting the rapid formation of pFXIIIa_2* which catalyzes the fibrinogen polymerization. As suggested by Cooke [8], we observed that the minimum calcium concentration to induced pFXIIIa_2b_2 dissociation is about 30mM (figure 4.5-lane5). In addition, the presence of either γγFI or γγFI induced the pFXIIIa_2b_2 subunit dissociation at physiological levels of Ca^{2+}. (figure 4.5 lane 9, lane 12).

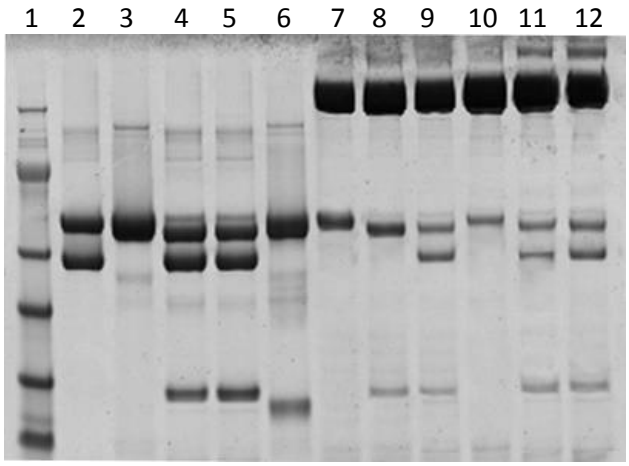

Figure 4.5: pFXIIIa_2b_2 activation SDS-PAGE gel analysis: **Lane1**: See Blue plus 2 Marker, **Lane 2**: Reduced pFXIIIa_2b_2, **Lane 3**: Non-reduced pFXIIIa_2b_2 , **Lane 4**: Reduced pFXIIIa_2b_2 +1.1U rFIIa, **Lane 5**: Non-reduced pFXIIIa_2b_2+1.1U rFIIa+30mM $CaCl_2$, **Lane 6**: Non-reduced pFXIIIa_2b_2+1.1U rFIIa+1.5 mM $CaCl_2$, **Lane 7**: Non-reduced γγrFI + pFXIIIa_2b_2, **Lane 8**: Non-reduced pFXIIIa_2b_2 + γγrFI + 1.1U rFIIa, **Lane 9**: Non-reduced pFXIIIa_2b_2 + γγrFI +1.1U rFIIa+1.5mM$CaCl_2$, **Lane 10**: Non-reduced γγ'rFI + pFXIIIa_2b_2, **Lane 11**: Non-reduced pFXIIIa_2b_2 + γγ'rFI + 1.1U rFIIa, **Lane 12**: Non-reduced pFXIIIa_2b_2 + γγ'rFI +1.1U rFIIa+1.5mM$CaCl_2$.

4.4.4. Estimation of kinetic constants: Michaelis-Menten (K_M) and Maximal Velocity (Vmax).

4.4.4.1. γγ rFI and pFXIIIa_2b_2 mixture.

The results of the estimation of K_M and Vmax obey to the reaction proposed in scheme C3. Figure 4.6A shows the linear regression of the Elapsed crosslink time vs Absorbance at different concentrations of the biotin peptide. Each linear regression equation has a correlation coefficient greater

than 0.98 which validates the accuracy of the obtained data. Table 3.1 shows the data used to prepare the Linewaever-burk plot (1/[S] vs 1/Vo). Figure 4.6B, shows the Lineweaver-Burk plot. The regression coefficient was estimated to be 0.97.

A

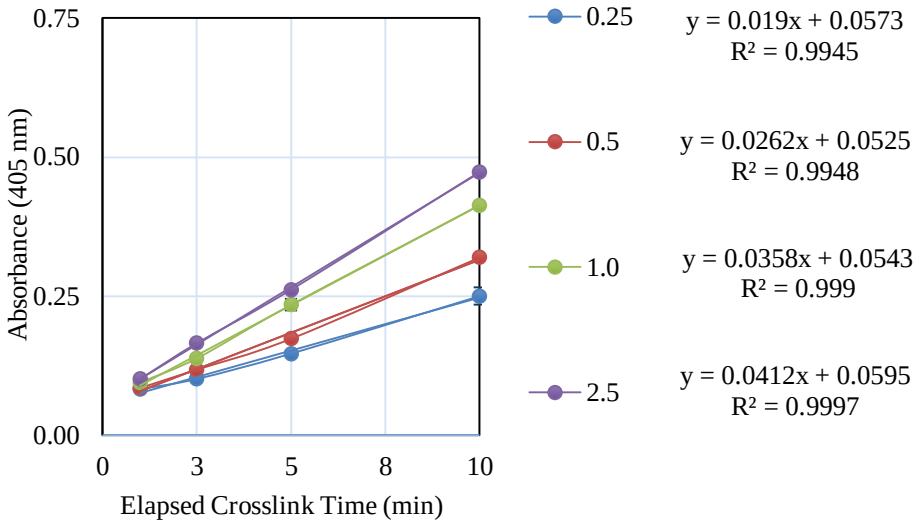

Table 4.1.: Lineweaver-Burk plot data γγ rFI and pFXIIIa_2b_2 mixture.

Substrate conc. 5BAPA (M)	Initial velocity Vo (min)	1/S	1/Vo
0.00025	0.0412	4000	52.6316
0.0005	0.0358	2000	38.1679
0.001	0.0262	1000	27.9330
0.0025	0.019	400	24.2718

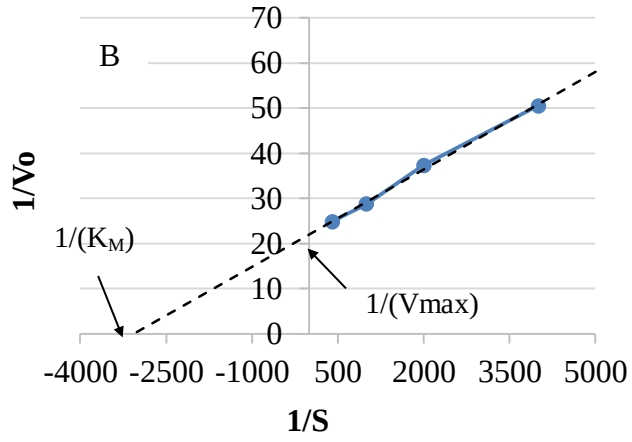

Figure 4.6: Estimation of K_M and Vmax. γγ rFI and pFXIIIa_2b_2.

4.4.4.2.**K_M and Vmax estimation for the γγ' rFI and pFXIIIa_2b_2 mixture**.

As previously presented for the γγ rFI and pFXIIIa_2b_2 mixture, the K_M and Vmax estimation for the γγ' rFI and pFXIIIa_2b_2 mixture was performed following the same procedure. Figure 4.7A represent the elapsed crosslink time of the peptide incorporation reaction. Linear regression of each is presented in figure 4.7A. The Lineweaver-burk plot is presented in figure 4.7B.

A

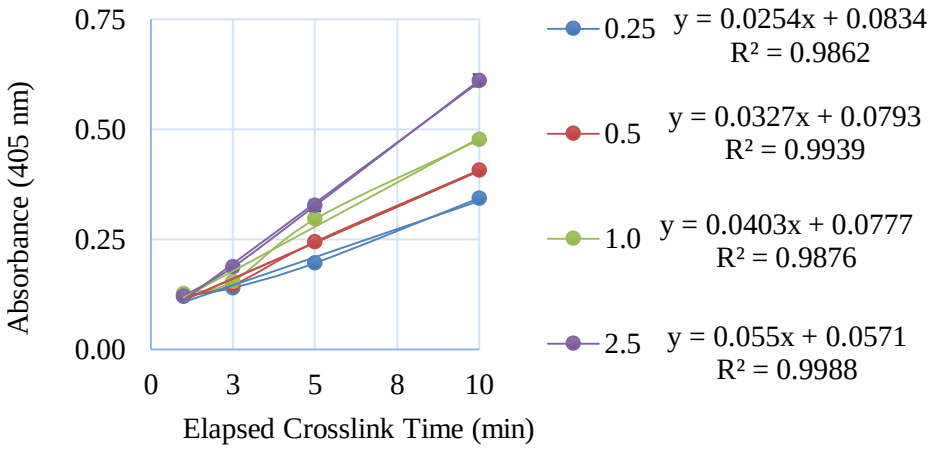

Table 4.2.: Lineweaver-Burk plot data γγ' rFI and pFXIIIa$_2$b$_2$ mixture

Substrate conc. 5BAPA (M)	Initial velocity Vo (min)	1/S	1/Vo
0.00025	0.0159	4000	62.8931
0.0005	0.0204	2000	49.0196
0.001	0.0252	1000	39.6825
0.0025	0.0344	400	29.0698

B

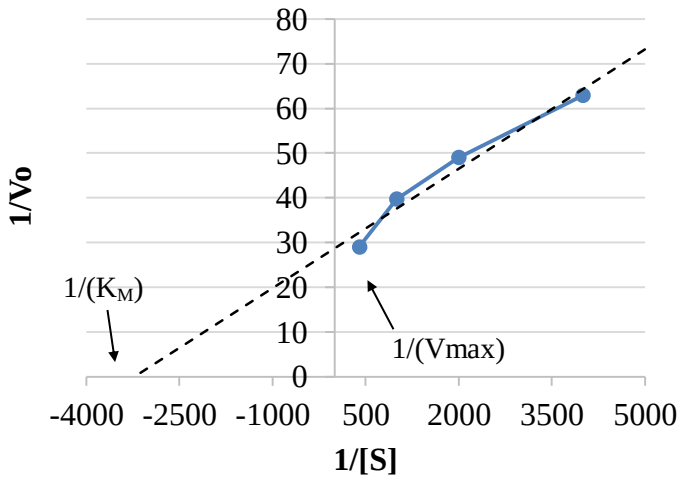

Figure 4.7: Estimation of K_M and Vmax. γγ' rFI and pFXIIIa$_2$b$_2$.

Table 4.3: Estimated Vmax and K_M for the mixtures: γγ rFI + pFXIIIa$_2$b$_2$ and γγ' rFI + pFXIIIa$_2$b$_2$

Mixture	Maximal Velocity (Vmax) mol/min	Michaellis-Menten Constant (K_M) (M)
γγ rFI + pFXIIIa$_2$b$_2$	0.044	3.27×10^{-4}
γγ' rFI + pFXIIIa$_2$b$_2$	0.035	3.11×10^{-4}

In table 4.3 the kinetic constant values K_M and Vmax for the γγrFI+pFXIIIa_2b_2 and γγ'rFI+pFXIIIa_2b_2 mixtures are showed. Both mixtures present similar K_M values. $3.27x10^{-4}$ and $3.11x10^{-4}$ for the γγrFI+pFXIIIa_2b_2 and the γγ'rFI+pFXIIIa_2b_2 respectively. The estimated Vmax for both mixtures are 0.0454(min) and 0.0349(min) for γγrFI+pFXIIIa_2b_2 and the γγ'rFI+pFXIIIa_2b_2. The differences between the last values are in the range of hundredths and do not represent a significant difference based on the methodology used to estimates these values.

4.5. Discussion

Our analysis assumes a lack of mass transfer restrictions with respect to the supply of Factor XIII zymogen occurring within the immobilized fibrinogen or fibrin hydrogel phases. The pFXIIIa_2b_2 activation mechanism requires thrombin and fibrinogen/fibrin as cofactors. [11, 29] The stages of the pFXIIIa_2b_2 activation begins with the thrombin proteolytic removal of the factor XIII activation peptide yielding the non-active pFXIIIa_2'b_2. Consecutively, the dissociation of pFXIIIa_2'b_2 which is facilitated and enhanced by the presence of fibrin and calcium at physiological levels, yields the dimers pFXIIIa_2' and pFXIIIb_2. In the final stage, the pFXIIIa_2' dimer undergoes conformational changes to expose the active cysteine site and form the active pFXIIIa_2*. Although the pFXIIIa_2b_2 activation mechanism was assessed in the presence of thrombin and fibrinogen, the impact of the γγ and γγ' fibrinogen and fibrin variants and the pFXIII-B subunit were not conclusive.

To obtain relevant data and reconcile previous experiments, three preparations that resemble the main stages of the pFXIIIa_2b_2 activation phases were evaluated along with

thrombin and the two major variants of γγ and γγ' recombinant fibrinogen / fibrin. We demonstrated that the presence of γγ' fibrin increases the rate of generation of $pFXIIIa_2b_2$ which may be related to the acceleration of the proteolytic activity of rFIIa. As previously suggested by Hornyak [4] the geometric disposition of the $pFXIIIa_2b_2$–fibrin–thrombin expedites the enzymatic activity of thrombin which accelerates the proteolytic removal of the AP_{FXIII}. However the fact that the γγ' rFbn increases the rate of AP_{FXIII} cleavage may be related to a particular high affinity binding site located in D domains on γ' chains as reported by Meh [25] suggesting the formation of termolecular complex ($pFXIIIa_2b_2$–fibrin–thrombin). Within this context, we can also suggest that the formation of the termolecular complex facilitates the proteolytic cleavage of the AP_{FXIII} which is necessary for the posterior $pFXIIIa_2b_2$ sub-unit dissociation.

We also demonstrated that the γγ'rFbn accelerates in about 23% the generation of $pFXIIIa_2$* when compared with the γγrFbn. This increase on the $pFXIIIa_2$* generation may be related to the rate of pFXIII-B subunit dissociation. First, we suggested that the formation of a termolecular complex is necessary to enhance the thrombin proteolytic activity. In concordance with our results, we can certainly conclude that γγ'rFbn accelerates the $pFXIIIa_2$* generation by inducing factorXIII-B subunit dissociation at faster rate than γγrFbn. As showed in figure 4.2 and 4.3, the presence of pFXII-B subunit plays an important role in the rate of $pFXIIIa_2$* generation. In fact, no statistical difference was found when either γγ or γγ' rFbn was incubated with $pFXIIIa_2$' or $rFXIIIa_1$. In addition, our studies indicated that fibrinogen conversion to fibrin was not indispensable to induce $pFXIIIa_2b_2$ subunit dissociation. As demonstrated by our HPSEC

analysis, the dissociation of pFXIII-B subunit was enhanced by the presence of γγ'rFI when mixed with $pFXIIIa_2'b_2$. However, as shown in western blots, not all this dissociation wasn't achieved at its maximum since some pFXIII-B subunit was detected on the fraction bound to either γγrFI or γγ'rFI. From this analysis we can suggest that conversion to fibrin is required to achieve the complete dissociation of pFXIII-B subunits from $pFXIIIa_2'b_2$. We can also concluded that the thrombin cleaved, $pFXIIIa_2'$, binds to either γγrFI or γγ'rFI as shown by our HPSEC analysis in which the formation of a single peak is shown.

4.6 References

[1] C. M. Naski, L. Lorand and J. A. Shafer, "Characterization of the kinetic pathway for fibrin promotion of alpha-thrombin catalyzed activation of plasma factor XIII," *Biochemistry,* vol. 30, pp. 934-941, 1991.

[2] J. T. Janus, D. S. Lewis, L. Lorand and A. J. Shafer, "Promotion of thrombin-catalyzed activation of factor XIII by fibrinogen," *Biochemistry,* vol. 22, pp. 6269-6272, 1983.

[3] S. D. Lewis, T. J. Janus, L. Lorand and J. A. Shafer, "Regulation of formation of Factor XIIIa by its Fibrin Substrates," *Biochemistry,* vol. 24, pp. 6772-6777, 1985.

[4] T. J. Hornyak and J. A. Shafer, "Interaction of factor XIII with Fibrin as Substrate and Cofactor," *Biochemistry,* vol. 31, pp. 423-429, 1992.

[5] M. Moaddel, L. A. Falls and D. H. Farrell, "The role of gammaA/gamma' firbrinogen in plasma factor XIII activation," *The Journal of Biological Chemistry,*

vol. 275, pp. 32135-32140, 2000.

[6] H. Handrkova, V. Schroeder and H. P. Kohler, "The activation peptide of coagulation factor XIII is vital for its expression and stability," *Journal of Thombosis and Haemostasis,* vol. 13, pp. 1449-1458, 2015.

[7] R. B. Credo, C. G. Curtis and L. Lorand, "Ca 2+ - related regulatory function of fibrinogen," *PNAS,* vol. 75, pp. 4234-4237, 1978.

[8] R. D. Cooke and J. J. Holbrook, "The calcium-induced dissociation of human plasma clotting factor XIII," *biochemistry Journal,* vol. 141, pp. 79-84, 1974.

[9] B. A. Anokhin, V. Stribinskis, W. L. Dean and M. C. Maurer, "Activation of factor XIII is accompanied by a change in oligomerization state," *FEBS,* vol. 22, pp. 3849-3861, 2017.

[10] S. Gupta, A. Biswas, M. S. Akhter, C. Krettler, C. Reinhart, J. Dodt, A. Reuter, H. Philippou, V. Ivaskevicius and J. Oldenburg, "Revisiting the mechanism of coagulation factor XIII activation and regulation from a structure functional perspective," *Scientific Reports,* vol. 6, 2016.

[11] K. B. Lewis, D. C. Teller, J. Fry, G. W. Lasser and P. D. Bishop, "Crosslinking kinetics of the human transglutaminase, factor XIII[A2], acting on fibrin gels and gamma-chain peptides," *Biochemistry,* vol. 36, pp. 995-1002, 1997.

[12] L. C. Pedersen, V. C. Yee, P. D. Bishop, I. Le Trong, D. C. Teller and R. E. Stenkamp, "Transglutaminase factor XIII uses proteinase-like catalytic triad to crosslink macromolecules," *Protein Science ,* vol. 3, pp. 1131-1135, 1994.

[13] C. G. Curtis, J. T. Janus, B. R. Credo and L. Lorand, "Regulation of factor XIIIa generation by fibrinogen," *Annals New York Academy of Science,* vol. 83, pp. 567-576, 1983.

[14] K. R. Siebenlist, D. A. Meh and M. W. Mosesson, "Plasma Factor XIII Binds Specifically to Fibrinogen Molecules Containing gamma prime chain," *Biochemistry,* no. 35, pp. 10448-10453, 1996.

[15] C. S. Greenberg, K. E. Achyuthan and J. W. Fenton II, "Factor XIIIa formation promoted by complexing of alpha-thrombin, Fibrin, and plasma factor XIII," *Blood,* vol. 69, pp. 867-871, 1987.

[16] C. S. Greenberg, K. E. Achyuthan, S. Rajagopalan and S. V. Pizzo, "Characterization of the fibrin polymer structure that accelerates thrombin cleavage of plasma factor XIII," *Archives of Biochemistry and Biophysics,* vol. 262, pp. 142-148, 1988.

[17] B. R. Credo, G. C. Curtis and L. Lorand, "Alpha-chain domain of fibrinogen controls gneration of fibrinoligase (coagulation factor XIIIa) Calcium Ion regulatory aspects," *Biochemistry,* vol. 20, pp. 3770-3778, 1981.

[18] S. I. Chung and J. E. Folk, "Kinetic studies with transglutaminases," *The Journal of Biological Chemistry,* vol. 247, pp. 2798-2807, 1972.

[19] D.-S. Park, J.-H. Kim, S. W. Lee and J.-M. Jeong, "Secretory expression of the alpha-subunit of human coagulation factor XIII in the yeast Pichia pastoris," *Biotechnology letters,* vol. 24, pp. 97-101, 2002.

[20] J. Calcaterra, K. E. Van Cott, S. P. Butler, G. C. Gil, M. Germano, H. A. Van Veen, K. Nelson, E. J. Forsberg, M. A. Carlson and W. H. Velander, "Recombinant human fibrinogen that produces thick fibrin fibers with incrased wound adhesion and clot density," *Biomacromolecules,* vol. 14, pp. 169-178, 2012.

[21] K. A. Smith, P. J. Adamson, R. J. Pease, J. M. Brown, A. J. Balmforth, P. A. Cordell, R. A. S. Ariens, H. Philippou and P. J. Grant, "Interactions between factor XIII and the alpha C region of fibrinogen," *Thrombosis and Hemostasis,* vol. 10, pp. 3460-3468, 2010.

[22] K. E. Achyuthan, M. A. Santiago and C. S. Greenberg, "A microtiter plate assay for factor XIII A-Chain-fibrin interactions," *Analytical Biochemistry,* vol. 219, pp. 43-48, 1994.

[23] T. F. Slaughter, K. E. Achyuthan, T.-S. Lai and C. S. Greenberg, "A microtiter plate transglutaminase assay utilizing 5-(Biotinamido)pentylamine as substrate," *Analytical Biochemistry,* vol. 205, pp. 166-171, 1992.

[24] M. Souri, T. Osaki and A. Ichinose, "The Non-catalytic B subunit of caogulation factor XIII accelerates fibrin cross-linking," *The Journal of Biological chemistry,* vol. 290, pp. 12027-12039, 2015.

[25] A. D. Meh, K. R. Siebenlist and M. W. Mosesson, "Identification and characterization of the thrombin binsing sites of fibrin," *The Journal of Biological*

Chemistry, vol. 271, pp. 23121-23125, 1996.

[26] D.-S. Park, J.-H. Kim, S. W. Lee and J.-M. Jeong, "Secretory expression of the alpha-subunit of human coagulation factor XIII in the yeast Pichia pastoris," *Biotechnology Letters,* vol. 24, pp. 97-101, 2002.

CHAPTER V

Solution phase associations between Human fibronectin and fibrinogen γγ' heterodimer observable using high pressure size exclusion chromatography and dynamic light scattering.

5.1.Summary

We previously reported the isolation of a binary mixture of γγ'-fibrinogen (γγ'-FI) and fibronectin (pFN) from human plasma that formed a novel fibrin structure with increased viscoelastic strength. Here we use HPSEC and DLS to characterize interactions between γγ'-FI and pFN occurring within that binary mixture. HPSEC fractionation showed distinct subpopulations having unique column residence times obtained when each of these subfractions were individually reprocessed by HPSEC. The relative hydrodynamic sizes of these reprocessed subfractions were intermediate to that observed for pure γγ'-FI and pFN as measured by both HPSEC and DLS. SDS-PAGE composition analysis indicated that the γγ'-FI and pFN were not covalently linked as can occur due to Factor XIII transglutaminase activity commonly associated with γγ'-FI preparations. Purified pFN was mixed with purified γγ'-FI or Aα-chain deficient (des-Aα) γγ'-FI or γγ-FI or des-Aα γγ-FI and associations between pFN and γγ'-FI or des-Aα γγ'-FI occurred spontaneously within 5 minutes. This was evident from the appearance of species having intermediate HPSEC and DLS relative hydrodynamic sizes and reduced presence of the original component species. A similar behavior was not observed after the mixing of pFN with γγ-FI or des-Aα γγ-FI. Previous reports were not able to observe these associations by SPR which immobilizes one of the species and therefore a complex

dependence on the freedom of motion occurring when γγ'-FI and pFN are both in solution is indicated. Furthermore, the presentation of γ' but not γ or Aα chains is required to catalyze this reversible process resulting in a compacted overall structure.

5.2.Introduction

Human fibrinogen (FI) and plasma fibronectin (pFN) are both large blood proteins produced by hepatocytes. They are essential precursors to the formation of fibrin polymer and its dual function as an adherent hemostatic barrier and provisional matrix to induce healing. pFN is incorporated directly from blood into the fibrin matrix during the polymerization of F1 where it augments fibrin strength. F1 and pFN occur in human plasma at a ratio of about 90 F1:10 pFN.

Solution phase interactions between F1 and pFN prior to fibrin formation have not yet been well elucidated. F1 and pFN have contrasting tertiary structures. For example, DLS analysis of F1 shows a narrow distribution of cylindrical structures having high aspect ratios. In contrast, purified FN typically exists as a Gaussian conformation consisting of a string of multiple beadlike domains. A high accessibility of conformationally internalized FN segments likely occurs in human plasma that imparts FN ligand functionality associated with solid phase binding to fibrin and extra cellular matrix (ECM) proteins.

FI is a hexameric glycoprotein having an Mr of 340 kDa: FI consists of two Aα (Mr=66.5 kDa), two Bβ (Mr=52.0 kDa) and two γ chains with subtly different Mr (Mr=46.5kDa and 50.0kDa) which can be resolved by SDS-PAGE electrophoresis. Its

cylindrical conformation arises from a disulfide bridging of these 6 chains creating a linear symmetry identified by two outer D domains connected to a central E domain [32, 33]. About 10% of FI molecules possess a heterodimeric pairing of γ and γ' chains (γγ'-FI) and the remaining 90% are homodimeric in γ-chains (γγ-FI). A γ-chain transcriptional variant results in a net replacement of 4 amino residues of the γ chain carboxy-terminus with a 20 aa extended γ'-carboxy terminal sequence. Two-sulfated tyrosines occur within the γ' impart a greater acidity making γγ'-FI isolatable from γγ-FI by DEAE chromatography [35, 36]. The physiologic role of abnormal γγ'-FI levels has been correlated with a complex and pleotropic impact on vascular health not observed with γγ-FI levels.

Plasma FN is a disulfide linked dimer consisting of two slightly different chains estimated at 198 kDa and 208 kDa. These chains are linked together at their carboxy-terminus terminus [22] but differ in their Domain V amino acid composition. The solubility of pFN distinguishes it from cellular matrix FN (cFN): cFN has a low solubility that leads to its incorporation into ECM soon after its secretion and that is likely due to the presence of an ED domain not present in pFN. Each pFN chain consists of a linear arrangement of repeating units known as: type I, type II and type III which exist as individual globular sub-domains. pFN contains 12 type I repeats (about 40 amino acid and 2 disulfide bonds), 2 type II repeats (60 amino acids and 2 intrachain disulfide) and 15 constitutive and 2 alternative spliced type III and one variable type III. [23, 24]. Each repeating unit operates as distinct domain and this imparts a significant degree of chain flexibility [19, 20, 21] facilitating interaction with ECM proteins like collagen and also

fibrin [21]. While past studies have shown that pFN contains two major fibrin binding sites (Fib-2) [25, 26], its interactions with whole population F1 were reported as highly temperature dependent and strongest at 4 ^{o}C [27].

Our recently reported results show that in addition to the acidity of each protein, γγ'F1 and pFN have interactions which may be contribute to their co-purification from normal human plasma using DEAE-chromatography. We also observed the formation of fibrin matrices that were stronger than that obtained with analogous mixtures of pFN and γγF1. In this study we use HPSEC and DLS to observe interactions between binary mixtures of pFN and γγ'-F1 uniquely purified from human plasma. Furthermore, we use reconstitution of purified FN with γγ-F1, or γγ'-F1 or Aα-chain deficient (des γγ'-FI) or des-Aα γγ-FI to study interactions between these species and unique involvement of γγ'-FI with pFN.

5.3.Materials and Methods

5.3.1.Materials

Chemicals of ACS grade were purchased from J.T. Baker (Phillipsburg, NJ) and Millipore-Sigma (St. Lois, MO). Human plasma was provided as a gift from the U.S. Army Materials Command (Fort Detrick, MD). Human plasma-derived fibrinogen (pdFI) depleted of plasminogen, von Willebrand factor and fibronectin was purchased from Enzyme Research Labs (South Bend, IN). Human fibronectin was purified from human plasma following a procedure previously described [41]. γγ and γγ' fibrinogen species were obtained from human plasma. Species isolation was performed according to a proposed procedure [10] Native γγ'FI:FN mixture was isolated from human plasma as

recently described by Ismail et al. [40] In Brief, 15 units of human plasma were centrifuged at 2702 RFC and 4°C for 20 min. the precipitated was resuspended in 20mM Tris-Base, 55mM sodium citrate, 27mM Lysine, pH 6.8. 0.15% TNBP and 0.5% triton X-100 was used for viral inactivation and stirred at room temperature for 1 hour. The treated solution was adjusted to 1M ammonium sulfate and centrifuged at 2702 RFC for 15 minutes at 25°C. the recovered pellet was dissolved in 20mM sodium citrate, 10mM NaCl pH 7.4 (wash buffer). Finally, the solution was filtered and loaded into a DEAE Sepharose fast flow. Bound protein was eluted with a linear gradient of 0.1–1.0 M NaCl in 20 mM sodium citrate and pH 7.4. Further characterization experiments were carried out using native γγ'FI:FN dialyzed against was buffer.

5.3.2.High Pressure Size Exclusion Chromatography (HPSEC).

For analytical purposes two Superose 6 10/300 (GE, Lifescience) columns were connected in series to a Knauer (Berlin, Germany) Smartline chromatography station and equilibrated with 50mM Tris buffer, 115 mM NaCl, pH 7.5 maintaining ionic strength of 0.15. Columns were loaded with 200µg of sample and isocratically eluted using equilibration buffer at a flow rate of 0.35 mL/min. Loaded samples were previously dialyzed and filtered through a 0.2 µm Pall membrane filter (Port Washington,NY) Effluent's absorbance was read at 280nm and collected fractions were assayed for protein content by SDS-PAGE, particle size distribution and R_H using a DLS instrument.

5.3.3.Native γγ'FI:FN HPSEC procedure

A total of 200µg dialyzed native γγ'FI:FN mixture solution was loaded into HPSEC columns and isocratically eluted using elution buffer (50mM TRIS, 115mM NaCl, pH 7.5). The eluate was collected in 11 Fractions in 1.5 minutes interval. A second HPSEC

pass of each collected fraction was performed following the procedure described above and the eluate product was then analyzed by SDS-PAGE and DLS.

5.3.4.γγFI or γγ'FI with FN mixture reconstitution HPSEC procedure

A 1:1 stoichiometric molar concentration of either γγFI or γγ'FI were mixed with FN and dialyzed against 50mM TRIS, 115mM NaCl, pH 7.5 Then, the mixtures were incubated at 37°C for 1 hour and loaded into the HPSEC column system. The eluted fractions were collected every 1.5 minutes and pooled in 3 groups to characterize each section of the chromatogram profile. Each pooled fractions were concentrated and reloaded into HPSEC . Collected fraction were evaluated by SDS-PAGE and DLS.

5.3.5.des α-γγFI or des α-γγ'FI with FN mixture reconstitution HPSEC procedure

fibrinogen des-α populations of either γγFI and γγ'FI were mixed with FN and the mixture was dialyzed and incubated as described before. 200 μg of mixture was loaded to the HPSEC system and collected fractions were pooled to evaluate sections of the chromatogram profile. Concentrated pooled fractions were reloaded to the HSPSEC system and collected fractions analyzed by SDS-PAGE and DLS.

5.3.6.Dynamic Light Scattering (DLS).

The hydrodynamic radius (R_H) and particle size distribution were assessed by DLS using the DynaPro99 Titan Instrument (Wyatt Technology, CA). In Brief, 20μL of samples containing 0.5 mg/mL of HPSEC native γγ'F1:FN fractions or purified γγF1, γγ'F1, FN or their mixture fractions were illuminated by a 830nm laser and the intensity of scattered light was measured by an avalanche photodiode. The fluctuations in the measured intensity specifies the diffusion coefficient is estimated by autocorrelation analysis and

the particle hydrodynamic radius is determined using the Stroke-Einsten relationship which assumes the uniform sphere shape of the analyzed particle.

5.3.7.SDS PAGE gel electrophoresis and Bicinchoninic acid assay (BCA)

Non-reduced and reduced samples of purified γγ'FI. γγFI, FN and their mixtures were evaluated by sodium dodecylsulfate polyacrylamide gel electrophoresis (SDS-PAGE) on 4-12% NuPage Bis-Tris pre-cast gels (Thermofisher, CA). All the gels ran for 1 hour at 200 volts and then stained with colloidal Blue gel stain (Invitrogen, Carlsbad, CA,). Gels were photographed with Canon S95 digital camera, and densitometry analysis was made using NIH ImageJ software [42]. The BCA total protein assay (ThermoFisher Scientific, New York) was performed to estimate protein concentration as described [43].

5.4.Results

5.4.1. Characterization of native γγ'FI:FN by HPSEC and DLS

The formation of a novel pFN wrapped fibrin structure having enhanced viscoelastic strength may be related to interactions that occur between pFN and γγ'-FI prior to fibrin formation. Both pdFN and each F1 subpopulation are large proteins that have contrasting tertiary conformations which may contribute to the formation of these fibrin structures. Figure 5.1a shows the HPSEC profiles of pFN, γγ'-FI and γγ-FI preparations studied here. The purity and integrity of these preparations are shown by reduced SDS-PAGE in Figure 5.1b. The Aα chain of either γγ-FI (lane 1) or γγ'-FI (lane 2) has two subpopulations having an Mr centered about 62 kDa that are typical of F1. The Bβ chain of either γγ-FI (lane 1) or γγ'-FI (lane 2) has a predominant subpopulation with an Mr centered about 55 kDa. The γ chain of the γγ-FI preparation is predominant

and has an Mr of about 49 kDa (lane 1). The heterodimeric nature of γγ'-FI (lane 2) shows an equal presence of γ and γ' where the γ' has an Mr that is about 1 kDa greater than the γ chain. pFN is a heterodimer possessing two different domain V structures migrated similarly with an Mr centered at about 198 kDa (lane 3). The HPSEC profiles show a distinctly larger hydrodynamic size for both γγ'-FI and γγ-FI relative to pFN. DLS analysis of these preparations show that γγ'-FI and γγ-FI are similar in hydrodynamic radius at about 12 nm while pFN is much smaller at about 10 nm (Table 1). The polydispersity of each species by DLS is also consistent with the HPSEC peak widths and symmetry.

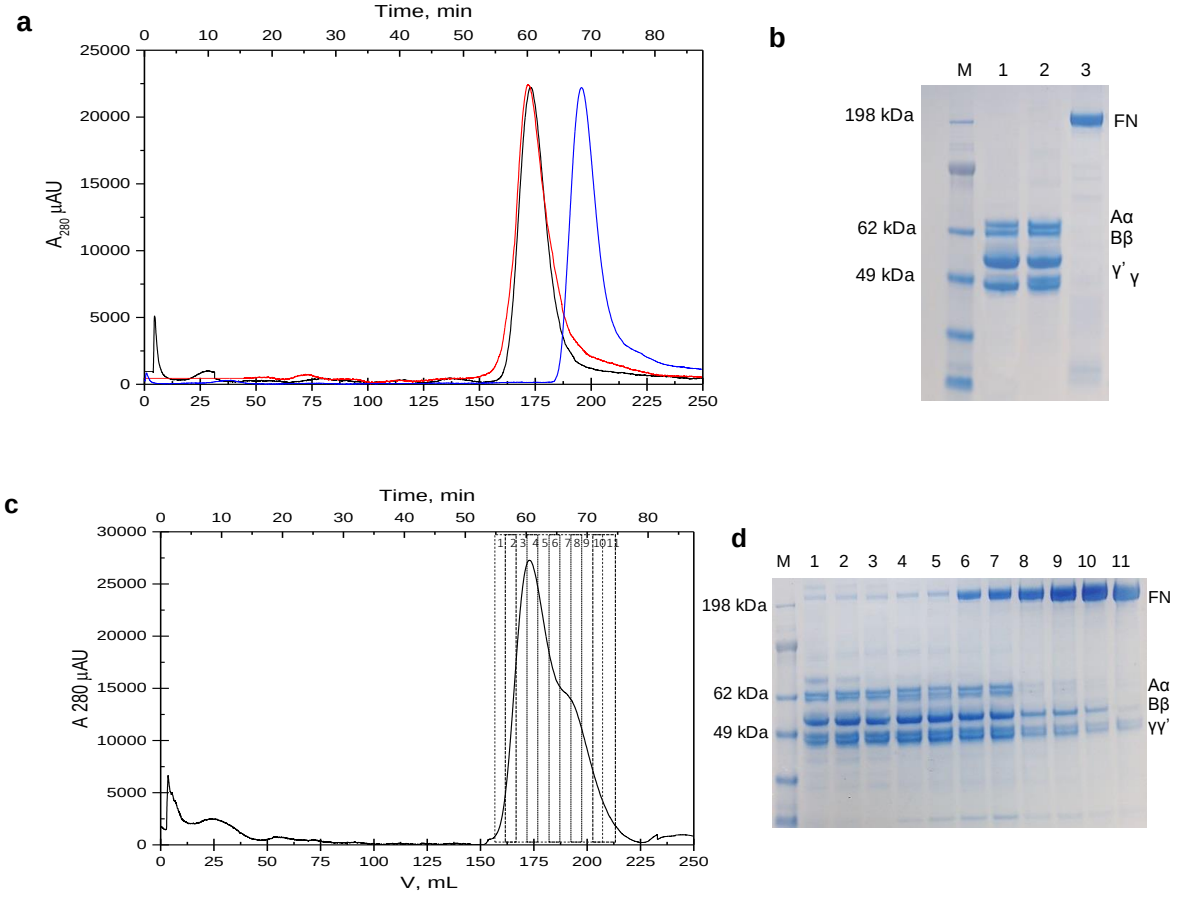

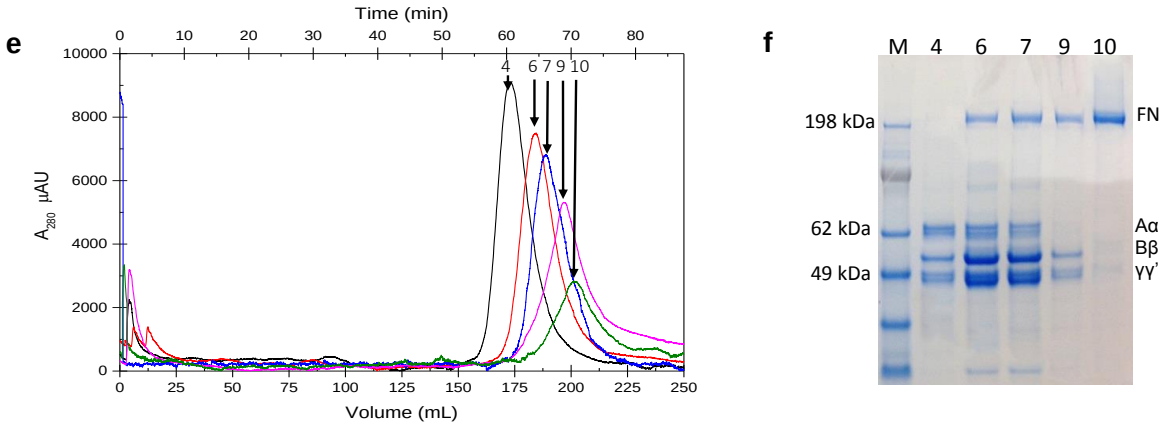

Figure 5.1: (a) High Performance Size-Exclusion Chromatography (HPSEC) profile of γγ FI, γγ'FI and FN. 200µg were loaded to two 25mL pre-packed Superose 6 10/300 GL (GE Healthcare) columns connected in series. HPSEC instrument was operated at 0.35 mL/min. using 50mM TRIS, 100mM NaCl pH 7.4 Buffer. 11 fractions were collected every 1.5 min interval **(b)** Reducing SDS-PAGE analysis of fibrinogen γγ, γγ' and fibronectn standards. Lane M: See blue plus marker, Lane 1: γγ pdFI, Lane 2: γγ' pdFI, Lane 3: FN. **(c)** High Performance Size-Exclusion Chromatography (HPSEC) profile of DEAE elution. **(d)** Reducing SDS-PAGE analysis of HPSEC fractions. Lane M: See blue plus marker, Lanes 1-11 correspond to HPSEC collected fractions 1 through 11. **(e)** Chromatography overlay profile of fractions 3 ,6, 7, 9 and 10 passed through HPSEC. Samples were loaded to two 25mL pre-packed Superose 6 10/300 GL (GE Healthcare) columns connected in series. HPSEC instrument was operated at 0.35 mL/min. using 50mM TRIS, 100mM NaCl pH 7.4 Buffer. **(f)** Reducing SDS-PAGE of fractions 3,6,7, 9 and 10 after second pass in HPSEC. Lane M: See blue marker, lane F3: fraction 3, lane F6: fraction 6, lane F7: fraction 7, lane F9: fraction 9, lane F10: fraction 10.

Table 5.1: γγ FI, γγ' FI, FN Hydrodynamic radius (R_H) measured by DLS at 25 °C. Samples were concentrated to 0.5 mg/mL in PBS buffer pH 7.4. Results indicate the mean and standard deviation of 3 independent preparations. Statistical analysis using one-way ANOVA indicates no significant differences between R_H measurements. ($P<0.035$, $\alpha=0.05$)

Species	Hydrodynamic radius (R_H), nm	Polydispersity, (%)	Intensity distribution (%)
γγ FI	12.2 ± 0.3	23.8 ± 0.9	97.3
γγ' FI	12.1 ± 0.2	23.9 ± 1.9	95.1
FN	10.5 ± 0.2	21.9 ± 1.1	96.3

Table 5.2: HPSEC retention time of γγ' FI-FN mixture isolated from human plasma. Collected fractions are numbered and showed in figure 5.1b and 5.1d

γγ' FI-FN mixture from human plasma		**HPSEC second fractioning**	
Sample	Retention Time (min)	Sample	Retention Time (min)
Fraction 4	60.7	Fraction 4	60.7
Fraction 6	64.1	Fraction 6	64.1
Fraction 7	65.8	Fraction 7	65.8
Fraction 9	69.9	Fraction 9	70.0
Fraction 10	70.8	Fraction 10	71.1

Table 5.3: γγ FI, γγ' FI, FN Hydrodynamic radius (R_H) and fractions 4,6,7,9 and 10 R_H measured by DLS at 25 °C. Samples were concentrated to 0.5 mg/mL in PBS buffer pH 7.4. Results indicate the mean and standard deviation of 3 independent preparations. Statistical analysis using one-way ANOVA indicates no significant differences between R_H measurements. ($P<0.035$, $\alpha=0.05$)

Species	**Hydrodynamic radius (R_H), nm**	**Polydispersity, (%)**	**Intensity distribution (%)**
Fraction 4 (F4)	12.4 ± 0.2	17.9 ± 3.9	95.4
Fraction 6 (F6)	11.8 ± 0.3	28.3 ± 2.1	84.6
Fraction 7 (F7)	11.4 ± 0.3	29.2 ± 1.5	82.9
Fraction 9 (F9)	11.0 ± 0.2	30.6 ± 4.1	88.0
Fraction 10 (F10)	10.7 ± 0.5	17.9 ± 1.8	93.9

Table 5.4: OD and mass of HPSEC fractions 1 to 11.

	Fraction 1	Fraction 2	Fraction 3	Fraction 4	Fraction 5	Fraction 6
OD	0.14	0.40	0.65	0.75	0.64	0.58
Mass* (µg)	5.4	15.5	25.2	29.0	24.8	22.5
Percentage	2.7	7.8	12.7	14.7	12.5	11.4

	Fraction 7	Fraction 8	Fraction 9	Fraction 10	Fraction 11
OD	0.52	0.46	0.39	0.30	0.28
Mass* (µg)	20.1	17.8	15.1	11.6	10.8
Percentage	10.2	9.0	7.6	5.9	5.5

5.4.2. Characterization of reconstituted γγ'FI with FN by HPSEC and DLS

HPSEC fractionation of a binary, plasma-derived mixture of pFN and γγ'-FI shows a less distinct separation between each species relative to references purified from that same parent mixture. (Figure 5.1c). Appreciable amounts of pFN appear in earlier eluting fractions that also contain γγ'-FI (Figure 5.1d, lanes 6,7). A minor des-α γγ'-FI degradation component co-emerges from the HPSEC along with pFN. In order to assess the impact of chromatographic dispersion and the identity of pFN and γγ'-FI subpopulations having intermediate hydrodynamic sizes, we individually reprocessed each fraction with the HPSEC. Surprisingly, each fraction retained its column residence time while having a symmetrical peak (Figure 5.1e and Table 5.2). Furthermore, DLS analysis confirmed the relative Rh values indicated by HPSEC behavior for each reprocessed fraction (Table 5.3, figure 5.1f). This suggested the possibility of pFN and γγ'-FI subpopulations having coincidental and intermediate hydrodynamic sizes and or an association between some of these species which formed a collapsed structure. A reprocessed fraction contained pFN and des-α γγ'-FI. The des-α γγ'-FI had intact Bβ, γ and γ' chains. We estimated by OD 280 nm reprocessed Fractions 6 and 7 to be about 20% of the total protein of the original binary mixture and consisted of pFN and γγ'-FI. (Table 5.4). In order to study the potential for forming associations between pFN and γγ'-FI, we mixed at a 1:1 mass ratio pFN (Figure 5.2d lane 1) and γγ'-FI (Figure 5.2d lane 2) similarly to that observed in the original plasma-derived binary mixture from which they were both isolated. Each of these preparations behaved as distinct, resolvable peaks when analyzed by HPSEC. After 5 minutes of incubation at 37 ^{o}C, the mixture

was applied to the HPSEC where the emergent peak was noticeably shifted in its balance relative to that of the original components with no accompanying peak resolution of the individual components. When fractions from this emergent peak were each individually reprocessed by HPSEC, they were observed to retain their original HPSEC residence times (Figure 5.2c Table 5.5). The intermediate residence times of reprocessed fractions 6, 7 and 8 contained both pFN and γγ'-FI (Figure 5.2 d). DLS analysis of these same reprocessed fractions showed an intermediate Rh to that of pure pFN and γγ'-FI that is congruent with their relative HPSEC residence times (Table 5.6). These results suggest that the shifts in residence times and merged peak behavior of the reconstituted mixture are likely due to formation of intermediately sized associations between pFN and γγ'-FI. This also indicates that these associations were collapsed structures but reversibly formed as they formed from pFN and γγ'-FI isolated from the original binary plasma-derived mixture.

Table 5.5: HPSEC retention time of γγ' FI and FN mixture. Collected fractions are numbered and showed in figure 5.3a, 3b and 3c

γγ' FI + FN mixture HPSEC first fractioning		**HPSEC second fractioning**	
Sample	Retention Time (min)	Sample	Retention Time (min)
γγ' FI	60.5		
FN	69.8		
Fraction 3	60.6	Fraction 6	60.8
Fraction 4	64.4	Fraction 7	64.4
Fraction 5	69.1	Fraction 8	69.0

‘

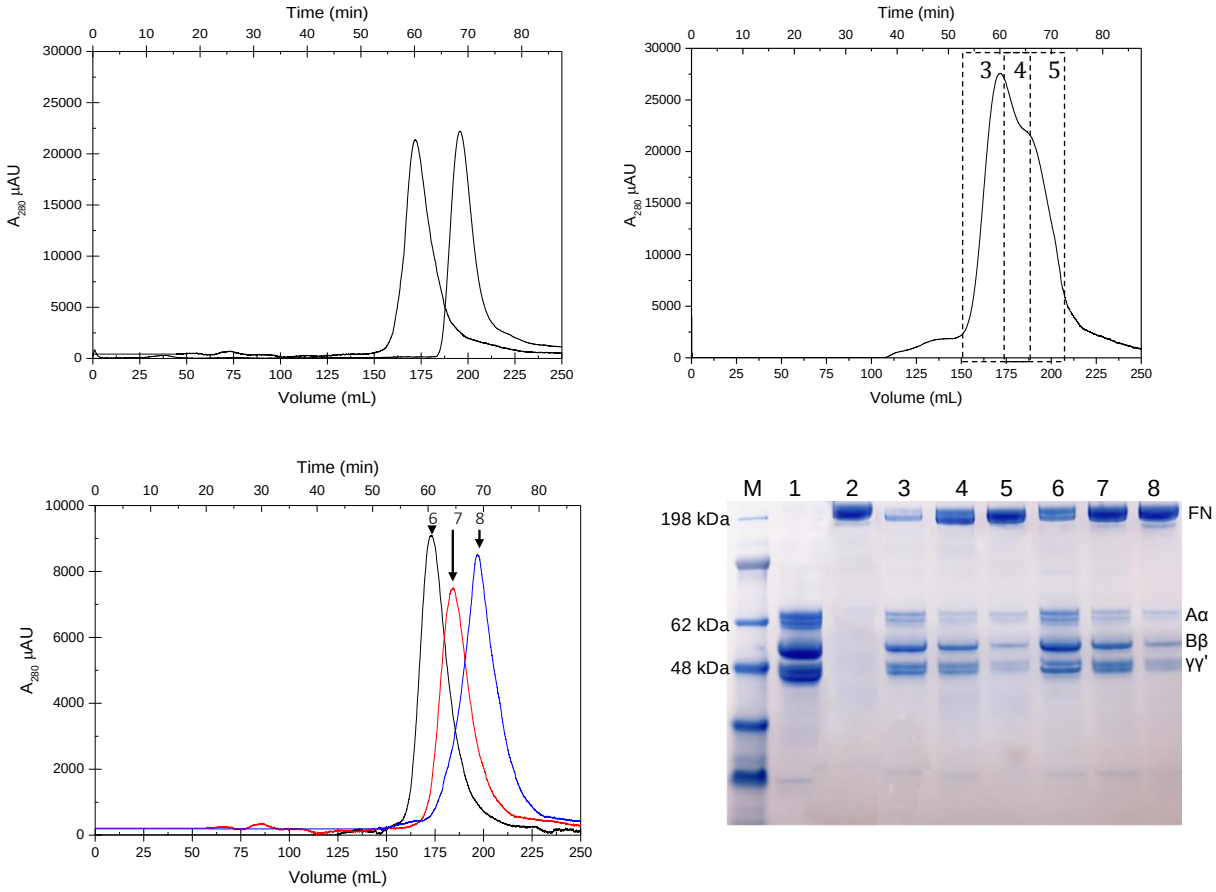

Figure 5.2: γγ'FI and FN mixture HPSEC chromatogram profile **(a)** Standard γγ'FI (1) and FN (2). **(b)** γγ'FI+FN mixture HPSEC chromatogram first pass. Collected fractions are numbered 3, 4, and 5. **(c)** γγ'FI+FN mixture HPSEC chromatogram overlay second pass. The previous collected fractions 3, 4, and 5 were concentrated and reloaded into the the HPSEC system. Collected fractions are numbered 6, 7, and 8 **(d)** SDS-PAGE analysis of standards and collected fractions.

Table 5.6: γγ' FI and FN mixture R_H and fractions 6,7 and 8 R_H measured by DLS at 25 °C. Samples were concentrated to 0.5 mg/mL in PBS buffer pH 7.4. Results indicate the mean and standard deviation of 3 independent preparations. Statistical analysis using one-way ANOVA indicates no significant differences between R_H measurements. ($P<0.044$, $\alpha=0.05$)

Species	Hydrodynamic radius (R_H), nm	Polydispersity, (%)	Intensity distribution (%)
γγ' FI	12.2 ± 0.3	23.8 ± 0.9	97.3
FN	10.5 ± 0.2	21.9 ± 1.1	96.3
Fraction 6 (6)	11.6 ± 0.5	25.3 ± 1.4	95.7
Fraction 7 (7)	11.4 ± 0.3	13.3 ± 5.5	99.5
Fraction 8 (8)	10.9 ± 0.3	16.2 ± 5.1	98.8

5.4.3. Characterization of reconstituted Desα-γγ'FI with FN by HPSEC and DLS

Because of the complex hexameric nature of fibrinogen and two chain pFN, we examined the potential for interactions with the des-α γγ'-FI degradation species that are α-chain deficient but still have intact Bβ, γ' and γ chains. We performed reconstitution experiments at 37 ^{o}C with des-α γγ'-FI and pFN (Figure 5.3b). The HPSEC residence time behavior of pure pFN and des-α γγ'-FI were distinct and resolvable from each other as was their hydrodynamic sizes analyzed by DLS (Figure 5.3a, Table 5.7 and 5.8). After 5 minutes incubation, the mixture showed an emergent peak having no

distinguishable component peaks. This emergent peak was fractionated and each fraction was reprocessed by HPSEC. (Figure 5.3c) In particular fraction 4 retained its residence time identity when reprocessed (Figure 5.3d: see reprocessed peak 7-lane 7 and table 5.7) having a composition containing strong gel signals of both pFN and des-α γγ'-FI. DLS showed that this fraction also exhibited an intermediate Rh to either of the participating constituents (Table 5.8). This result indicated the rapid formation of an association between these constituents while in the absence of α-chain. We hypothesized that the presence of the γ' was important to the interaction of the γγ'-FI with pFN and conversely the absence the γ' chain in either γγ-FI or des-α γγ-FI would diminish the formation of interactions with pFN.

Table 5.7: HPSEC retention time of Des-α γγ FI and FN mixture. Collected fractions are numbered and showed in figure 5.4a, 4b and 4c

Des-α γγ' FI + FN mixture HPSEC first fractioning		**HPSEC second fractioning**	
Sample	Retention Time (min)	Sample	Retention Time (min)
Des-α γγ' FI	65.6		
FN	69.8		
Fraction 3	60.7	Fraction 6	64.5
Fraction 4	67.5	Fraction 7	67.6
Fraction 5	69.7	Fraction 8	69.8

Table 5.8: Des-α γγ' FI and FN mixture R_H and fractions 6,7 and 8 R_H measured by DLS at 25 °C. Samples were concentrated to 0.5 mg/mL in PBS buffer pH 7.4. Results indicate the mean and standard deviation of 3 independent preparations. Statistical analysis using one-way ANOVA indicates no significant differences between R_H measurements. ($P<0.029$, $\alpha=0.05$)

Species	**Hydrodynamic radius (R_H), nm**	**Polydispersity, (%)**	**Intensity distribution (%)**
Des-α γγ' FI	11.7 ± 0.5	26.0 ± 2.5	95.2
FN	10.5 ± 0.2	21.9 ± 1.1	96.3
Fraction 6 (6)	11.4 ± 0.4	17.6 ± 1.3	97.8
Fraction 7 (7)	11.3 ± 0.3	17.3 ± 3.3	96.0
Fraction 8 (8)	10.9 ± 0.4	14.9 ± 2.2	99.0

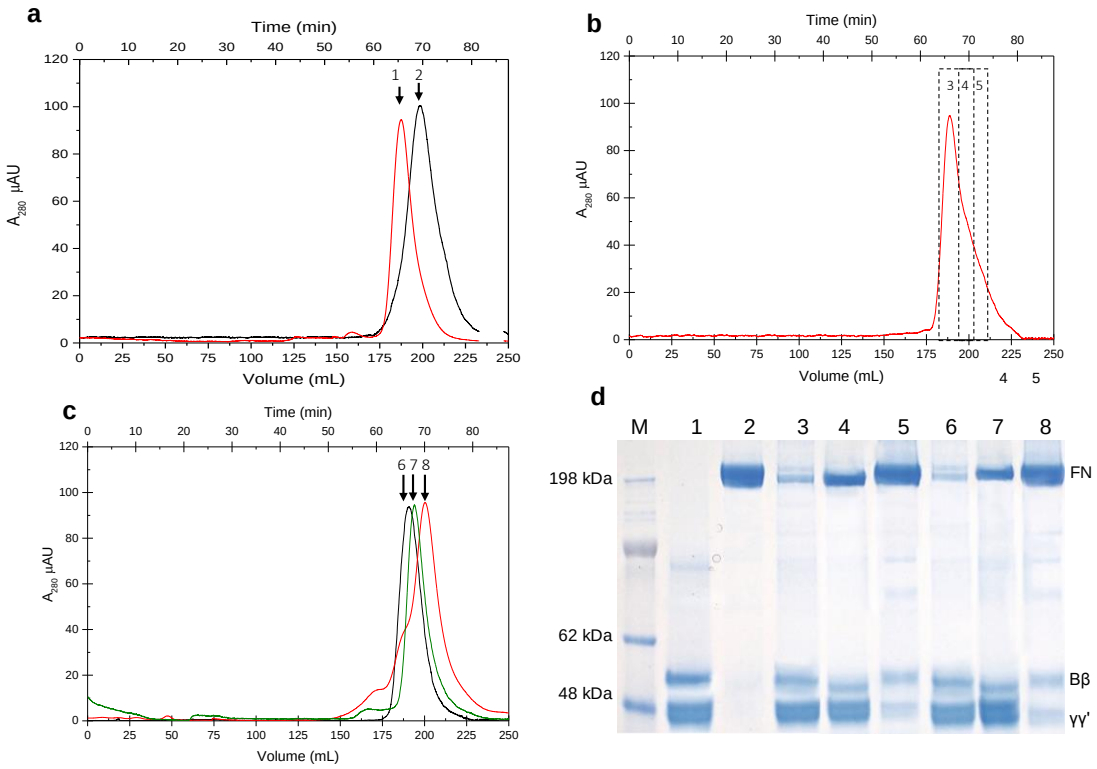

Figure 5.3: Des-α γγ' FI and FN mixture HPSEC chromatogram profile **(a)** Standard Des-α γγ' FI (1) and FN (2). **(b)** Des-α γγ' FI+FN mixture HPSEC chromatogram first pass. Collected fractions are numbered 3, 4, and 5. **(c)** Des-α γγ' FI +FN mixture HPSEC chromatogram overlay second pass. The previous collected fractions 3, 4, and 5 were concentrated and reloaded into the the HPSEC system. Collected fractions are numbered 6, 7, and 8 **(d)** SDS-PAGE analysis of standards and collected fractions.

5.4.4. Characterization of reconstituted γγFI with FN by HPSEC and DLS

We next performed analogous mixing experiments using pure pFN and γγ-FI (Figure 5.4) in order to deduce the potential for forming associations between these species. As above, we used the same pFN (lane 2, figure 5.4d) made from the original

plasma-derived binary mixture having both pFN and γγ'-FI. The pure γγ-FI (lane 1, figure 5.4d) was made from the processing step prior to the isolation of the binary pFN and γγ'-FI mixture. Prior to mixing and incubating these together at 37 ^{o}C, each of these preparations behaved as distinct peaks when analyzed by HPSEC (Figure 5.4a). After 5 minutes of incubation, the mixture was applied to the HPSEC: unlike the pFN and γγ'-FI merged peak behavior, the pFN and γγ-FI were still resolvable as identifiable constituent peaks (Figure 5.4b). Furthermore HPSEC fractions selected from this product were each reprocessed by HPSEC: each of these fractions retained their individual HPSEC residence times obtained prior to reprocessing (Figure 5.4c, Table 5.9). DLS analysis of these same reprocessed fractions reflected Rh values more closely resembling that of the nearly pure γγ-FI and pFN. (Table 5.10) The composition by SDS PAGE of those fractions was mostly indicative of chromatographic dispersion overlap. These results indicate that spontaneous formation of intermediately sized associations between pFN and γγ-FI did not appreciably occur relative to that of the analogous pFN and γγ'-FI mixture.

Table 5.9: HPSEC retention time of γγ FI and FN mixture. Collected fractions are numbered and showed in figure 5.2a, 5.2b and 5.2c

γγ FI + FN mixture HPSEC first fractioning		**HPSEC second fractioning**	
Sample	Retention Time (min)	Sample	Retention Time (min)
γγ FI	60.7		
FN	69.8		
Fraction 3	60.7	Fraction 6	60.8
Fraction 4	65.3	Fraction 7	65.5
Fraction 5	68.7	Fraction 8	68.7

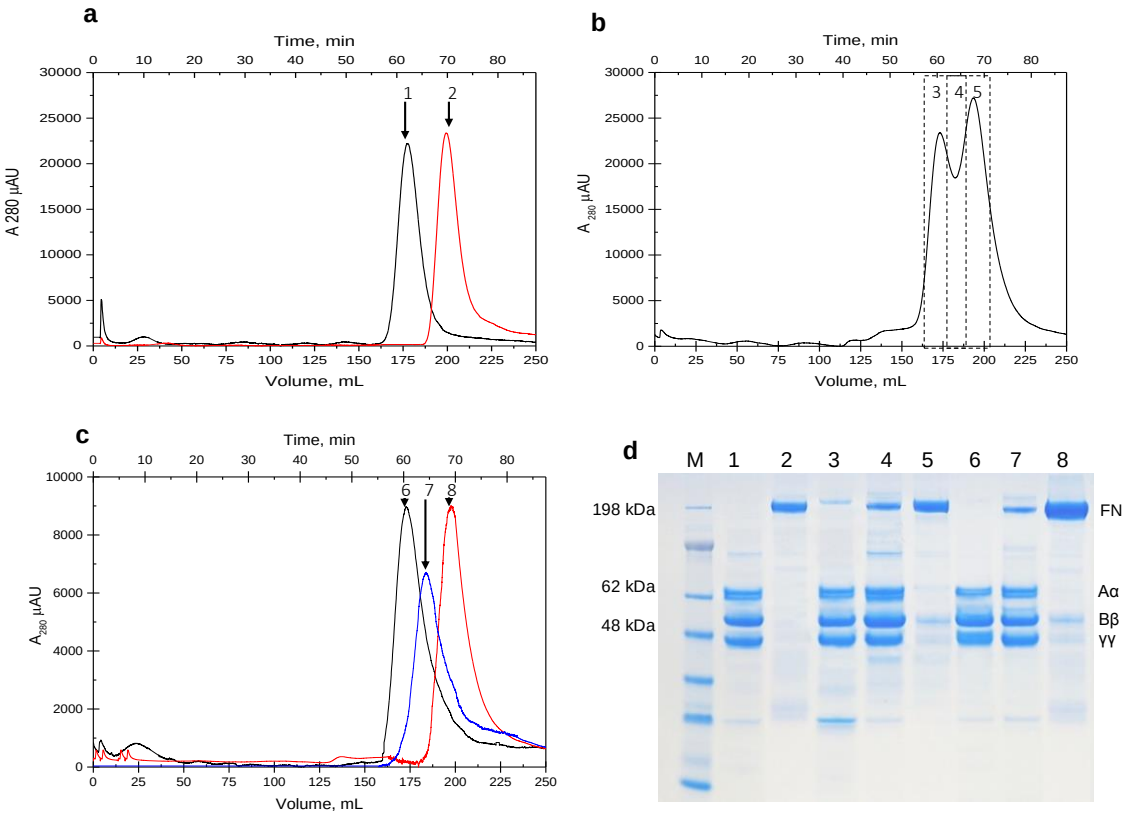

Figure 5.4: γγFI and FN mixture HPSEC chromatogram profile **(a)** Standard γγFI (1) and FN (2). **(b)** γγFI+FN mixture HPSEC chromatogram first pass. Collected fractions are numbered 3, 4, and 5. **(c)** γγFI+FN mixture HPSEC chromatogram overlay second pass. The previous collected fractions 3, 4, and 5 were concentrated and reloaded into the the HPSEC system. Collected fractions are numbered 6, 7, and 8 **(d)** SDS-PAGE analysis of standards and collected fractions.

Table 5.10: γγ FI and FN mixture R_H and fractions 6,7 and 8 R_H measured by DLS at 25 °C. Samples were concentrated to 0.5 mg/mL in PBS buffer pH 7.4. Results indicate the mean and standard deviation of 3 independent preparations. Statistical analysis using one-way ANOVA indicates no significant differences between R_H measurements. ($P<0.041$, $\alpha=0.05$)

Species	Hydrodynamic radius (R_H), nm	Polydispersity, (%)	Intensity distribution (%)
γγ FI (1)	12.1 ± 0.2	23.9 ± 1.9	95.1
FN (2)	10.5 ± 0.2	21.9 ± 1.1	96.3
Fraction 6 (6)	11.9 ± 0.6	25.0 ± 8.4	97.8
Fraction 7 (7)	11.4 ± 0.5	26.8 ± 6.9	95.4
Fraction 8 (8)	10.8 ± 0.3	20.5 ± 3.6	95.5

5.4.5. Characterization of reconstituted Desα-γγFI with FN by HPSEC and DLS

We performed mixing experiments using pure pFN and des-α γγ-FI in order to deduce the potential for forming associations between these species reflective of the absence of the α-chain. As above, we used the same pFN made from the original plasma-derived binary mixture having both pFN and γγ'-FI where the pure des-α γγ-FI was made from the processing step prior to isolation of the binary pFN and γγ'-FI mixture. Prior to mixing and incubating these together at 37 ^{o}C, each of these preparations behaved as distinct peaks when analyzed by HPSEC. (Figure 5.5a) After 5 minutes of incubation, the mixture was applied to the HPSEC: unlike the merged peak behavior of the pFN: des-α

γγ'-FI mixture, the pFN:des-α γγ-FI mixture still exhibited resolvable constituent peaks (Figure 5.5b). HPSEC fractions from this product were each reprocessed by HPSEC (Figure 5.5c) where the subfraction composition indicated by SDS PAGE reflected a greater pure components character with cross species content due to chromatographic dispersion.(figure 5.5d) Each of these fractions retained their individual HPSEC residence times prior obtained to reprocessing (Figure 5.5c, Table 5.11). The DLS analysis of these same reprocessed fractions reflected Rh more closely that of the nearly pure des-α γγ-FI and pFN. (table 5.12) These results indicate that spontaneous formation of intermediately sized associations between pFN and des-α γγ-FI did not appreciably occur upon mixing.

Table 5.11: HPSEC retention time of Des-α γγ FI and FN mixture. Collected fractions are numbered and showed in figure 5.4a, 5.4b and 5.4c

Des-α γγ FI + FN mixture HPSEC first fractioning		**HPSEC second fractioning**	
Sample	Retention Time (min)	Sample	Retention Time (min)
Des-α γγ FI	65.6		
FN	69.8		
Fraction 3	60.7	Fraction 6	64.5
Fraction 4	67.5	Fraction 7	67.6
Fraction 5	69.7	Fraction 8	69.8

Table 5.12: Des-α γγ FI and FN mixture R_H and fractions 6,7 and 8 R_H measured by DLS at 25 °C. Samples were concentrated to 0.5 mg/mL in PBS buffer pH 7.4. Results

indicate the mean and standard deviation of 3 independent preparations. Statistical analysis using one-way ANOVA indicates no significant differences between R_H measurements. ($P<0.021$, $\alpha=0.05$)

Species	Hydrodynamic radius (R_H), nm	Polydispersity, (%)	Intensity distribution (%)
Des-α γγ FI	11.4 ± 0.5	26.0 ± 2.5	95.2
FN	10.5 ± 0.2	21.9 ± 1.1	96.3
Fraction 6 (6)	11.8 ± 0.2	19.8 ± 2.1	99.0
Fraction 7 (7)	11.5 ± 0.5	30.9 ± 7.0	89.4
Fraction 8 (8)	10.7 ± 0.2	23.3 ± 0.6	98.3

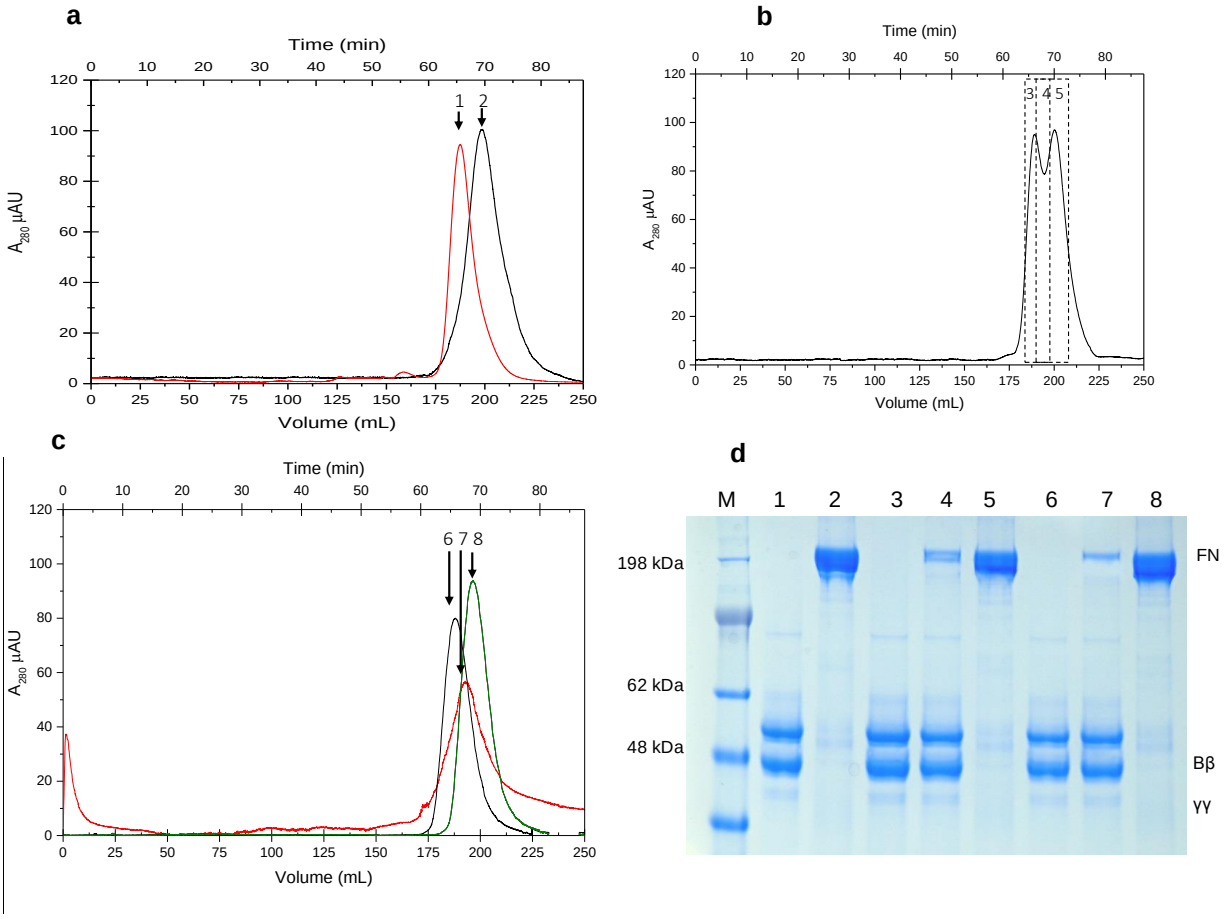

Figure 5.5: Des-α γγ FI and FN mixture HPSEC chromatogram profile **(a)** Standard Des-α γγ FI (1) and FN (2). **(b)** Des-α γγ FI+FN mixture HPSEC chromatogram first pass. Collected fractions are numbered 3, 4, and 5. **(c)** Des-α γγ FI +FN mixture HPSEC chromatogram overlay second pass. The previous collected fractions 3, 4, and 5 were concentrated and reloaded into the the HPSEC system. Collected fractions are numbered 6, 7, and 8 **(d)** SDS-PAGE analysis of standards and collected fractions.

5.5.Discussion

The Interaction of fibrinogen with fibronectin initially observed on the formation of cold insoluble precipitates [27]. A later study indicated that this interaction was limited in fibrinogen due to the cryptically hidden αC chain which was exposed in fibrin after the thrombin proteolytic removal of the fibrinogen peptides [29]. However, Nagatmatsu et. al. used DLS to evaluate the diffusion coefficient of a FI-FN complex purified from plasma as a complex from patients with rheumatoid arthritis [14]. Their work indicated that FN flexibility contributed to the formation of a FI-FN complex that enabled the spatial exposure of binding sites. The above studies were limited to whole populations F1 as the γγ'FI plasma F1 subspecies was not yet well studied. We have recently published the purification of a γγ'FI-FN mixture using DEAE chromatography [40]. This study focused on the development of strong plasma derived fibrin sealants made at low fibrinogen concentrations. In this work, we have reported the study of interactions between γγ'FI and FN. We show that a reversible formation of a compacted γγ'FI-FN association exists by reassembling it from FN and γγ'FI where each species was purified from and by disrupting the original complex. We use des-α chain γγ'FI and γγFI species

arising from proteolysis to show that γγ'FI-FN association is specifically catalyzed by the presence of the γ' chain. These experiments show that rapid *in situ* formation of compacted overall γγ'FI-FN structure happens even when alpha chains are not natively present. The compacted structure is hydrodynamically smaller than γγ'FI alone and larger than FN.

Previous studies have not reported solution phase interactions with F1 and FN. These studies used techniques that immobilized portions of whole F1, fibrin or FN molecules that we probed by the remaining species that was in solution. Only associations with immobilized fibrin and fibrinogen with solution phase FN were reported. For example, SPR identified a FN high affinity segment located in fibrin αC chain. [29] In addition, fibrin-Sepharose coupled columns proved to bind FN with greater affinity than FI-Sepharose columns. [27] In both cases fibrin was immobilized to a solid surface restricts freedom of motion. We hypothesize that DLS observation of these interaction enables the complex association and resulting compacted γγ'FI-FN complex. This is consistent with the formation of a 1:1 FI-FN complex purified by affinity chromatography from heparinized plasma of patients with RA reported by Nagamatsu et. al. which showed that this complexation with fibrinogen and not fibrin. [14] [44, 45]. In addition, Nadamatsu concluded that the high flexibility of FN in solution is needed for the formation of a compact molecule. Nadamatsu and our observations do not conflict with neither Makogonenko et al [29] nor Stathakis et al [27] findings as exposure of cryptic sites within fibrinogen due to its conversion to fibrin has been shown to occur within FN that is incorporated into fibrin matrices.

FN shows specific affinity toward the FI γ' chain in the absence of the α chain. Although the FI α chain presence is required for the FN interaction with fibrin [29], the formation of insoluble CIg cryoprecipitates [27] and the cryoprecipitation of Heparin-CIg mixtures [28], our experiments suggested that in addition to the FI α chain the FI γ' presents a binding region for FN not studied in previous studies of whole population F1. For example, Stathakis et. al. concluded that for the CIg-induced precipitation to occur the presence of the FI Aα chain was essential. In addition, in their experiments they also reported the necessity of fibrin-fibrinogen complexes and CIg to form insoluble precipitates. They showed that fractions lacking of the FI Aα chain failed to precipitate in the presence of CIg as well as FI fractions containing intact α chain suggesting the necessity of fibrin molecules with intact α chains for precipitate formation [27]. Their findings were further evaluated using heparin for the formation of a heparin-precipitable fraction of plasma. Their studies suggested the importance of the carboxyl terminal segment of the Aα chain for the formation of a cold precipitable complex formed of heparin-CIg and fibrinogen [28]. Further evidence of the involvement of the FI α chain in the interaction with FN was reported by Makogonenko et. al. In their experiments, they used SPR and ELISA to confirm the selective interaction between FN and the fibrin α chain and to localize the Aα221-391 segment as an important FN binding region which was exposed only after the fibrinogen conversion to fibrin. Indeed, in our present study we were able to observe and characterize the Des-α γγ'FI-FN interaction by HPSEC.

FN induces γγ'FI conformational changes forming a compact molecule. Our study shows that the initial catalysis of the rapid formation of this compacted structure is caused by the presence of the γ' chain. The compactness of the final structure indicates

that all chains become involved in the final wrapped structure. Even though both FN and FI conformation are highly dependent on temperature, pH and ionic strength [19, 20], the flexible configuration of FN under physiological conditions may induce conformational changes in FI when interacting together. In fact, our previous DLS studies indicated the structural rearrangement of the native γγ'FI-FN mixture to form a compact molecule [40]. Here, our DLS experiment focused on the size and particle polydispersity assessment indicated the monomodal monodisperse behavior of the Des-α γγ'FI-FN mixture (SF5: %P=17.3±3.3) and differ from all the other preparations which presented intermediate level of polydispersity (15%<%P<30). Our study suggests that the intermediate level of polydispersity produced in all other preparations but Des-α γγ'FI-FN mixture may be generated by the FN binding to the FI α chain which generates different size molecules due to FN flexibility. This hypothesis is supported by our γγFI-FN and γγ'FI-FN interactions evaluation (table 5.3 and 5.4) which suggest that the γγFI-FN intermediate level of polydispersity (SF2: %P=26.8±6.9) arises from the FN binding of the FI α chain which may generates non-homogeneous distribution of structures. When mixed with FN, our assessment show decrease in the R_H to less than that of native γγ' FI suggesting the formation of a complexed molecule accommodated and enabled by the flexible nature of FN.

5.6 References

[1] T.-Y. Huang, L.-M. Chi and K.-Y. Chien, "Size-exclusion chromatography using reverse phase columns for protein separation," *Journal of Chromatography A,* 2018.

[2] M. Netopilik, "Toward ideal separation by size exclusion chromatography," *Journal of Chromatography A,* vol. 1487, pp. 139-146, 2017.

[3] G. B. Irvine, "Determination of molecular size by size-exclusion chromatography (gel filtration)," *Current Protocols in Cell Biology,* vol. Chapter 5, pp. 5.5.1 - 5.5-16, 2001.

[4] C. L. Mayer, W. K. Snyder, M. A. Swietlicka, A. D. VanSchoiack, C. R. Austin and B. J. mcFarland, "Size exclusion chromatography can identify faster-associating protein complexes and evaluate design strategies," *BCM research notes,* vol. 2, pp. 135 - 143, 2009.

[5] J. Bloustine, V. Berejnov and S. Fraden, "Measurements of protein-protein interactions by size exclusion chromatography," *Biophysical journal,* vol. 85, pp. 2619-2623, 2003.

[6] K. Ahrer, A. Buchacher, G. Iberer, D. Josic and A. Jungbauer, "Analysis of aggregates of human immunoglobulin G using size-exclusion chromatography, static and dynamic light scattering," *Journal of Chromatography A,* vol. 1009, pp. 89-96, 2003.

[7] K. Loster, O. Baum, W. Hofmann and W. Reutter, "Characterization of molecular aggregates of a1b1-integrin and other rat liver membrane proteins by combination of size exclusion chromatography and chemical cross-linking," *Journal of Chromatography A,* vol. 711, pp. 187 - 199, 1995.

[8] N. C. Vanderslice, A. S. Messer, K. Vadivel, P. Bajaj, M. Phillips, M. Fatemi, W. Xu and W. H. Velander, "Quantifying vitamin K dependent holoprotein compaction caused by differential gamma carbolxylation using high-pressure size exclusion," *Analytical Biochemistry,* vol. 479, pp. 6-14, 2015.

[9] J. Djuro, H. Horn, P. Schulz, S. Horst and L. Britsch, "Size-Exclusion chromatography of plasma protein with high molecular masses," *Journal of chromatography A,* pp. 289-298, 1998.

[10] K. R. Siebenlist, D. A. Meh and M. W. Mosesson, "Plasma factor XIII binds specifically to fibrinogen molecules containing gamma-prime chains".

[11] R. D. Ricker, L. A. Sandoval, J. D. Justice and F. O. Geiser, "Multivariate visualization in the size exclusion chromatography and pattern recognition of biological samples," *Journal of Chromatography A,* vol. 691, pp. 67 - 69, 1995.

[12] S. Fekete, A. Beck, J.-L. Veuthey and D. Guillarme, "Theory and practice of size exclusion chromatography for the analysis of protein aggregates," *Journal of Pharmaceutical and Biomedical Analysis,* vol. 101, pp. 161 - 173, 2014.

[13] R. D. Ricker and L. A. Sandoval, "Fast, reproducible size-exclusion chromatography of biological macromolecules," *Journal of chromatography A,* vol. 743, pp. 43-50, 1996.

[14] K. Nagamatsu, M. Komori, S. Kuroda and K. Tanaka, "Dynamic Light scattering studies on hydrodynamic properties of fibrinogen-fibronectin complex," *Journal of Biomolecular structure & Dynamics,* vol. 9, pp. 807-820, 1992.

[15] J. Wen, T. Arakawa, J. Talvenheimo, A. A. Welcher, T. Horan, Y. Kita, J. Tseng, M. Nicolson and J. S. Philo, "A light scattering/size exclusion chromatography method for studying the stoichimoetry of a protein-protein complex," *Techniques in protein chemistry,* vol. 7, pp. 23 - 31, 1996.

[16] J. Wen, T. Arakawa and J. S. Philo, "Size-Exclusion chromatography with on-line light-scattering, absorbance, and refractive index detectors for studying proteins and their interactions," *Analytical Biochemistry,* vol. 240, pp. 155 - 166, 1996.

[17] O. A. Grillo, K.-L. T. Edwards, R. S. Kashi, M. K. Shipley, L. Hu, M. J. Besman and C. R. Middaugh, "Conformational Origin of the Aggregation of Recombinant Human Factor VIII," *Biochemistry,* vol. 40, pp. 586-595, 2001.

[18] L. Huang and S. T. Lord, "The isolation of fibrinogen monomer dreamatically influences fibrin polymerization," *Thrombosis Research,* vol. 131, pp. 258-263, 2013.

[19] J. Pelta, H. Berry, G. C. Fadda, E. Pauthe and D. Lairez, "Statistical Conformation of Human Plasma Fibronectin," *Biochemistry,* vol. 39, pp. 5146-5154, 1999.

[20] E. C. Williams, P. A. Jammey, J. D. Ferry and D. F. Mosher, "Conformational States of Fibronectin: Effects of pH, Ionic strength and collagen binding," *The Journal of*

Biological Chemistry, vol. 257, pp. 14973-14978, 1982.

[21] M. W. Mosesson and D. L. Amrani, "The structural and biologic activities of plasma fibronectin," *Blood,* vol. 56, pp. 145-158, 1980.

[22] P. Speziale , L. Visai, S. Rindi and A. Di Poto, "Purification of human fibronectin using immobilized gelatin and Arg affinity chromatography," *Nature protocols,* vol. 3, pp. 525-533, 2008.

[23] W. S. To and K. S. Midwood, "Plasma and cellular fibronectin: distinct and independent funtions during tissue repair," *fibrinogenesis & tissue repair,* vol. 4, 2011.

[24] M. K. Magnusson and F. D. Mosher, "Fibronectin: Structure, assembly and cardiovascular implications," *Arteriosclerosis Thrombosis and Vascular Biology,* vol. 18, pp. 1363-1370, 1998.

[25] A. Rostagno, M. J. Williams, M. Baron, I. D. Campbell and L. I. Gold, "Further characterization of the NH-2 terminal fibrin binsding site on fibronectin," *Journal of Biological Chemistry,* vol. 269, pp. 31938-31945, 1994.

[26] Y. V. Matzuka, L. V. Medved, S. A. Brew and K. C. Ingham, "the NH2-terminal Fibrin-binding site of fibronectin is formed by interacting fourth and fifth finger domains," *Journal of Biological Chemistry,* vol. 269, pp. 9539-9546, 1994.

[27] N. E. Stathakis, M. W. Mosesson, A. B. Chen and D. K. Galanakis, "Cryoprecipitation of fibrin-fibrinogen complexes induced by the cold-insoluble globulin of plasma," *Blood,* vol. 51, pp. 1211-1222, 1978.

[28] N. E. Stathakis and M. W. Mosesson, "interactions among heparin, cold insoluble globulin and fibrinogen in formation of the heparin precitable fraction of plasma," *Journal of Clinical Investigation,* vol. 60, pp. 855-865, 1977.

[29] E. Makogonenko, G. Tsuruoa, K. Ingham and L. Medved, "Interaction of fibrin(ogen) with fibronectin: further characterization and localization of the fibronectin-binding site," *Biochemistry,* vol. 41, pp. 7907-7913, 2002.

[30] M. Wasilewska, Z. Adamczyk and B. Jachimska, "Structure of fibrinogen in electrolyte solutions derived from dynamic light scattering (DLS) and viscosity measurements," *Langmuir,* vol. 25, pp. 3698-3704, 2009.

[31] Z. Adamczyk, B. Cichocki, M. Ekiel-Jezewska, A. Slowicka, E. Wajnryb and M. Wasilewska, "Fibrinogen conformations and charge in electrolyte solutions derived from DLS and dynamic viscosity measurements," *Journal of Colloid and Interface Science,* vol. 385, pp. 244-257, 2012.

[32] M. W. Mosesson, "Fibrinogen and fibrin structure and functions," *Journal of Thrombosis and Haemostasis,* vol. 3, pp. 1894-1904, 2005.

[33] M. W. Mosesson, J. S. Finlayson, R. A. Umfleet and D. Galanakis, "Human Fibrinogen Heterogeneities: Structural and related studies of plasma fibrinogens which are high solubility catabolic intermediates," *Journal of Biological Chemistry,* vol. 247, pp. 5210-5219, 1972.

[34] J. W. Wiesel and R. I. Litvinov, "Fibrin formation, structure and properties," *Subcell Biochemistry,* vol. 82, pp. 405-456, 2017.

[35] M. W. Mosesson, J. S. Finlayson and R. A. Umfleet, "Human Fibrinogen Heterogeneities: Identification of gamma chain variants," *Journal of Biological Chemistry,* vol. 247, pp. 5223-5227, 1972.

[36] D. W. Chung and E. W. Davie, "gamma and gamma-prime chains of human fibrinogen are produced by alternative mRNA processing," *Biochemistry,* vol. 23, pp. 4232-4236, 1984.

[37] M. Moaddel, D. H. Farrell, M. A. Daugherty and G. M. Fried, "Interactions of human fibrinogens with factor XIII: roles of calcium and the gamma-prime peptide," *Biochemistry,* vol. 39, pp. 6698-6705, 2000.

[38] R. S. Lovely, M. Moaddel and D. H. Farrell, "Fibrinogen gamma-prime chain binds thrombin exosite II," *Journal of thrombosis and heamostasis,* vol. 1, pp. 124-131, 2002.

[39] D. A. Meh, K. R. Siebenlist and M. W. Mosesson, "Identification and characterization of the thrombin binding sites on fibrin," *Journal of biological chemistry,* vol. 271, pp. 23121-23125, 1996.

[40] E. A. Ismail, F. M. Fabian, O. Wang, Y. Lei, M. A. Carlson, W. H. Burgess and W. H. Velander, "The isolation of a plasma derived gamma/gamma-prime fibrinogen:fibronectin mixture that forms a novel polymeric matrix," *Process Biochemistry,* 2019.

[41] A. S. Brew and C. K. Ingram, "Purification of human plasma fibronectin," *Journal of tissue culture methods,* vol. 16, pp. 197-199, 1994.

[42] C. A. Schneider, W. S. Rasband and K. W. Eliceiri, "NIH Image to image J: 25 years of image analysis," *Nature methods,* vol. 9, pp. 671-675, 2012.

[43] P. K. Smith, R. I. Krohn, G. T. Hermanson, A. K. Mallia, F. H. Gartner, M. D. Provenzano, E. K. Fujimoto, N. M. Goeke, B. J. Olson and P. C. Klenk, "Measurement of protein using bicinchoninic acid," *Analytcal biochemistry,* vol. 150, pp. 76-85, 1985.

[44] T. Rooney, R. Scherzer, J. K. Shigenaga, J. Graf, J. B. Imboden and C. Grunfeld, "Levels of plasma fibrinogen are elevated in well-controlled rheumatoid arthritis," *Rheumatology,* vol. 50, pp. 1458-1465, 2011.

[45] D. L. Scott and K. W. Walton, "The significance of fibronectin in rheumatoid arthritis," *Seminars in Arthritis and rheumatism,* vol. 13, pp. 244-254, 1984.

CHAPTER VI

CONCLUSIONS

The biophysical and kinetic characteristics of factor XIII, fibrinogen and fibronectin and these interactions were studied in this work. This was undertaken in the context of gaining understanding to phenomena which may be useful to therapeutic applications of recombinant versions of these complex proteins that are essential for establishing a provisional polymeric barrier needed for regaining hemostasis and for initiating healing after tissue is wounded. These proteins contribute to this important physiologic function by nanoscale material structural properties as a barrier to fluid loss and through cell signaling need to initiate wound healing as a provisional matrix. This work focuses on the molecular analysis of the interactions of these proteins, their enzymatic versus substrate roles and strives to visualize and further the conceptualization and nature of their interactions that will be useful in the future to physiologic manipulations as biotherapeutics. From these studies, we conclude the following:

1. Consistent with past reports, our studies confirm the interaction of plasma factor XIII ($pFXIIIA_2B_2$) with the fibrinogen (FI) γ' chain via the B subunit of FXIII. We uniquely conform this association by a combination of molecular size measurements and also with kinetics observable from phenomena occurring within a fibrin or fibrinogen hydrogel phase immobilized on an assay surface. Importantly we have used contrasting interactions using a monomeric recombinant Factor XIII having only an A subunit to further support this conclusion. Importantly, we newly adapted a prior published version of this assay to serve our kinetic observation purpose. Our studies have resulted in the characterization of the underlying kinetic phenomena of fibrin cross-linking associated

with the monomeric, rFXIII made in Pichia pastoris and useful for use in fibrin sealant applications.

2. Unlike past reports, our experiments were uniquely performed using the recombinant homodimer γγF1, the heterodimer γγ' FI having no background activity of plasma factor XIII. These demonstrate that the γγ' FI subspecies of F1 is responsible for the intrinsic interaction via the factor XIII B subunit. The phenomena observed by size exclusion chromatography and confirmed by the use of Sepharose 6 column showed a greater affinity of tetrameric, plasma factor XIII ($pFXIIIA_2B_2$) towards the γγ' FI than the γγ FI. Conversely, experiments also demonstrated that the $pFXIIIA_2B_2$ has a low affinity level related by slower kinetic processing of γγ FI as confirmed by transglutaminase mediated peptide incorporation assay. The $pFXIIIA_2B_2$–FI γγ' interaction induces structural rearrangements. This was suggested by dynamic light scattering (DLS) studies where the high level of polydispersity was observed indicative of the rearrangements induced by the tetrameric nature of $pFXIIIA_2B_2$. Our studies suggest that $pFXIIIA_2B_2$ – FI γγ' interaction can occur as a 1:2 molecular ratio. This conclusion suggests that one $pFXIIIA_2B_2$ can support two FI γγ' possibly via the two separate FXIII B subunits.
3. The rate of $pFXIIIA_2B_2$ activation is accelerated by the γ' fibrin chain. Our adapted incorporation peptide assay showed a faster rate of $pFXIIIA_2B_2$ activation than occurred in γγ FI. Moreover, our studies indicate that the rate of factor XIII B subunit dissociation is catalyzed by either the fibrinogen/fibrin forms of γγ' FI. This is consistent with previous studies that suggested the γ' chain acts as a cofactor facilitating the FXIII B subunit dissociation.

4. This work presents physical chemical evidence of the reversible interactions specifically between the γγ' fibrinogen (FI) and fibronectin (FN) that lead to the formation of a compacted complex. Previously it was suggested that complexation was only observable between whole population fibrin and FN and that identified the importance of the α–chain for the interaction to occur. Our studies are unique in their use of pure FI species: γγF1, γγ'F1, des α-γγF1, des α-γγ'F1 and FN. Our studies using SEC analysis of the interaction between each of the isolated FI species, γγF1, γγ'F1, des α-γγF1, des α-γγ'F1 and FN showed the presence of the γ' chain was needed to initiate FN complexation. The unique use of purified des-α FI γγ', des α-γγF1 and FN enabled discernment that the absence of α-chain shows that γ' chain initiates the complexation with FN.
5. Our studies isolate an (FN)–FI complex from normal human plasma and not plasma from RA patients. The biophysical analysis of these molecules performed using SEC and DLS indicated that the molecular size did not experiment changes suggesting that the linear and semi-globular structure of FI and FN collapse into a wrapped structure with molecular size which clearly ranges between that of the hydrodynamic size FI and FN.